NASA Technical Memorandum 85842

NASA Geodynamics Program: Annual Report for 1982

Geodynamics Program Office
Office of Space Science and Applications
Washington, DC 20546

National Aeronautics and Space Administration

Scientific and Technical Information Branch

1983

TABLE OF CONTENTS

I. INTRODUCTION

This document is the fourth annual report of the NASA Geodynamics Program, covering calendar year 1982. The purpose of these annual reports is to inform interested agencies and individuals of the status, progress, and plans of the program.

The first annual report (NASA, 1980) contained a section of background and historical information covering the period from the beginning of the program in 1964 as the National Geodetic Satellite Program, up to the end of 1979. The second annual report (NASA, 1981b) highlighted the progress in instrumentation development and theoretical research, and the preparation for initiation of crustal motion measurements in the western United States. The third annual report (NASA, 1982b) emphasized progress made in 1981 in achieving improved measurement precision and in establishing the foundation for the acquisition and analysis of scientific data.

In 1982, the Geodynamics Program was combined with the Planetary Program to form the Earth and Planetary Exploration Division of the NASA Office of Space Science and Applications. As part of this reorganization, the Geodynamics Program was restructured into three program elements: Crustal Dynamics, Earth Dynamics, and Geopotential Fields.

This report summarizes program activities and achievements in 1982, and includes for the first time abstracts of papers presented at the annual NASA Geodynamics Conference, which was held from January 24 to 28, 1983. The significant results presented at this conference are summarized in Section IV, and abstracts are included in Appendix 4.

The investigations and investigators selected in response to the 1982 Geodynamics Notice, and current publications based on studies supported by the Geodynamics Program, are listed in the appendices.

HIGHLIGHTS AND ACHIEVEMENTS OF 1982

Substantial effort was devoted in 1982 to the development and upgrading of laser and very long baseline interferometry (VLBI) systems, in order to improve both the system measurement performance and the mobility of transportable systems. Some reduction in the rate of data acquisition occurred as a result of fiscal constraints. However, significant progress was made in the analysis and interpretation of data and in the concluding of international agreements for global geodynamics studies. This progress can be summarized as follows:

- Baseline measurements, using mobile laser and VLBI systems, were obtained for use in crustal deformation studies at eight sites in the western United States.

- Interplate baseline measurements for plate motion studies were continued using fixed laser and VLBI stations located on the North American, South American, Australian, Pacific, and Eurasian plates.

- The transportable laser ranging station TLRS-2 was completed and deployed to Easter Island. In cooperation with France and Mexico, Moblas stations were established at Huahine Island, near Tahiti in French Polynesia, and at Mazatlan, Mexico.

- The Global Positioning System (GPS) geodetic receiver development moved into test phases at JPL (SERIES) and MIT (MITES); measurements over distances of several tens of kilometers generally provided repeatabilities of 6 cm or less; the major source of error is the uncertainties in determination of the orbits of the GPS satellites.

- A contractual agreement was implemented with the National Mapping Division (Natmap), Australian Department of National Development and Energy, for upgrade of the Orroral Valley lunar laser station, and the incorporation of capability for satellite laser ranging at that station.

- An agreement was concluded with the Italian CNR/PSN for cooperative geodynamics activities, including a laser site at Matera, Italy, and studies for mobile laser ranging system development and a joint Lageos-II mission.

- A Federal Implementation Plan for Crustal Dynamics and Earthquake Research was approved by the participating agencies (ICCG, 1981).

- In response to a Geodynamics Notice, 93 research proposals were received and 32 were selected for funding in Fiscal Year 1983.

- Workshops were held on the Earth's gravity and magnetic fields, and a Geopotential Research Plan (GRP) developed to guide this research over the next decade.

- Studies of the Geopotential Research Mission (GRM) were continued and a GRM Science Steering Group (GRM/SSG) was established to strengthen the scientific rationale for the GRM (NASA, 1983b).

- Analysis of perturbations of the Lageos orbit showed that part of the perturbation is explainable by a variation in J_2, the lowest-degree coefficient in the spherical harmonic representation of the Earth's gravity field. The observed change agrees well with theoretical estimates of the changes in the Earth's gravity field due to the effects of post-glacial uplift.

- A study of the optimum spacecraft and orbit characteristics of Lageos-II was completed by the NASA/PSN Lageos-II Study Group, which recommended that Lageos-II be the same physical size, mass, and construction as Lageos-I, and that it be launched into a 6,000 km circular orbit with inclination 52°.

II. PROGRAM OVERVIEW

A. OBJECTIVES

The objectives of the NASA Geodynamics Program are:

To contribute to the understanding of the solid Earth; in particular, the processes that result in movement and deformation of the tectonic plates;

To improve measurements of the Earth's rotational dynamics and its gravity and magnetic fields, in order to better understand the internal dynamics of the Earth.

Studies of new instrumentation and space missions are supported by the Geodynamics Program to facilitate the improvement of precise measuring systems by which these phenomena may be assessed.

The Geodynamics Program is subdivided into three areas: Earth Dynamics, Crustal Dynamics, and Geopotential Research.

The objective of the Earth Dynamics Program is to develop models of polar motion and Earth rotation, and to relate studies of global plate motion to the dynamics of the Earth's interior. This program is expected to lead to an increased understanding of the global structure of the Earth and the evolution of the crust and lithosphere. The research conducted in this program includes studies of the dynamic interaction between different regions of the Earth's interior and its relationship to crustal magnetization, gravity anomalies and tectonic features. A significant portion of this program element includes activities performed under the Crustal Dynamics Project (CDP), which makes highly accurate measurements of Earth rotation and polar motion.

Field Measurements and modeling studies of crustal deformation in various tectonic settings are the primary objectives of the Crustal Dynamics Program. These activities provide measurements, analyses, and models which describe the accumulation and release of crustal strain, and the crustal motion between and within the tectonic plates, particularly the North American, Pacific, Eurasian, South American, and Australian plates. Activities include development of quantitative descriptions of the geophysical and geological constraints on the motions of measuring sites, including refinements of global plate motion models and block-tectonic models of the western United States. The investigations also compare the geologically determined motion vectors between project sites with the geodetically determined values, to test the predictions of geological models.

The Geopotential Research Program uses space and ground measurements to construct gravity and magnetic field models and to investigate data analysis techniques and software systems. Studies of the Lageos orbit and the orbits of near-Earth satellites are part of the efforts directed toward advancing gravity field studies. Gravity field data derived from satellite altimetry, satellite-to-satellite tracking, and gradiometry; magnetic field data from satellite magnetometers, and ancillary data, are used in constructing the models.

B. FUNDING

Funding for the NASA Program for Fiscal Years 1981-1983 and planned funding for 1984 is shown in Table 1, in terms of the reorganized program areas. The Crustal Dynamics Program funding includes the Crustal Dynamics Project, the laser network operations, crustal modeling research, and advanced instrumentation development for rapid measurement of crustal motion.

Fiscal constraints in 1982 and 1983, amounting to a 23% reduction below required funding, necessitated curtailment of laser ranging observations from sixteen to eight hours per day, a reduction in the number of sites and site visits in the western U.S., a reduction in global plate motion observations, restriction of South American regional deformation studies to four sites, and indefinite postponement of studies in the Caribbean basin, New Zealand, and the eastern Mediterranean. However, planned funding for FY 1984 was increased by $1.9M in early 1983 to provide for restoration of the Caribbean basin and South American studies.

The funding levels for the Earth Dynamics Program are not representative of the actual research in this area, since additional activities (amounting to several million dollars per year) is conducted as part of the Crustal Dynamics Project. NOAA funding of the Polaris project contributes directly to this program element in that all resulting data is applied to the NASA research program under interagency agreement.

C. 1982 STATUS

In 1982 program activity focused on the continued improvement of position measuring systems, the deployment of systems outside the U.S., the establishment of international agreements for joint observing sessions, and the formulation of federal agency plans for crustal research and geopotential studies.

For the laser and VLBI systems, a broad level of progress was achieved towards the attainment of the goal of one-centimeter precision first stated in 1969. Modifications were incorporated into the SAO laser stations which improved the accuracy of ranging to Lageos (normal points) from 10 cm to less than 5 cm. The SAO stations at Natal, Brazil, and Orroral Valley, Australia, were closed in 1981 and 1982 respectively, due to funding limitations. However, arrangements were made for future upgrading of this equipment for reinstallation and use elsewhere. Upgrade of Moblas stations (Moblas 4-8) was initiated, based on test results which showed that subcentimeter ranging (normal point) was attainable.

The Transportable Laser Ranging Station TLRS-1 performed well during its first year of operations, and TLRS-2 was completed and certified as ready for field use. Fabrication of MLRS, the McDonald Observatory Laser Ranging System at Fort Davis, Texas, was completed and testing was begun. In addition, work was started on the Orroral Valley Laser Ranging System (NLRS) and on tests of the Lurescope at the LURE Observatory at Haleakala, Hawaii, in order to have three lunar laser ranging systems ready for the MERIT campaign beginning in September, 1983.

Modifications of mobile VLBI systems MV-1 and MV-2, and fabrication of the new system (MV-3), were continued. Field tests were initiated on the SERIES (Satellite Emission Range Inferred Earth Surveying) GPS receivers, and studies were completed for an Airborne Laser Ranging System (ALRS). Further work on development of the ALRS was postponed pending availability of funding. Configuration Control Boards were established by the CDP to assure that before their implementation, proposed system changes and improvements would be adequately assessed as to performance and cost.

Provisions were made for the establishment of laser ranging sites on Easter Island (TLRS-2), in French Polynesia (Moblas), at Mazatlan, Mexico (Moblas), sites in Baja California (TLRS-1), and Socorro Island (TLRS-2). Discussions were held on the use of Transportable VLBI Data Systems (TVDS) units for VLBI measurements at radio antenna sites in Hawaii, Kwajalein, Quito (Ecuador), São Paulo (Brazil), and Santiago (Chile). In addition, assistance was provided to scientific organizations in Japan, Australia, Italy, and West Germany for the development of their own VLBI stations.

Agreements for CDP Principal Investigator studies were concluded with France, The Netherlands, West Germany, Switzerland, Sweden, Canada, Mexico, England, Peru, Australia, and China. The agreements with France, The Netherlands, West Germany, and China also provided for the exchange of laser and VLBI data. Other agreements were discussed with organizations in Japan for long-term VLBI experiments (Radio Research Laboratories) and for laser data exchange (Japanese Hydrographic Department).

An agreement was concluded in July 1982 for a broad cooperative geodynamics program with the Italian government (CNR/PSN). This agreement provides for indefinite loan of an SAO laser station to be located at Matera, Italy, to be operated by PSN, for a joint NASA/PSN study group to explore the scientific contributions of a second Lageos satellite, and for exchange of technical data for the development of mobile VLBI and laser systems. The Lageos-II study group report (NASA/PSN, 1983), completed in late December 1982, found that significant improvement in baseline accuracy, tidal component separation, and gravity field model could be attained with a second Lageos, identical to the first but in a 50-57° prograde orbit.

Plans for joint studies between NASA and ESA of time transfer laser techniques using the LASSO instrumentation on SIRIO-II were abruptly terminated following the failure of the SIRIO-II launch vehicle.

In recognition of the importance of gravity and magnetic field models to geodynamics research, detailed planning for the GRM was accelerated in 1982 with the initiation of system definition studies at APL and the establishment of a GRM/SSG. Workshops were held on gravity field modeling (February 1982) and magnetic field modeling (May 1982). A single-axis cryogenic gravity gradiometer instrument was completed and tested. To guide future geopotential research and to maximize opportunities for refinement of field models at an early date, a Geopotential Research Program Plan (NASA, 1982d) was written to outline the necessary activities through the mid-1990's. This plan describes methods for the achievement of a factor of two or more improvement in field models; the preparation for, acquisition, and use of new data from the GRM; and refinement of field surveys beyond GRM using gravity gradiometry (Gravity Gradiometry Mission) and long-duration magnetic field monitoring (Magnetic Monitor Mission).

The NASA Geodynamics Program is conducted as a joint program with other federal agencies. This Federal Program For The Application of Space Technology to Crustal Dynamics and Earthquake Research was established by interagency agreement in 1980. In 1982 a federal plan for implementation of the joint program was completed by the Interagency Coordinating Committee for Geodynamics (ICCG) and approved by the Geodynamics Program Review Board (PRB), which is composed of signatories to the agreement, at its first meeting in July 1982. The Board also approved, in principle, a plan for the transfer of operational responsibility for mobile VLBI systems developed by NASA to NOAA/NGS. Under this plan (ICCG, 1981), NOAA will establish a National Crustal Motion Network (NCMN) incorporating many of the sites initiated by NASA, and will use mobile VLBI for long-term monitoring of its first-order geodetic control networks. Historically, definition of requirements for gravity field and positioning have been the responsibility of the Satellite Geodesy Applications Board (SGAB). At its June 1982 meeting, the SGAB approved a joint NASA/NOAA plan for development of gravity and magnetic field models, and reviewed progress in development of GPS geodetic receivers and spaceborne altimeter missions (Geosat and Topex). A special panel was established by the SGAB in 1980 to plan and coordinate interagency development of geodetic receivers. In November 1982 the GPS Panel agreed to proceed with plans for intercomparison of several technical GPS receiver designs in late 1983, using a baseline defined by the OVRO and Mojave VLBI stations in California.

D. PLANS FOR 1983

Considering the status of instrumentation developments for geodynamics research and the finalizing of interagency and international plans, 1983 is a pivotal year for the NASA program. The acquisition and analysis of data is expected to accelerate and discussions will be initiated on the requirements and capabilities for geodynamics research in the 1990's. An outline of the major planned activities follows:

1. In 1983, laser and VLBI data will be acquired at some 50 global sites by fixed stations and mobile systems. More than half of these observations will involve the TLRS and MV systems. These measurements are planned to support studies of regional deformation in the western U.S., North American plate stability, and the relative motions of the North American, Pacific, Australian, Nazca, South American, and Eurasian plates. Preparations will continue for initiation of regional deformation studies in Alaska in mid-1984 and for an extensive Pacific plate experiment involving VLBI observations from Alaska, Japan, the continental U.S., Hawaii, and Kwajalein.

2. The upgrade of MV-1 and 2 will be completed and the Mojave VLBI station will become operational. Plans for transfer of these systems, including MV-3, to NOAA/NGS will be finalized. NGS will begin operations with Mojave and MV-3 in January 1984, and with MV-1 and MV-2 in January 1985.

3. Fabrication of TLRS-3 and TLRS-4 will be initiated with expected availability in late 1984 and early 1985 respectively. Upgrade of the Moblas units 4, 5, and 6 will be completed. Lunar laser ranging will be resumed with the MLRS and initiated at Haleakala, Hawaii. The upgrading of the NLRS station will be completed and tested in early 1984.

4. Based on the funding restoration approved in January 1983, plans will be initiated for studies in the Caribbean Basin using GPS receivers and for regional deformation studies in western South America (scientific proposals from Peru and Bolivia were selected for approval in March 1983).

5. Participation in the MERIT and COTES observational campaigns will be initiated in September 1983 using fixed VLBI, satellite laser ranging, and lunar laser ranging stations; provision is being made for collocation of laser and VLBI systems at selected sites in the U.S.

6. The VLBI correlator at Caltech will be completed and redundant processing with the Haystack correlator will be used to verify data processing. A new correlator, to be be located at USNO, will be the primary correlator for use by the Crustal Dynamics Project. The new correlator will be initiated by NGS, NASA, NRL and USNO, and should be operational in early 1985.

7. Confirmation of the requirements for the GRM and the system studies will be completed; the GRM/SSG report was issued in February 1983.

8. As part of the 1982 activities, workshops were planned in early 1983 to identify scientific needs and technologies for geodynamics research in the 1990's. A geodynamics workshop was held at Airlie House, Warrenton, Virginia, in February 1983, and a Gravity Gradiometer Workshop was held at GSFC February 28 to March 2, 1983. The reports of these workshops will be completed in 1983 and used in the formulation of a long-range NASA Geodynamics Program plan.

III. CRUSTAL DYNAMICS PROJECT

A. MEASUREMENTS

Summaries of 1982 VLBI and SLR observations for tectonic plate motion, plate stability, and regional deformation are given in Tables 2 and 3. Two VLBI plate motion experiments were conducted in 1982, yielding a total of 28 individual measurements over six baselines between North America and Europe. Monthly SLR solutions between nine pairs of stations produced a total of 305 measurements over 41 baselines between the North American, Pacific, Australian, South American, and Eurasian plates (Figure III-1).

During 1982, the western U.S. regional deformation measurements were concentrated in California, with a few observations from stations in adjoining or nearby states (Figure III-2). Many of these regional measurements served a dual purpose in that validation and intercomparison of the VLBI and SLR techniques became a continuous process. Rather than scheduling separate observation sessions for validation and intercomparison, both types of systems are scheduled for simultaneous observations from certain selected stations during regularly scheduled measurement campaigns. It is anticipated that this procedure will continue for the remainder of the Project.

A ten-day regional deformation and systems intercomparison experiment was conducted during October 1982. An MV-3/2 hybrid configuration of the mobile VLBI system (MV-3 antenna with MV-2 electronics van) obtained 60 hours of data while collocated first with the SLR base station at Monument Peak, California, and then with the station at Quincy, California. The MV-3/2 and the MV-1 at JPL, working with the VLBI base stations at OVRO, Ft. Davis, and Goldstone, measured a total of 32 baselines in the western U.S.

The TLRS-1 visited Mt. Hopkins, Arizona; Vernal, Utah; Ft. Davis, Texas; and Owens Valley, California, producing 72 measurements of regional deformation baselines to and between SLR base stations in western North America.

B. VLBI SYSTEM DEVELOPMENT

During 1982 several observatory VLBI stations were upgraded, some new stations were added to the network, and the Haystack correlator facility at Westford, Massachusetts, was improved. Similarly, upgrade of the two mobile VLBI systems was continued and a new system, MV-3, was nearing completion (Figure III-3). Plans for the orderly transfer of mobile VLBI operations from NASA/JPL to NOAA/NGS were developed and coordinated by the two agencies. A formal Mobile VLBI Operations Transfer Agreement, which embodies the necessary actions to properly effect transfer, as well as a statement of operational principles and related future support commitments between NASA and NOAA, is expected to be signed in 1983.

Some of the significant VLBI system milestones in 1982 included:

1. A contract for the commercial production of three VLBI Mark-III Data Acquisition Terminals (DAT) was awarded, with delivery scheduled for June 1983. VLBI groups from the Federal Republic of Germany, Japan, and Italy have also ordered Mark-III DAT's from U.S. commercial sources, with several other countries expected to place orders in the near future.

2. A new dual S-X band receiver feed modification was developed and installed on the VLBI antennas at OVRO, Fort Davis, and Maryland Point, Maryland. This modification has improved the S-band system temperature an average of 30 degrees Kelvin.

3. A prototype cryogenically cooled field effect transistor and low noise amplifier package was developed and tested for NASA by the University of California at Berkeley. New low-noise amplifiers were installed on the Haystack Observatory antenna at Westford, Massachusetts, and a unit for the Mojave antenna at Goldstone, California, was delivered.

4. The MV-3 antenna system was completed and tested in time for the hybrid MV-2/3 to be used for the October 1982 measurement campaign. The system performed very well, with an exceptionally high yield of good data. The MV-3 electronics van is scheduled for completion in January 1983, and the entire MV-3 system is scheduled for its first operational use in February 1983.

5. Three new hydrogen masers were completed by APL and introduced into the CDP operational inventory. Operational use of water vapor radiometers (WVR's) began at several stations, but with less than satisfactory results. The CDP initiated an intensive WVR system review, and the required upgrade modifications will be made in order to have reliable WVR capability.

6. Two other VLBI R&D efforts made impressive progress in 1982. A high-density tape recorder development is under way at Haystack and JPL, with demonstration units expected by the spring of 1983. A VLBI holography technique for antenna dish surface remote measurement was demonstrated in tests on the Westford, Haystack, and Maryland Point antennas.

7. The implementation of several fixed VLBI stations was either completed or nearing completion by the end of 1982:

a. The Maryland Point station, constructed and operated by the U.S. Naval Research Laboratory, became operational in April 1982.

b. The Mojave station was well under way, with a new antenna drive system and building modifications nearing completion. First operations are expected in June 1983.

c. The Richmond, Florida, VLBI station was erected. This third station of the Polaris network is being built by NOAA, with first operations planned for September 1983.

d. The VLBI station at Wettzell, West Germany, being constructed by the Institute for Applied Geodesy in Frankfurt and the Max-Planck Institute for Radio Astronomy in Bonn, was nearing completion, with first turn-on expected in August 1983.

e. Development of the VLBI system at Kashima, Japan, being undertaken by the Japanese Radio Research Laboratories, was well under way.

8. The mobile VLBI systems MV-1 and MV-2 were nearing completion of their upgrading programs:

a. The MV-1 electronics van was in the final stages of completion, and full-up systems operation is planned for August 1983.

b. The MV-2 antenna was fitted with a Voyager dichroic reflector plate to provide dual S/X band capability, and calibration tests were conducted on the antenna range. Full operation of the MV-2 was scheduled for February 1983.

c. An Alaskan site reconnaissance trip was conducted, and five mobile VLBI sites were selected. These sites, and one still to be selected in the summer of 1983, will be prepared for a measurement campaign to be conducted in the summer of 1984.

9. Development of the Caltech/JPL correlator facility continued in 1982. Two-station capability should be demonstrated by mid-1983, with the full three-station capability expected by the end of the year.

C. LASER SYSTEM DEVELOPMENT

The Geodynamics Program laser network consists of several types of laser systems located throughout the world (Figure III-4). Sites in South America and Mexico are not yet constructed (except for the SAO observatory at Arequipa, Peru, and the Moblas station at Mazatlan, Mexico), but are planned to be completed within the next two years. The NASA laser operations have been continuously improving since their beginning, with the rms ranging precision being reduced from 70 cm in 1965 to less than 3 cm for the most recently upgraded systems. The tracking efficiency has increased from 12% in 1976 to over 55% during 1982.

The significant laser system milestones during 1982 included:

1. Upgrade of the Moblas system at Quincy, California, with a passively mode-locked Nd:YAG laser manufactured by Quantel International, was completed in October 1982. This new laser, with a pulse width of 200 picoseconds, is a significant improvement over the 7 nanosecond pulse width of the previous laser. The new laser has proven to be reliable for both daytime and nighttime tracking. The CDP plans to complete the upgrade of all eight Moblas systems over the next two years, with this new laser and newer-model components in the receiver subsystem. These new receiver components (photomultipliers, gating circuits, amplifiers, time interval units, and discriminators) are required to optimize performance of the narrower-pulse Quantel laser, to give a single-shot ranging precision of better than 1 cm rms. Three Quantel lasers were delivered to NASA in December 1982, and upgrade of Moblas-4 at GSFC was started at that time. The other two lasers are scheduled for installation in Moblas-5 at Yarragadee, Australia, and Moblas-6 at Mazatlan, Mexico, during the first six months of 1983.

2. Completion of the SAO laser system upgrade at Arequipa, Peru, in May 1982 improved overall system performance in accuracy, range noise, data yield, and reliability. With the narrower two-nanosecond pulse and a new analog pulse processing system, the systematic range errors have been reduced to 3-5 cm and range noise has been reduced to 5-15 cm on low satellites and 10-18 cm on Lageos. The pulse repetition rate has been increased to 30 pps, and considerable improvement has been made in signal-to-noise ratio by using a three-angstrom interference filter and by reducing the range gate window to 200-400 nsec. A second SAO system (formerly located at Natal, Brazil) was similarly upgraded at SAO during 1982, and has been shipped to Matera, Italy, for installation under a cooperative agreement between NASA and CNR/PSN. This agreement provided for NASA to upgrade this system and provide it to Italy on indefinite loan, and for CNR/PSN to install and operate the system, with SAO providing technical support and coordination. The system is scheduled to begin operations in June 1983. A third SAO system ended operations at Orroral Valley, Australia, in early 1982, due to the decision to upgrade the Natmap lunar laser ranging station with satellite laser ranging capability. This system will also be returned to SAO in Cambridge, Massachusetts, for upgrading and possible subsequent installation elsewhere.

3. Final integration of the TLRS-2 subsystems (Figure III-5) was completed in July 1982, and satellite tracking operations were successfully accomplished in July and August 1982. Collocation testing was carried out with Moblas-7 at

GSFC from September through November 1982, in which more than 60 tracking operations were completed. The system was declared operational and was deployed to its first field operation site on Easter Island at the end of December 1982. This second-generation TLRS employs modular construction, a low-power laser, and single-photon detection techniques to meet the rapid deployment high-precision tracking requirements of the CDP. It is packaged in shipping containers that are used as part of the system during tracking, and will fit in the cargo hold of normal commercial passenger jet aircraft for transportation. The system includes a passively mode-locked frequency-doubled Nd:YAG laser transmitter, a single-photoelectron receiver system, a 100 psec resolution multistop range measurement system, a 32K DEC LSI 11/23 computer for system control and data handling, a 25 cm aperture refracting optical system mounted in an azimuth-elevation tracking mount, and a cesium beam oscillator with WWV and GPS receiver epoch time system.

4. Construction of the McDonald Laser Ranging System (MLRS, Figure III-6), built and operated by the University of Texas at Austin for NASA, was completed in early 1982. This is a dual-purpose facility for laser ranging both to man-made satellite and to the Moon. The system is designed around a 76 cm telescope assembly, with a 532 nanometer wavelength laser. MLRS operations are very similar to those of TLRS-1, which was also built and operated for NASA by the University of Texas at Austin, in that it employs single-photoelectron ranging, performs internal calibration, and has an almost identical timing system. The satellite ranging laser is a Quantel YG400 doubled neodymium type that outputs a single mode-locked 0.3 mjoule pulse of 100 psec length, at 10 pps. The lunar laser is a Quantel YG442P doubled neodymium type, which shares much of the control electronics and cooler with the satellite laser. The lunar system outputs a 3 nsec (FWHP) 400 mjoule pulse, also at 10 pps. MLRS established Lageos ranging capability in the spring, and underwent collocation tests with TLRS-1 in late summer and early fall 1982. Having obtained adequate data by October 1982, collocation was ended in time for TLRS-1 to participate in the October 1982 VLBI campaign. TLRS-1 had been scheduled for intercomparison measurements at OVRO and Vandenberg AFB in California during this experiment.

In early 1983 some discrepancies were found in the MLRS data processing procedures. This problem required that all MLRS data obtained from the beginning of collocation through February 1983 be reprocessed and re-analyzed. At the date of this report, the reprocessed data, which now appears to be of high quality, has not yet been released to the DIS for distribution to investigators. The CDP must decide if it will be necessary to perform another collocation with TLRS-1; in the meantime, implementation tests and acceptance of lunar laser capability has been delayed due to the higher priority placed on satellite laser ranging at McDonald in order to meet CDP objectives. However, with the MERIT campaign due to start in September 1983 and the importance of lunar laser ranging to that project and to the CDP, higher priority has been given to achieving lunar laser ranging capability at MLRS during the optimum lunar observing periods.

5. The LURE Observatory at Haleakala, Maui, Hawaii, built and operated for NASA by the University of Hawaii, completed six months of satellite laser ranging collocation testing with Moblas-1 in January 1982. After the observatory was severely damaged by a storm in early 1980, complete refurbishment of the installation was started in June 1980. The GTE Sylvania laser is a frequency-doubled ND:YAG type operating at 3 pps, with each 200-500 psec pulse providing

250-350 mjoule at 532 nanometers wavelength. The laser is coupled into a 40 cm aperture refractor telescope which expands and collimates the laser pulses and directs them to a 68 cm flat coelostat mirror, the Lunastat. The Lunastat, which is also used as a transceiver for satellite laser ranging, is positioned so that the laser beam is directed by a computer-controlled absolute pointing system. New gated constant-fraction discriminators and a photomultiplier receive package were installed. The computer is a DEC LSI 11/23 microprocessor with 160K RAM and 10 Mbyte hard disc storage. The round trip time of the laser pulse is measured by an HP 5370A time interval unit with a resolution of 10 psec, and epoch time is provided by a cesium beam standard with Loran-C reference. The original lunar laser ranging receiver used the Lurescope, a multilensed telescope designed to collect the laser return through eighty 19-cm achromatic lenses and route it to a common focus where it was detected by a photomultiplier tube. A photon counting system has been built to be used for evaluating the Lurescope efficiency. The Lurescope was first driven by the new control system in April 1982, and the software to track stars, model the mount, and evaluate the Lurescope efficiency has been developed and tested. However, the software and the completely separate time interval measurement subsystems for lunar laser ranging are still under development. Various techniques for equalizing the four distinct optical path lengths within the Lurescope are being evaluated. Lunar laser ranging capability at Haleakala is expected to be available in time to participate in the MERIT campaign which will begin in September 1983.

6. In April 1982 NASA entered into a joint venture with the Australian National Mapping Division (Natmap) to refurbish the lunar laser ranging observatory at Orroral Valley so that this observatory would be able to range with high accuracy to both man-made satellites and to the Moon. Natmap is responsible for the design, fabrication, integration, and operation of the new system (NLRS), while NASA is funding the purchase of new equipment and modification of major subsystems such as the telescope, laser, receiver, and control.

In June 1982 the 60" telescope mount at Orroral Valley was shipped to Contraves Goerz in Pittsburgh, Pennsylvania, for reconfiguration from equatorial to X-Y (alt-alt) type, addition of a Coude path capability to replace the Nysquith optics of the old telescope, and for inclusion of high-precision guiding and pointing. The new telescope will be driven by a pair of torque motors on each axis, controlled by computer to give a pointing precision of three arc-seconds. The laser is a Quantel International model YG402DP/AP, a frequency-doubled Nd:YAG type with 532 nmeter output wavelength, pulsed at up to 10 pps. Its average power is one watt in single pulse mode, with 300 psec pulse width, or 3.3 watts in mode-locked comb mode with 7-9 250-psec pulses transmitted over a 7-nsec spacing. The higher-power mode is intended for lunar laser ranging. Coude optics have been adopted so that the laser will remain in a fixed position. The receiver, a replica of the MLRS receiver, is being built by the University of Texas at Austin, and an HPA-700 computer with 1 Mbyte of main memory and 65 Mbyte disc storage will provide telescope pointing and laser transmit/receive control, as well as all types of real-time data handling. The system timing will have 50 psec resolution, capable of recording eight pulses over a dynamic range of 100 nsec, or single pulses with 78 psec resolution over 1 msec. The NLRS is scheduled to be fully operational with both lunar and satellite laser ranging by spring 1984, and is expected to contribute significantly to the MERIT campaign.

D. DATA BASE

The CDP Data Information System (DIS) provides for cataloging all Project-acquired data from 1974-1982 as well as new data to be acquired during the lifetime of the Project through 1988 (NASA, 1981a). The main objective of the DIS is to provide Project-funded investigators with the necessary scientific data for their studies toward the advancement of the understanding of Earth dynamics, tectonophysics, and earthquake mechanisms. The DIS includes a large selection of pre-processed laser and VLBI data acquired at fixed and mobile stations. In addition, analyzed data products are made available from the laser and VLBI observations, such as baselines, station position coordinates, polar motion data, length-of-day data, and other related ancillary data products. The information is stored in a Crustal Dynamics Data Bank and is directly accessible by the DIS via a menu-driven user language. The DIS uses a data base management system to enable the users to query, access, and cross-reference the information.

After the completion of conceptual design phase of the DIS in July 1981, the detailed design of the data base was followed by system implementation. Shared utilization of a VAX 11/780 computer at GSFC enabled a rapid implementation of the system. Pilot operation for outside users through dial-up telephone lines was started in May 1982, and the system became fully operational in September 1982. A User's Guide for the DIS, published in October 1982 (NASA, 1982c), gives many examples of typical queries in the DIS and to its Data Bank.

E. CRUSTAL DYNAMICS SCIENCE WORKING GROUP MEETINGS

The Principal Investigators met twice during 1982, at the Spring and Fall Crustal Dynamics Science Working Group meetings at Goddard Space Flight Center. At each of these meetings, Crustal Dynamics Project personnel and the investigators exchanged views about the observing program and observing strategies, and the investigators presented their most recent scientific results.

IV. SCIENTIFIC RESULTS: FIFTH ANNUAL NASA GEODYNAMICS CONFERENCE

The Fifth Annual NASA Geodynamics Conference, held January 24-28, 1983, in Washington, DC, was attended by over 200 participants from eleven countries. The Conference consisted of presentations of research results by the program investigators and a panel discussion in which the future of space geodynamics was discussed. This was followed by reviews of the status and plans of the NASA Crustal Dynamics Project. Abstracts of papers presented at the Conference (NASA, 1983a) are included in this report (Appendix 4). The following is a summary of the significant scientific results discussed at the conference,

A. CRUSTAL DYNAMICS

Plate Motion and Deformation

B. Tapley (University of Texas), and D. Smith and D. Christodoulidis (GSFC), reported on results of plate motion determined from Lageos laser ranging. Although the present accuracies are not quite adequate to resolve plate motions, Smith and Christodoulidis reported baseline length changes differing from zero by more than one standard deviation - Hawaii to the Australian stations at Yaragadee and Orroral Valley, where the measurements of baseline length change are -7 ± 3 cm/year. The Minster-Jordan model predicts about -6 cm/year. Improvements in data reduction procedures are currently being implemented, and these should lower the uncertainties by about 30%.

Sovers (JPL) reported on intercontinental VLBI measurements using DSN stations in California, Spain, and Australia. The change in the Goldstone-Tidbinbilla baseline is estimated at -9 ± 3 cm/year, and the change in the Goldstone-Madrid baseline is estimated at $+11 \pm 3$ cm/year, rates which are several times those predicted by the Minster-Jordan model. J. Ryan (GSFC) reported on repeated VLBI measurements between Westford, Massachusetts, and Fort Davis, Texas, which have a scatter about the mean of about 2 cm rms. The same data set was analyzed by NGS, and the NGS baseline lengths differed from those estimated by GSFC by 2.5 cm (rms); this demonstrates the present level where subjective decisions during the analysis procedure become significant.

A number of authors reported the results of supporting theoretical and observational studies which do not make use of space-acquired data. Reilinger and his colleagues at Cornell have used ground-based leveling to provide upper bounds on the rates of intracontinental deformation, which will serve as guidelines for determining the precision required to monitor intracontinental deformation using space measurements. Long-term and long-range tilts are less than about one part in 10^7 in the eastern United States, and about twice that in the western United States. Bergman and Solomon (MIT) studied seismicity data from the Indian Ocean to determine whether stress provinces (well-defined regions of uniform orientation of principal intraplate stresses) exist in oceanic as well as continental plates. Among their results are indications that tend to confirm that the Ninetyeast Ridge may represent a boundary between separate Indian and Australian plates, with the relative motion between these plates diminishing toward the south.

Lowman (GSFC), with colleagues from UCSB and the University of Utah, has been studying the tectonics of the Basin and Range Province. Results to date indicate that present seismic activity may be largely due to listric faulting; several unmapped faults in the southwestern Mojave Desert suggest a southward bending of the central Mojave shear system. R. Smith (Utah) used a new compilation of historical seismicity, and slip rate determinations on late Cenozoic faults, to calculate present and Quaternary moment rates for the southwestern United States. These rates apply to deformation due only to earthquakes, not aseismic creep. The present strain rate in the Basin and Range is not uniform, and occurs at rates corresponding to maximum extension of about 4 mm/year, with the principal deformation in the central Nevada seismic zone and the southern intermountain seismic belt (Figure IV-1). The Quaternary deformation rates are remarkably similar. New seismic reflection profiles have revealed at least three reflections in the upper and intermediate crust that are probably low-angle detachments; normal slip on these detachments may have accomodated much of the east-west extension during the Cenozoic. The uppermost detachment occurs at the top of a previously known low-velocity layer in the crust, where 80% of earthquake foci occur. Smith has made a model for deformation in this area involving present extension above an extending and plastically deforming lower crust in the Basin and Range, with intraplate shear coupling across southern California into the Basin and Range.

S. Daly (MIT) and A. Raefsky (JPL) have studied how diapirs penetrate overlying material, attempting to answer the question of whether the rise of the diapir occurs at a sufficiently rapid rate to prevent the associated magma from cooling and solidifying. Results to date indicate that other parameters (such as shape) and other mechanisms such as preheating, must be included.

Regional Crustal Deformation

The first results of measurements with mobile VLBI, mobile laser ranging, and SERIES were presented by research groups from JPL and the University of Texas. The SERIES experiments were over short baselines, and show scatter of 4-8 cm rms in horizontal and vertical position and 6 cm rms in baseline length. No tropospheric or ionospheric corrections have yet been made. Mobile VLBI measurements of baseline lengths in California differ show zero changes in length, with estimated standard errors of 2-4 cm/year; one problem in analysis of data through 1981 appears to be errors in the BIH Earth orientation parameters used. The Texas group analyzed TLRS horizontal ranging data taken over the Los Angeles Basin from Mount Wilson, and showed that shear strain rates may be estimated to a few parts in 10^7, without corrections for atmospheric conditions, using the line ratio method.

Ground-based geodetic surveying data were interpreted by Cline and his coworkers (NGS), who modeled four regions of southern California (Los Angeles, San Diego, San Bernardino, and the Channel Islands) by a combination of secular strain and fault slip in large earthquakes. The observed deformation is consistent with right lateral motion in the San Bernardino region, left lateral motion through the Transverse Ranges, and the expected motion on the Malibu and Newport-Inglewood faults. No motion was found between JPL and Pearblossom, on opposite sides of the San Andreas Fault. Fault movements in southern California were studied by Slade and his coworkers (JPL), who used three-dimensional

finite element modeling to calculate displacement fields due to the 1979 Imperial Valley earthquake. These fields are in agreement with some geodetic data in the area, but disagree with other data; the authors suggest that the latter contain substantial aseismic deformation.

Theoretical and numerical studies of fault mechanism are being done by Cohen (GSFC) and Lyzenga and Raefsky (JPL). Cohen is continuing to study the effect of viscoelastic lithosphere/asthenosphere structure on temporal and spatial dependence of deformation due to earthquakes. Lyzenga and Raefsky are seeking to determine what physical conditions are necessary in order to reproduce earthquake sequences with a given distribution of recurrence intervals.

Caputo and colleagues (Texas A&M) studied the relation between gravity anomalies and seismicity in central Italy, and found that the highest level of seismicity is found where the gradient of gravity anomalies is greatest and where the largest load-generated shear stress is found.

J. Beavan and a group from LDGO have been measuring tilt in the Shumagin Islands seismic gap using leveling data since 1972. Until 1978 tilt was as expected for strain accumulation on this locked plate boundary, but the tilt reversed direction and doubled in magnitude in 1978, at the same time that the yearly seismic energy release increased by a factor of six. In 1980 the tilt returned to its pre-1978 level. The authors interpret this phenomenon as an episode of aseismic slip beneath the Shumagin Islands, resulting in stress concentration on the locked boundary.

B. EARTH DYNAMICS

Polar Motion, Earth Rotation, and Solid Earth Tides

Plate motion and crustal deformation occur at rates so small that at present not many results are available, given the accuracies of the measurement systems in use. However, information on Earth orientation (length of day and position of the instantaneous pole of rotation) is regularly obtained by both laser ranging and VLBI. Consequently, the state of analysis of space-acquired polar motion and Earth rotation data is far advanced compared to that of plate motion and deformation. The results of three types of measurements of polar motion and Earth rotation were discussed at the Conference: satellite laser ranging, lunar laser ranging, and VLBI.

Atmospheric Angular Momentum. An area receiving major attention at present is the relationship between mass movements in the atmosphere and Earth rotation. Five different groups (GSFC, JPL, AER, MIT, and Princeton University) reported on studies of this correlation. Rosen (AER) studied the seasonal variations in atmospheric angular momentum for the northern and southern hemispheres separately, and showed that the annual July-August speeding up of the earth results from annual changes in the relative atmospheric angular momentum in the two hemispheres (Figure IV-2). It now seems clear that at periods less than one year, almost all the variations in length of day can be explained on the basis of changes in atmospheric angular momentum, and one of the principal scientific uses of observed fluctuations in Earth rotation may well lie in the field of atmospheric sciences. The length of data available is not adequate to study longer periods, although T. M. Eubanks of the JPL group noted a slow divergence

of length of day with respect to atmospheric angular momentum that may be due to exchange of angular momentum between the core and mantle of the Earth. [It was also reported at the conference that R. Hide of the Meteorological Office in Great Britain has a paper in press in the Proceedings of the Royal Society of London showing that a very large fraction of the polar motion in a twenty-month segment of BIH data can be explained on the basis of changes in atmospheric angular momentum.]

S. Dickman (SUNY Binghamton) reported on results of studies of the solid Earth and oceans as a coupled two-body system; these modeling studies are able to predict wobble modes similar in frequency, sense of rotation, and ellipticity to the Chandler and Markowitz wobbles. It appears that studies of polar motion must take into account interaction with the ocean as well as with the atmosphere.

Lunar Laser Ranging. This method continues to be hampered by there being only one operational lunar laser ranging observatory - McDonald Observatory of the University of Texas. All the lunar laser ranging results are for McDonald data, although sporadic returns have been obtained from the LURE Observatory at Haleakala, Hawaii, the Lunar Laser Ranging Observatory at Orroral Valley, Australia, the IfAG observatory at Wettzell, West Germany, the GRGS observatory at Grasse, France, and the Crimean Astrophysical Observatory.

Improved results for several geophysical parameters have been obtained from lunar laser ranging data by scientists at JPL, the most important of which is a new determination of the secular acceleration of the Moon (-25.2 ± 1.2 arcseconds per century per century) and the correction to Wahr's amplitude of the 18.6 year obliquity nutation (7 ± 6 milliarcseconds). The JPL group continues to improve the lunar ephemeris and libration models, and have included improved polar motion corrections along the meridian of McDonald Observatory, and relativistic effects. With these improvements, the weighted rms lunar ranging residual is now 18.7 cm over the thirteen years since McDonald observations began, a reduction of 15% compared to the previous solution.

Comparisons Between Different Data Types. Comparisons were presented between results on polar motion and Earth rotation from lunar laser ranging, satellite laser ranging, doppler, connected-element interferometry, VLBI, and the BIH values; results using the different data types are generally in good agreement. Babcock and McCarthy of USNO discussed comparisons made by USNO, and plans for publication of polar motion and Earth rotation measurements based on USNO observations. Capitaine and Feissel (BIH) and Zhu and Mueller (OSU) discussed the effect of introducing the 1980 IAU nutation theory. Ye Shu-Hua of Shanghai Observatory reported on a comparison of data types in which systematic differences were found between BIH data and independent Chinese measurements in the period 1972-1982. Dickey and Williams (JPL) showed that lunar laser ranging values of UT1 agree closely with BIH values for 1980 (Figure IV-3).

Earth and Ocean Tides. Hsu and Mao of the Chinese Academy of Sciences reported on improvements of tidal loading models using realistic structural parameters for the lithosphere and upper mantle. The University of Texas group discussed the application of ocean tide models to computation of satellite orbits, finding that different numerical models differ in their effect on the Lageos orbit only at the level of the Lageos residuals. Dunn and Torrence of

EG&G discussed the corrections to ocean tidal models due to adopting Wahr's Earth tide model.

Geophysical Aspects. Chao (GSFC) discussed the result of high-resolution spectral analysis of ILS polar motion data; he found that the ILS data are consistent with a Chandlerian polar motion having four spectral components. Pavlis and Mueller (OSU) discussed the effect of errors in Earth orientation on baseline measurements, pointing out that the present accuracy of Earth rotation data is inadequate to achieve centimeter-level baseline measurements. Pavlis and Mueller also proposed a method of 'simultaneous range differences' for satellite laser ranging, which on the basis of numerical simulations may be capable of significant reduction of rms errors compared to satellite laser ranging procedures now in use.

C. GEOPOTENTIAL FIELDS

Magnetic Field Modeling

Three papers were presented on magnetic field development and modeling. Langel (GSFC) has overcome numerical instabilities inherent in the equivalent magnetization modeling approach by using principal component analysis. A POGO magnetic anomaly map, reduced to pole, was presented; the equivalent map for Magsat data is in preparation. Langel's group also discussed models of the external field, which are important for determining crustal magnetic anomalies. Risbo (Copenhagen) discussed extrapolation of Magsat data to the core-mantle boundary; he found that magnetic flux enters and leaves the core in a few high-intensity regions which have a pronounced westward drift.

Gravity Field Modeling

One general gravity model and several specialized models were described. Lerch (GSFC) discussed the most recent Goddard Earth Model, GEM-L2, which was developed solely from orbital tracking observations and represents a twofold improvement over previous models for the long-wavelength geoid; the field up to degree and order four now has an accuracy of eight cm in geoid height (Figure IV-4). Baselines observed by Lageos laser ranging should be improved significantly, since the estimated orbital recovery for Lageos is now about 30 cm. Rapp (OSU) continues to improve his set of one-degree area mean gravity data, which has been augmented by about 5% compared to the 1979 gravity data collection. J. Marsh (GSFC) showed results of Starlette laser tracking, including a set of low-degree ocean tidal terms that are in good agreement with tidal constituents estimated from oceanographic sources. Frey and Klosko (GSFC) described a gravity model based on crustal gravity anomalies and upward-continued to satellite altitudes for comparison with the magnetic field observations of Magsat.

Geopotential Field Interpretation

Satellite observations of the gravity and magnetic field put important constraints on models of the solid Earth. Two topics received particular attention in this session: constraints on the effective viscosity of the mantle, from Lageos observations; and thermomechanical models of the lithosphere and

upper mantle, derived from Seasat altimetry. A highlight of the meeting was the discussion of possible changes in the Earth's gravity field. Rubincam (GSFC) and Yoder and his co-workers (JPL) presented interpretations of the observed acceleration of the node of the Lageos orbit, and both groups found that the observations are consistent with a time rate of change of the J_2 gravity field coefficient of about 3×10^{-11} year^{-1}. Figure IV-5, from Rubincam, shows the evidence for a change in J_2 in the nonlinear change of the Lageos node with time. Peltier and Wu (Toronto) used a new model of the solid Earth's viscoelastic response to deglaciation to predict a value of dJ_2/dt of -3.5×10^{-11} per year, in good agreement with the observations. The major glaciation involved is that in North America, the effect of which is seen in Figure IV-6 (also from Rubincam), a geoid referred to a hydrostatic reference figure.

Hager (Caltech) found a significant correlation between geoid undulations and density anomalies in subducting slabs for degrees four through nine of the gravity field; he pointed out that the dynamic response of the Earth governs the way that internal density distribution affects the geoid, and was able to estimate the average value of this dynamic response using the correlation noted above. Hager concluded that this average value was consistent either with whole-mantle convection or with strong dynamic coupling across the 670-km discontinuity.

Several groups reported on studies of the structure of the oceanic lithosphere using altimetric geoid measurements. B. Marsh and J. Hinojosa (JHU) found the expected east-west age banding in the Pacific from two-dimensional spectral analysis of the altimetry data, but found that intermediate-wavelength anomalies due to hot spots could not be resolved at present. Watts and Ribe (LDGO) reported on their continuing studies of seamounts; they found that the regional compensation of a seamount is a function of the age and thickness of the mechanical lithosphere at the time of emplacement of the seamount. Angevine and Turcotte (Cornell) are constraining models of isostatic compensation using the correlation between the altimetric geoid and bathymetry; they concluded that a layer of mantle material of anomalously low density underlies the Agulhas Plateau. McAdoo's group at GSFC also used Seasat altimetry data to study the correlation between bathymetry and geoid undulations, confirming earlier suggestions that the outer rise and slope topography seaward of deep ocean trenches is uncompensated (Figure IV-7). These results confirm that the effective elastic thickness of the lithosphere increases with age. Parsons and Daly (MIT) have found integral relations between bathymetry or geoid undulations and the temperature structure produced by mantle convection, and predict that the temperature variations in the neighborhood of the upper thermal boundary layer contribute strongly both to the geoid and to topography, which is consistent with the observed depth and geoid anomalies over mid-ocean swells.

Ihnen and Whitcomb (CIRES) studied the gravity low in the northern Indian Ocean, and constructed a model which fits the observed free-air gravity anomalies and geoid height; the model involves a large region of crust which is not isostatically compensated, which is consistent both with a downgoing arm of a convection cell and the presence of a 'wake' left behind India as it moved northward toward Asia.

D. GENERAL DISCUSSION

A panel discussion was held to bring out comments on what the most significant scientific results reported during the conference were, and on what the program trend should be in the future. It was agreed that the highlights of the meeting were the correlation of polar motion and Earth rotation results with atmospheric dynamics, and the detection and theoretical prediction of a change in the J_2 component of the gravity field. The latter result is particularly important for understanding mantle rheology, but better gravity measurements over the continents are required to make the necessary measurements of changes in higher-order harmonics of the gravity field. The combined interpretation of gravity, altimetry, and bathymetry data is producing impressive results in studies of the marine lithosphere. One of the most important aspects of the meeting was the extensive interaction between geodesists and other Earth scientists, demonstrating that the Geodynamics Program is an integrated Earth sciences program.

It is clear that sub-decimenter accuracies are now being routinely achieved in measurement of baseline lengths, and the next few years should see marked improvement in accuracy and the beginning of scientifically useful results from the crustal deformation measurements. It was pointed out that a 6-8 year project is not a sound approach to understanding Earth dynamics through space measurements of polar motion, Earth rotation, plate motion, and crustal deformation, partly because the crustal movements are probably episodic, and also because long-period effects (such as the solar cycle) cannot be understood on the basis of what a brief project can accomplish. It was recommended that a long-range program to develop, continue, and extend the present activities of the Geodynamics Program be established well before the termination of the Crustal Dynamics Project, with proper attention to the development of methods for making space-related position measurements on the ocean floor.

V. ADVANCED STUDIES AND MISSIONS

The activities in this program area are encompassed in two main subdivisions: gravity and magnetic field measuring systems, and the utilization of GPS for regional crustal deformation measurements.

A. GRAVITY AND MAGNETIC FIELD MEASUREMENTS

The major effort in this area has been the continuing design studies and simulations in support of initiation of the GRM (Figure V-1). Satellite-to-satellite tracking during the GRM between two drag-free satellites at 160 km altitude separated by 300 km will measure accelerations caused by gravity anomalies. One satellite will be equipped with magnetometers similar to those flown on Magsat. The goal for GRM is to produce gravity and magnetic field maps with an accuracy of one mgal and one nT respectively, and a horizontal resolution of 100 km. In order to do this for the gravity field, relative velocity must be measured with an accuracy of about one micron per second with four-second averaging times. The results of engineering tests with a laboratory breadboard system, coupled with detailed guidance and control system simulations, indicate that 0.15 micron per second measurements can be achieved with

four-second averaging times. For one-second averaging times, 0.25 micron per second values could be obtained. This would imply that gravity information with 50 km and 25 km resolution could also be obtained by GRM, but with a degraded accuracy.

The development of the single-axis cryogenic gravity gradiometer has been completed and a laboratory unit has undergone initial testing. This instrument is a candidate for a post-GRM gravity field mapping mission.

Initial tests on the gravity gradiometer were carried out using several vibration-isolation and common-mode rejection techniques to achieve successful operation of the device in a laboratory cryostat. The noise spectrum observed in the recent cooldowns corresponded to 0.3 E $Hz^{-1/2}$ in the 6-7 Hz frequency range, and 1-2 E $Hz^{-1/2}$ below one Hz; the noise was mainly seismic in origin. Coupling mechanisms of the seismic noise through various mechanical modes of the suspension system are under investigation. With a sufficiently high degree of common-mode rejection, a SQUID-limited sensitivity of 0.07 E $Hz^{-1/2}$ is expected for the present design.

This superconducting gravity gradiometer has been used as a null detector in a new test for the gravitational inverse square law. The tensor characteristic of the gravitational field produced by a 1.6 ton pendulum was examined to obtain an experimental limit for the inverse square law at a range of one meter.

A three-axis unit of slightly increased dimension is under consideration. In the meantime, the prototype single axis instrument will be further evaluated and improved. The current plan is to make some modifications in the design of the unit and to fabricate and test the new single-axis unit before proceeding to the three-axis version.

A second type of cryogenic gravity gradiometer is in the conceptual design phase. This gradiometer relies on a new type of accelerometer for gravity gradiometry, and uses a superconducting microwave cavity-controlled oscillator (SCO) as the displacement sensor. Unlike other accelerometers being proposed or developed, which convert displacements into frequency changes, SCOs have achieved fractional frequency stabilities of better than 10^{-15}, which translates into a dimensional stability of 3×10^{-15} cm. Also being studied is a practical SCO accelerometer design using a mass-spring accelerometer as one wall of the superconducting microwave cavity. A detailed error analysis shows that this device, when used in a gravity gradiometer, would have a sensitivity of 10^{-4} to 10^{-5} E for averaging times of 1-1000 seconds, and would have fewer dynamic range limiting problems than voltage-based devices.

Plans for utilizing the tethered satellite system were initiated. Three investigators were selected under the 1982 Geodynamics Notice, with their tasks to begin in 1983.

B. GLOBAL POSITIONING SYSTEM UTILIZATION

With the advent of the GPS, geodesists recognized the importance of this system to positioning and surveying. At least three independent efforts are under way to test whether and under what circumstances this system can be used

to obtain measurements with the requisite accuracy for measurements of crustal motion over reasonable time spans (i.e., baselines with accuracies of the order of 5 cm or better).

The first of these, being sponsored by DMA, NGS, and USGS, is called GEOSTAR (GEOdetic navSTAR). It makes use of an advanced single-channel digital receiver capable of tracking four GPS satellites simultaneously in P-code for both the L1 and L2 frequencies or in C/A code. The other two systems are SERIES (Satellite Emission Range Inferred Earth Surveying), which is being developed by NASA, and MITES (Miniature Interferometric Terminals for Earth Surveying), which is being developed jointly by NASA and USGS.

The SERIES receivers are fundamentally codeless spectral compressors, by means of which the spread spectra modulations of several NAVSTAR satellites can be simultaneously received at L-band and compressed by seven orders of magnitude into audio or sub-audio frequency range. A computer extracts the frequency and phase of the signal from each satellite in view. The data processing proceeds by a combination of Doppler positioning and phase ranging to such levels of precision as may be required, even to the millimeter level, by using the L-band carriers. The possibility of exploiting this high precision as to achieve high accuracy in baseline length measurements remains substantially a problem of the calibration of the system for instrumental, ionospheric, and tropospheric delay effects. Because the SERIES devices are pseudo-ranging receivers, it is possible for a single receiver to measure the ionsophere along each line of sight and to perform point positioning, given the satellite ephemerides.

Several tests were run to assess the precision and accuracy being obtained with the SERIES system. For nine experiments concluded over a one-month interval in 1982, each lasting over 1.5 hours, the scatter in the measurement of a 150-meter baseline was 3-5 cm, a result consistent with that calculated from the signal-to-noise ratio estimates. A very similar level of precision was obtained for nine experiments over a 21-km baseline at Goldstone. The mean of the 21-km baseline length determinations for SERIES was compared to a composite of VLBI and conventional survey measurements. The differences were 2 cm in baseline length, 13 cm in the east-west component, 3 cm in the N-S component and 15 cm in the vertical component. Preliminary results have also been obtained for several measurements over a 171-km line between JPL and Goldstone. Several experiments were performed, and the results of nine of these have been examined so far. Six out of these nine experiments yielded the following rms scatter (no tropospheric or ionospheric correction):

X-component:	4 cm scatter
Y-component:	5 cm
Z-component:	8 cm
Length:	6 cm.

These results show that the SERIES stations are operating near the signal-to-noise limit. Future work will be directed toward improving the signal-to-noise ratio, and further comparison with other measuring systems.

Experimental results have also been obtained using the MITES system terminals. These terminals are designed to utilize the 19-cm wavelength signal

broadcast by the GPS system. Over the past ten months these systems have undergone field testing, and show good results. An accuracy of one ppm for each component of the baseline vector has been achieved for lines ranging up to 61 km in length. With the introduction of dual-frequency reception and the consequent elimination of first-order ionospheric refractive effects, accuracies of 0.2 ppm are foreseen. This level of accuracy should make the portable interferometers very useful for local and regional crustal motion monitoring. Plans are being made to compare the results obtained by the different systems over the same baseline. These comparison tests are being planned for late 1983.

TABLE 1

Geodynamics Program Funding

(in millions)

	FY 1981	FY 1982	FY 1983	FY 1984*
Crustal Dynamics	23.3	21.4	23.8	26.7
Earth Dynamics	1.2	0.6	0.8	1.0
Geopotential Research	2.6	1.7	2.5	2.2
Total	27.1	23.7	27.1	29.9

* Planned

TABLE 2

VLBI Observations in 1982

Plate Motion

North America - Europe — 28 measurements, 6 baselines

Plate Stability

North America — 31 measurements, 10 baselines

Regional Deformation

From:	To: OVRO	DSS-13	Ft. Davis	JPL
Monument Peak	2	2	2	1
Quincy	2	2	2	1
JPL	2	2	2	-
OVRO	-	4	4	2
DSS-13	4	-	4	2

TABLE 3

SLR Observations for 1982

Plate Motion

North America - Eurasia	63 measurements,	11 baselines
North America - Pacific	76	8
North America - Australia	41	4
North America - South America	29	4
Pacific - Eurasia	33	6
Pacific - Australia	22	2
Pacific - South America	15	2
Australia - Eurasia	18	8
Australia - South America	8	1

Plate Stability

North America	51 measurements,	6 baselines
Pacific	11	1
Eurasia	6	1

Regional Deformation

From:	To: Quincy	Platteville	Ft. Davis	Monument Peak
Mt. Hopkins	3	3	-	2
Vernal	2	2	1	2
OVRO	2	2	2	2
Monument Peak	11	10	6	-
Quincy	-	11	6	11
Platteville	11	-	5	10

APPENDIX 1

GLOSSARY OF ACRONYMS AND ABBREVIATIONS

AER	Atmospheric and Environmental Research, Inc.
ALRS	Airborne Laser Ranging System
AO	Announcement of Opportunity
APL	Applied Physics Laboratory, Johns Hopkins University
BIH	Bureau International de l'Heure
CDP	Crustal Dynamics Project
CEI	Connected-Element Interferometry
CIRES	Cooperative Institute for Research in Environmental Sciences (University of Colorado)
CIT	California Institute of Technology
CNES	Centre National d'Etudes Spatiales (France)
CNR	Consiglio Nazionale delle Recerche (Italy)
Cospar	Committee on Space Research
COTES	Conventional Terrestrial Reference System
CSTG	Commission for International Coordination of Space Techniques for Geodesy and Geodynamics (IAG/Cospar)
DAT	Data Acquisition Terminal
DIS	Data Information System
DISCOS	Disturbance Compensation System
DMA	Defense Mapping Agency
DOC	Department of Commerce
DOD	Department of Defense
DSN	Deep Space Network
DSS	Deep Space Station
E	Eötvös Unit
EG&G	Edgerton, Germeshausen, and Greer, Inc.
ESA	European Space Agency
FY	Fiscal Year
GEM	Goddard Earth Model
GEODYN	Goddard Computer Program for Geodynamics and Orbital Computations
GEOS	Geodynamic Experimental Ocean Satellite
GEOSAT	DoD Altimeter Satellite
GEOSTAR	Geodetic Navstar
GGM	Gravity Gradiometer Mission
GN	Geodynamics Notice
GPS	Global Positioning System
GRGS	Groupe de Recherches de Geodesie Spatielle
GRM	Geopotential Research Mission
GRP	Geopotential Research Program
GSFC	Goddard Space Flight Center
GUWG	GRM User Working Group
HO	Haystack Observatory
HRAS	Harvard Radio Astronomy Station
IAG	International Association of Geodesy
IAGA	International Association of Geomagnetism and Aeronomy
IAU	International Astronomical Union
ICCG	Interagency Coordinating Committee for the Application of Space Technology to Geodynamics
ICL	Inter-Union Commission on the Lithosphere

ICSU	International Council of Scientific Unions
IfAG	Institut fur Angewandte Geodasie (Frankfurt)
IGRF	International Geomagnetic Reference Field
ILP	International Lithosphere Program
ILS	International Latitude Service
IUGG	International Union of Geodesy and Geophysics
IUGS	International Union of Geological Sciences
JHD	Japanese Hydrographic Department
JHU	Johns Hopkins University
JPL	Jet Propulsion Laboratory
Lageos	Laser Geodynamics Satellite
LASSO	Laser Synchronization (of atomic clocks) from Stationary Orbit
LDGO	Lamont-Doherty Geological Observatory (Columbia University)
LLR	Lunar Laser Ranging
LURE	Lunar Ranging Experiment
Magsat	Magnetic Field Satellite
Mark-III	Advanced VLBI Data System
MERIT	Monitoring Earth Rotation and Intercomparison of Techniques
mgal	Milligal
MIT	Massachusetts Institute of Technology
MITES	Miniature Interferometric Terminals for Earth Surveying
MLRS	McDonald Laser Ranging System
MMM	Magnetic Field Monitor Mission
Moblas	Mobile Laser System
MSFC	Marshall Space Flight Center
MV	Mobile VLBI
NASA	National Aeronautics and Space Administration
NAS/NRC	National Academy of Sciences - National Research Council
NASCOM	NASA Communications Network
Natmap	Division of National Mapping (Australia)
NAVSTAR	Navigation Satellite for GPS Constellation
NBS	National Bureau of Standards
NCMN	National Crustal Motion Network
NEROC	Northeastern Radio Observatory Corporation
NGS	National Geodetic Survey
NGSP	National Geodetic Satellite Program
NLRS	National Mapping Laser Ranging Station
NOAA	National Oceanic and Atmospheric Administration
NRAO	National Radio Astronomy Observatory
NRL	Naval Research Laboratory
NSF	National Science Foundation
NSSDC	National Space Science Data Center
NSWC	Naval Surface Weapons Center
nT	Nanotesla
OSSA	Office of Space Science and Applications
OSU	Ohio State University
OVRO	Owens Valley Radio Observatory
PM/ER	Polar Motion/Earth Rotation
PMT	Photomultiplier Tube
POGO	Polar Orbiting Geophysical Observatory
Polaris	Polar Motion Analysis by Radio Interferometric Systems
PRB	Program Review Board (Geodynamics)
PSN	National Space Plan (Italy)
RMS	Root-mean-square

RRL	Radio Research Laboratories (Japan)
RTD	Research and Technology Development
RTOP	Research and Technology Objectives and Plan
SAFE	San Andreas Fault Experiment
SAO	Smithsonian Astrophysical Observatory
SCO	Superconducting Cavity-Controlled Oscillator
SERIES	Satellite Emission Range Inferred Earth Surveying
SGAB	Satellite Geodesy Applications Board
SIRIO	Satellite Italiano per la Ricerca Opuntato
SLR	Satellite Laser Ranging
SQUID	Superconducting Quantum Interference Device
SSG	Science Steering Group
Stalas	Stationary Laser System
STDN	Space Flight Tracking and Data Network
SUNY	State University of New York
TLRS	Transportable Laser Ranging System
Topex	Ocean Topography Experiment
UCSB	University of California at Santa Barbara
USGS	U.S. Geological Survey
USNO	U.S. Naval Observatory
UT	Universal Time
VLA	Very Large Array
VLBI	Very Long Baseline Interferometry
WVR	Water Vapor Radiometer

APPENDIX 2

INVESTIGATIONS SELECTED IN RESPONSE TO THE GEODYNAMICS NOTICE, 1982

Benton, E. R. (University of Colorado): Constrairts on Geomagnetic Secular Variation Modeling from Electromagnetism and Fluid Dynamics of Earth's Core.

Bose, S. C. (Applied Science Analytics, Inc.): Error Analysis of Geopotential Modeling from Satellite-to-Satellite Tracking.

Burchfiel, B. C. (MIT): Seismicity and Active Tectonics of the Andes and the Origin of the Altiplano.

Burke, K. (SUNY Albany): Wilson Cycle Studies.

Caputo, M. (Texas A&M University): Altimetry Data and the Elastic Stress Tensor of Subduction Zones.

Chase, C. G. (University of Minnesota): The Geoid as Indicator of Large-Scale Mantle Convection and the Proper Motion of Hotspots.

Cohen, S. C. (GSFC): Models of Crustal Deformation During The Earthquake Cycle.

Colombo, G. (SAO): Investigation of Dynamic Noise Affecting Geodynamics Instrumentation in a Tethered Subsatellite.

Daly, S. F. (JPL): On the Influence of Variable Viscosity on Flow in the Earth's Mantle.

Dickey, J. O. (JPL): Earth Rotation Studies Using Lunar Laser Range (LLR) Data.

Dickman, S. R. (SUNY Binghampton): Effects of the Oceans on Polar Motion.

England, P. C. (Harvard University): Study of Miocene and Pliocene Foredeep Development and Lithospheric Flexure of the Adriatic Foreland (Italy and Yugoslavia).

Frey, H. V. (GSFC): Numerical Modeling of Lithospheric Variations Between Southern Australia and Wilkes Land, Antarctica, Using Satellite-Derived Anomaly Data.

Fuligni, F. (Istituto Fisica Spazio Interplanetario): Feasibility Study of a Gravity Gradiometer for Measurements of the Earth's Gravity Field from the Low Altitude Tethered Subsatellites of the TSS (Tethered Satellite System): Class.

Gaposchkin, E. M. (Mathematical Geosciences Inc.): Development of High Accuracy and Resolution Global and Local Geoid and Gravity Maps Using Satellite-to-Satellite Tracking Data Suitable for Geophysics and Oceanography.

Grossi, M. D. (SAO): Study of Critical Technology Required for the Development of a Cryogenic Microwave Cavity Gravity Gradiometer for Orbital Use.

Hager, B. H. (Caltech): Dynamic Interpretation of Geoid Anomalies.

Hinze, W. J. (Purdue): Improving the Geological Interpretation of Magnetic and Gravity Satellite Anomalies.

Kaula, W. M. (UCLA): Analysis of Satellite-To Satellite Range-Rate Data.

Kaula, W. M. (UCLA): Earth Dynamics Analysis.

Lerch, F. J. (GSFC): Gravity Modeling with Localized Functions.

Lyzenga, G. A. (JPL): Studies of Recurrent Earthquakes and the Propagation of Stress in the Lithosphere.

Marsh, B. D. (Johns Hopkins University): Delineation and Interpretation of Earth's Gravity Field.

Marsh, J. G. (GSFC): Development of Techniques for Gravity Model Improvement Based Upon Tranet Doppler Satellite Observations.

McAdoo, D. C. (GSFC): Subduction Dynamics and Strength of the Lithosphere.

Molnar, P. (MIT): Study of Seismic Wave Velocity Structure in the Downgoing Slab and the Olivine-Spinel Phase Change.

Mueller, I. I. (OSU): Intercomparison of Different Space Geodetic Measurement and Computational Techniques for the Establishment of a Terrestrial Reference Coordinate System for Earth Dynamics.

Rapp, R. H. (OSU): Improvement of the Earth's Gravity Field from Terrestrial and Satellite Data.

Richardson, R. M. (University of Arizona): Deformation Within and Between Lithospheric Plates: A Finite Element Analysis.

Schubert, G. (UCLA): Thermal and Mechanical Evolution of Oceanic Fracture Zones and Effects of a Layered Mantle on Postglacial Rotational Response.

Schutz, B. E. (University of Texas, Austin): Advanced Technique Development for the Determination of the Earth's Gravity Field.

Spiess, F. N. (Scripps): Development of a Method for Accurately Tying Sea Surface Positions to a Deep Sea Floor Reference Point.

Taylor, H. A. (GSFC): An Investigation of Relations Between Atmospheric Angular Momentum and Variations in the Earth's Rotation.

Turcotte, D. L. (Cornell): Mechanisms of Crustal Deformation in the Western United States.

Williams, J. G. (JPL): Nutations from Lunar Laser Ranging.

APPENDIX 3

PUBLICATIONS ON RESEARCH SUPPORTED BY THE NASA GEODYNAMICS PROGRAM

Anderson, S. L., and K. Burke, Suture zones of the Grenville Province. Geol. Soc. Amer. Memoir, Proterozoic Studies (in press, 1983).

Benvenuti, M., and M. Caputo, Pattern recognition of gravity anomaly-seismicity relationship. Atti Accad. Naz. Lincei (in press, 1983).

Bentley, C. R., Magsat magnetic anomalies over Antarctica and the surrounding oceans. Geophys. Res. Lett. 9, 285-288, 1982.

Bock, Y., and Zhu Sheng-Yuan, On the establishment and maintenance of a modern conventional terrestrial reference system. Proc. General Meeting, International Association of Geodesy, Tokyo, Japan, May 1982.

Bock, Y., Estimating crustal deformations from a combination of baseline measurements and geophysical models. Bull. Geod. (in press, 1983).

Bock, Y., The Use of Baseline Measurements and Geophysical Models for the Estimation of Crustal Deformations and the Terrestrial Reference System. Report No. 337, Department of Geodetic Science and Surveying, Ohio State University, Columbus, Ohio. December 1982.

Bordoni, F., and F. Fuligni, Parametric antenna as a tunable detector for continuous gravitational radiation. Phys. Rev. (submitted, 1983).

Brown, R. D., M_2 ocean tide at Cobb Seamount from Seasat altimeter data. J. Geophys. Res. 88, 1637-1656, 1983.

Brown, R. D., Ocean tide measurement by Seasat altimeter data. Oceans 82 Conference Record, 439-444. Marine Technology Society, September 1982.

Brown, R. D., Toward a more dynamical geoid. Proc. Ninth International Symposium on Earth Tides (in press, 1983).

Brown, R. D., W. D. Kahn, D. C. McAdoo, and W. E. Himwich, Roughness of the marine geoid from Seasat altimetry. J. Geophys. Res. 88, 1531-1540, 1983.

Burke, K., C. Cooper, J. F. Dewey, P. Mann, and J. L. Pindell, Caribbean tectonics and relative plate motions. Geol. Soc. Amer. Memoir, Caribbean Studies (in press, 1983).

Burke, K., J. F. Dewey, W. S. F. Kidd, and A. M. C. Sengor, Continental collisions analogous to that forming the Qinghai-Xizang Plateau, in Geological and Ecological Studies of the Winghai-Xizang Plateau, 743-746. Science Press Beijing and Gordon and Breach, New York, 1981.

Burke, K., Two problems of intracontinental tectonics - relevation of old mountain belts and subsidence of intracontinental basins, in Proc. International Conference on Intracontinental Earthquakes, ed. J. Petrowski and C. Allen, Skopje, 1981.

Burke, K., W. S. F. Kidd, and D. L. Turcotte, Tectonics of basaltic volcanism, in Basaltic Volcanism, Chapter 6, pp. 804-898. Lunar and Planetary Institute, Houston, Texas, December 1981.

Caputo, M., A linear model for population growth, Atti Accad. Sc. Ferrara 59, 1-20, 1982.

Caputo, M., and G. F. Faito, Statistical analysis of the tsunamis of the Italian coasts. J. Geophys. Res. 87, 601-604, 1982.

Caputo, M., Are there one-to-one relations between magnitude, moment, intensity, and acceleration of the ground? Geophys. J. Roy. Astron. Soc. 72, 83-92, 1983.

Caputo, M., Determination of the creep, fatigue, and activation energy from constant strain rate experiment. Tectonophysics 91, 157-164-1983.

Caputo, M., G. Milana, and J. Rayhorn, Topography and its isostatic compensation as a cause of seismicity. Tectonophysics (in press, 1983).

Caputo, M., Physical constraints for the estimates of strain on the Earth's surface. Bollettino Geodesia Scienze Affini 2, 161-175, 1982.

Caputo, M., R. Console, A. M. Bagrielov, V. I. Keilis-Borok, and T. V. Sidorenko, Long-term premonitory seismicity patterns in Italy. Geophys. J. Roy. Astron. Soc. (in press, 1983).

Caputo, M., Seismicity in the Messina straits; geodetic and geophysical observations. Tectonophysics (in press, 1983).

Caputo, M., The occurrence of large earthquakes in southern Italy. Tectonophysics (in press, 1983).

Caputo, M., The reddening of the spectra of the parameters and the energy of earthquakes. Earthquake Prediction Res. 1, 173-181, 1982.

Cohen, S., A multilayer model of time-dependent deformation following an earthquake on a strike-slip fault. J. Geophys. Res. 87, 5409-5421, 1982.

Cohen, S., and T. Peck, Reports on Crustal Movements and Deformations. NASA TM 83872, National Aeronautics and Space Administration, Washington, DC, 1981.

Cohen, S., Relationships among the slopes of lines derived from various data analysis techniques and the associated correlation coefficient. Geophysics 46, 1606, 1981.

Cruz, J., Improved Global Prediction of 300 Nautical Mile Mean Free Air Anomalies. Report No. 331, Department of Geodetic Science and Surveying, Ohio State University, Columbus, Ohio. May 1982.

Dickey, J. O., H. F. Fliegel, and J. G. Williams, Comparison of polar motion results using lunar laser ranging, in High-Precision Earth Rotation and Earth-Moon Dynamics: Lunar Distances and Related Observations, Proc. IAU Colloquium 63, ed. O. Calame, 125-137. Dordrecht, D. Reidel Co., 1982.

Dickey, J. O., H. F. Fliegel, and J. G. Williams, Universal time from laser ranging, in Bureau International de l'Heure, 1981 Annual Report, D35-D62, 1982.

Dickey, J. O., J. G. Williams, and C. F. Yoder, Results from lunar laser ranging data analysis, in High-Precision Earth Rotation & Earth-Moon Dynamics: Lunar Distances and Related Observations, Proc. IAU Colloquium 63, ed. O. Calame, 209-216. Dordrecht, D. Reidel Co., 1982.

Eubanks, T. M., J. A. Steppe, J. O. Dickey, and P. S. Callahan, Spectral analysis of the Earth's angular momentum budget. J. Geophys. Res. (submitted, 1983).

Fliegel, H. F., J. O. Dickey, and J. G. Williams, Intercomparison of lunar laser ranging and traditional determinations of earth rotation, in High-Precision Earth Rotation and Earth-Moon Dynamics: Lunar Distances and Related Observations, Proc. IAU Colloquium 63, ed. O. Calame, 53-88. Dordrecht, D. Reidel Co., 1982.

Fliegel, H. F., J. O. Dickey, and J. G. Williams, Earth rotation by lunar distances: JPL Report, in Project MERIT: Report on the Short Campaign and Grasse Workshop With Observations on Earth Rotation During 1980 August-October, ed. G. A. Wilkins and M. Feissel, 1982.

Grossi, M. D., Limitations imposed by ionospheric turbulence on satellite-to-satellite doppler measurement accuracy. Geophys. Res. Letters 9, 1183-1186, 1982.

Hager, B. H., Global isostatic geoid anomalies for plate and boundary layer models of the lithosphere. Earth Plan. Sci. Lett. 63, 97-109, 1983.

Hager, B. H., R. J. O'Connell, and A. Raefsky, Subduction, back-arc spreading, and global mantle flow. Tectonophysics (in press, 1983).

Hager, B. H., Subducted slabs and the geoid: constraints on mantle rheology and flow. J. Geophys. Res. (submitted, 1983).

Hager, B. H., The geoid and geodynamics. Nature 299, 104-105, 1982.

Hastings, D. A., A look at the preliminary Magsat anomaly map, emphasizing Africa, in Proc. Sixth Conference on African Geology, Nairobi, 1982.

Hastings, D. A., An interpretation of the preliminary total-field Magsat anomaly map, in Proc. Fifth Latin American Geological Congress, 199-200, 1982.

Hastings, D. A., An updated Bouguer anomaly map of south-central West Africa. Geophysics (in press, 1983).

Hastings, D. A., editor, Geophysics, tectonics, and mineral deposits of Africa. Geoexploration 20, 197-329, 1982.

Hastings, D. A., J. L. Dwyer, D. D. Greenlee, J. W. Reynolds, C. M. Trautwein, and D. G. Orr, Case histories in the manual and digital synthesis of Landsat, geophysical, and other data. Geophysics 47, 433-444, 1982.

Hastings, D. A., On the tectonics and metallogenesis of West Africa: A model incorporating new geophysical data. Geoexploration 20, 295-327, 1982.

Hastings, D. A., On the availability of geoscientific collaborators of and in Africa. Geoexploration 20, 201-205, 1982.

Hastings, D. A., Preliminary correlations of Magsat anomalies with tectonic features of Africa. Geophys. Res. Lett. 9, 303-306, 1982.

Hastings, D. A., Synthesis of geophysical data with space-acquired imagery: a review. Adv. Space Res. (in press, 1983).

Hinze, W. J., R. R. B. von Frese, M. B. Longacre, L. W. Braile, E. G. Lidiak, and G. R. Keller, Regional magnetic and gravity anomalies of South America. Geophys. Res. Lett. 9, 314-317, 1982.

Jekeli, C., Alternative Methods to Smooth the Earth's Gravity Field. Report No. 327, Department of Geodetic Science and Surveying, Ohio State University, Columbus, Ohio. December 1981.

Longacre, M. B., W. J. Hinze, and R. R. B. von Frese, A satellite magnetic model of northeastern South American aulocogens. Geophys. Res. Lett. 9, 318-321, 1982.

Mann, P., and K. Burke, Structure and stratigraphy of the Northern Wagwater Belt, Jamaica. Trans. Ninth Caribbean Geological Congress, Santo Domingo, vol. 1, pp. 94-97, 1983.

Mann, P., F. W. Taylor, K. Burke, and R. Kulstad, Subaerially exposed Holocene coral reef, Enriquillo Valley, Dominican Republic. Bull. Geol. Soc. Amer. (in press, 1983).

Mann, P., K. Burke, M. Hempton, and D. Bradley, Evolution of pull-apart basins. J. Geol. (in press, 1983).

Marsh, B. D., J. G. Marsh, and R. G. Williamson, On gravity from SST, geoid from Seasat, and plate age and fracture zones in the Pacific. J. Geophys. Res. (submitted, 1983).

Marsh, J. G., F. Lerch, and R. Williamson, Geodynamics and geodetic parameter estimation from Starlette laser tracking data. Marine Geodesy (to be submitted, 1983).

McAdoo, D. C., and C. F. Martin, Seasat observations of lithospheric flexure seaward of deep ocean trenches. NASA TM 85046, National Aeronautics and Space Administration, Washington, DC, 1983.

McAdoo, D. C., On the compensation of geoid anomalies due to subducting slabs. J. Geophys. Res. 87, 8684, 1982.

Mueller, I. I., and B. A. Archinal, Geodesy and the Global Positioning System, in Proc. International Symposium on Geodetic Networks and Computations, International Association of Geodesy, vol. IV: Modern Observation Techniques for Terrestrial Networks. Deutsche Geodätische Komission, Series B., Vol. 258/IV, pp. 26-36, Munich, 1982.

Mueller, I. I., Zhu Sheng-Yuan, and Y. Bock, Reference Frame Requirements and the MERIT Campaign. Report No. 329, Department of Geodetic Science and Surveying, Ohio State University, Columbus, Ohio. June 1982.

Newhall, X. X., E. M. Standish, and J. G. Williams, DE-102: a numerical integrated ephemeris of the Moon and planets spanning forty-four centuries. Astronomy and Astrophysics (in press, 1983).

Parsons, B., and S. Daly, The relationship between surface topography, gravity anomalies, and temperature structure of convection. J. Geophys. Res. 88, 1129-1144, 1983.

Pavlis, E. C., On the Geodetic Applications of Simultaneous Range Differencing to Lageos. Report No. 338, Department of Geodetic Science and Surveying, Ohio State University, Columbus, Ohio. December 1982.

Rapp, R. H., and C. Wichiencharoen, A comparison of doppler implied and gravimetric geoid undulations considering terrain-corrected gravity data. J. Geophys. Res. (submitted, 1983).

Rapp, R. H., Aspects of geoid definition and determination, in Proc. General Meeting, International Association of Geodesy, Tokyo, Japan, May 1982.

Rapp, R. H., Degree variances of the Earth's potential, topography, and its isostatic compensation. Bull. Geod. 56, 84-94, 1982.

Rapp, R. H., Geoid undulation computations for doppler positioning requirements, in Proc. Annual Meeting, American Congress of Surveying and Mapping, March 1983.

Richter, F. M., H. C. Nataf, and S. F. Daly, Heat transfer and horizontally averaged temperature of convection with large viscosity variations. J. Fluid Mech. (in press, 1983).

Richter, F. M., S. F. Daly, and H. C. Nataf, A parameterized model for the evolution of isotropic heterogeneities in a convecting system. Earth & Plan. Sci. Lett. 60, 178-194, 1982.

Schneeberger, R., D. Pavlis, and I. I. Mueller, Use of simultaneous doppler-derived ranges in the geometric mode, in Proc. Third International Geodetic Symposium on Satellite Doppler Positioning, Las Cruces, New Mexico, February 1982.

Sengor, A. M. C., Kevin Burke, and J. F. Dewey, Tectonics of the North Anatolian transform fault, in Multidisciplinary Approach to Earthquake Prediction, ed. A. M. Isikara and A. Vogel. Vieweg u. Sohn, 1982.

Sexton, J. L., W. J. Hinze, R. R. B. von Frese, and L. W. Braile, Long wavelength aeromagnetic anomaly map of the conterminous U.S.A. Geology 10, 364-369, 1982.

Soller, D. R., R. D. Ray, and R. D. Brown, A new global crustal thickness map. Tectonics 1, 125-149, 1982.

Stein, S., J. F. Engeln, D. A. Wiens, K. Fujita, and R. C. Speed, Subduction seismicity and tectonics in the lesser Antilles arc. J. Geophys. Res. 87, 8642-8664, 1982.

Taylor, H., On the relationship between secular variations in Earth rotation rate, length of day, and global temperature. Nature (submitted, 1983).

Vassiliou, M. S., B. H. Hager, and A. Raefsky, Distribution of earthquakes with depth, and stress in subducting slabs. Science (submitted, 1983).

von Frese, R. R. B., and W. J. Hinze, Regional North American gravity and magnetic anomaly correlations. Geophys. J. Roy. Astron. Soc. 69, 745-761, 1982.

von Frese, R. R. B., W. J. Hinze, J. L. Sexton, and L. W. Braile, Verification of the crustal component in satellite magnetic data. Geophys. Res. Lett. 9, 293-295, 1982.

Wichiencharoen, C., The Indirect Effects on the Computation of Geoid Undulations. Report No. 336, Department of Geodetic Science and Surveying, Ohio State University, Columbus, Ohio. December 1982.

Williams, J. G., and W. G. Melbourne, Comments on the effects of adopting new precession and equinox corrections, in High-Precision Earth Rotation and Earth-Moon Dynamics: Lunar Distances and Related Observations, Proc. IAU Colloquium 63, ed. O. Calame, 293-303. Dordrecht, D. Reidel Co., 1982.

Williams, J. G., Lunar and planetary ephemerides: accuracy, inertial frames, and zero points, in Proc. Fourth International Workshop on Laser Ranging Instrumentation, vol. 1, 309-312, Geodetic Institute, University of Bonn, Bonn, West Germany, 1982.

Yoder, C. F., J. G. Williams, J. O. Dickey, B. E. Schutz, R. J. Eanes, and B. D. Tapley, Secular variation as Earth's Gravitation Harmonic J_2 from Lageos and the nontidal acceleration of Earth rotation. Nature (in press, 1983).

Zhu, Sheng-Yuan, and I. I. Mueller, The effect of corrections in precession, nutation, and equinox. Bull. Geod. 57, 1983.

Zhu, Sheng-Yuan, Comments on 'Frequency modulation of the Chandlerian component of polar motion,' by W. E. Carter. J. Geophys. Res. 87, 1982.

Zhu, Sheng-Yuan, Prediction of Earth Rotation and Polar Motion. Report No. 320, Department of Geodetic Science and Surveying, Ohio State University, Columbus, Ohio. September 1981.

APPENDIX 4

GEOPOTENTIAL RESEARCH PROGRAM

GEOPOTENTIAL RESEARCH PROGRAM - MODELING

GEOPOTENTIAL RESEARCH PROGRAM - INTERPRETATION

APPENDIX 4 (Continued)

GEOPOTENTIAL RESEARCH PROGRAM - INTERPRETATION

CRUSTAL DYNAMICS RESEARCH - PLATE MOTION/PLATE STABILITY

APPENDIX 4 (Continued)

CRUSTAL DYNAMICS RESEARCH - PLATE MOTION/PLATE STABILITY

CRUSTAL DYNAMICS RESEARCH - REGIONAL CRUSTAL DEFORMATION

EARTH DYNAMICS RESEARCH - POLAR MOTION/EARTH ROTATION AND SOLID EARTH TIDES

APPENDIX 4 (Continued)

EARTH DYNAMICS RESEARCH - POLAR MOTION/EARTH ROTATION AND SOLID EARTH TIDES

CRUSTAL DYNAMICS PROJECT REVIEW

APPENDIX 4 (Continued)

CRUSTAL DYNAMICS PROJECT REVIEW

PAPERS PRESENTED BY TITLE ONLY

GEOPOTENTIAL RESEARCH PROGRAM

J. P. Murphy
Geodynamics Branch, NASA Headquarters
Washington, DC 20546

Nearly a quarter of a century of gravity and magnetic field measurements from space have been collected. For the most part, individual projects were conducted with specific model improvements as objectives. Significant improvements in data quality and quantity have recently been realized and considerable amounts of new satellite data have been acquired. Advances have been made in terrestrial data quality and analysis methods as well as techniques for their combination with satellite measurements for model improvement.

A research program for maximizing the information extraction potential from this data to produce the best possible global gravity and magnetic field models for the mid 1980's has been formulated along with a plan for development of advanced instruments and missions.

The first of these new missions is the Geopotential Research Mission (GRM). Gravity and magnetic field measurements are made during the seven month GRM through the use of two satellites equipped with a Doppler tracking system capable of making 1 μ m/s relative range-rate measurements. They are placed in a 160 km altitude circular polar orbit separated by 300 km. Changes in relative range-rate between the two satellites caused by variations in gravity along the suborbital track are used to solve for gravity anomalies. One is also equipped with boom-mounted scalar and vector magnetometers to repeat the survey of Magsat. However, the lower orbit provides a threefold improvement in resolution and the launch several years after Magsat provides an accurate measurement of secular change.

The mission objective is to accurately map the global earth gravity and magnetic fields with a resolution of 100 km and an accuracy of 1 mgal for gravity and 2 nT for geomagnetism in order to meet requirements in solid earth and ocean science and practical applications. Specifically, the information will be used to: 1) study the relationship of mantle convection and plate motion; 2) determine mechanical properties of the crust; 3) differentiate between competing mechanisms for creating mountains; 4) construct regional geological models for resource assessment; 5) better understand core dynamics; 6) provide the global ocean geoid for ocean circulation studies; 7) provide updated magnetic charts for navigation and removal of the background field in terrestrial surveys; 8) provide improved gravity models for precise orbit and trajectory determination; and 9) study the origin and decay of the earth's magnetic field. (Gravity field, magnetic field, geoid, crustal anomalies).

Geopotential Research Mission (GRM) Design

T. Keating
Goddard Space Flight Center
Code 402
Greenbelt, MD 20771

ABSTRACT

The design of the GRM spacecraft(s) and the associated instrumentation is presented. Descriptions of the major instrumentation; i.e., satellite-to-satellite doppler tracking, Disturbance Compensation System, and scalar and vector magnetometers as well as the spacecraft propulsion, power, thermal, attitude control, telemetry, and command, and the spacecraft-to-ground doppler tracking are provided.

A scenario flight program describing launch, deployment, orbital altitudes, orbit perturbations, mission life, tracking requirements, and data flow is presented.

A summary of the status of the mission with an outline of the present activities is included.

GEOPOTENTIAL RESEARCH MISSION SCIENCE

David E. Smith
Robert A. Langel
Goddard Space Flight Center, Greenbelt, MD 20771

ABSTRACT

The broad scientific objectives of the Geopotential Research Mission are to improve our knowledge and understanding of the evolution and structure of the earth's crust and interior from the analysis of the earth's gravity and magnetic fields. Gravity data, accurate to about a milligal (at the earth's surface) and magnetic data, accurate to about a nanotesla (at the satellite altitude, 160 km), will be obtainable from the mission at a resolution of about 100 km. This represents an improvement of nearly an order of magnitude in accuracy at these short-wavelengths and includes both the oceans and the land areas. These data will be used in the development of global models of the earth's potential fields for application to a variety of studies of the solid earth. The magnetic field data and models will be used to investigate the dynamics of the core and the generation and decay of the main field. The global gravity models will be used for studies of the lithosphere, mantle, and the driving mechanisms of plate motion. Crustal models are expected to be developed from the combination of the gravity and magnetic data sets (together with other geophysical data) and should significantly increase our understanding of the formation and evolution of geological structures, such as basins and mountain ranges.

The gravity data will also permit the development of a high accuracy geoid which will benefit the analysis of satellite altimetry for ocean circulation, and make a major improvement in satellite orbit determination capability for nearly all satellites. The magnetic data will also be used to update magnetic field charts for an improvement in navigation.

Improved GRM Simulation Results

Francis J. Lerch/Barbara H. Putney
Goddard Space Flight Center
Greenbelt, MD 20771

ABSTRACT

Computer simulation resutls for the Geopotential Research Mission (formerly Gravsat) have been obtained which support accuracy goals of the mission, namely, 4 mgals for gravity anomaly and 10 cm for geoid height with a half-wavelength resolution of 1 degree. The computer simulations were performed with satellite-to-satellite doppler tracking (±1 micron/sec) between two low altitude satellites at 160 km in polar orbits and separated by 300 km in a drag-free environment for a 6-month mission lifetime. Results have been obtained from the following studies: (1) the recovery of spherical harmonics with potential coefficients complete through degree and order 36 gave an accuracy of 2 to 3 orders of magnitude better than current knowledge; (2) recovery of geoid height and gravity anomaly in a local region (50° LAT x 20° LONG) in the presence of unmodeled errors external to the region gave an accuracy of 7 cm for geoid height and 4 mgal for gravity anomaly for 1° x 1° blocks within the interior of the region; (3) the recovery of 1/2° x 1/2° blocks of geoid height and gravity anomaly in a local area containing a trench region gave commission errors of 5 cm for geoid height and 3 mgal for gravity anomaly for 1° x 1° block sizes; and (4) a Fourier analysis of the trench region in (3) confirmed the results of this study.

Future analysis should be conducted to extend the spherical harmonics to high degree (70 to 100) to reduce the aliasing effect on the solution due to the truncation of the harmonics. Because of computer time limitations it is necessary to truncate the spherical harmonic series. The residual potential including the smaller wavelengths of the truncated harmonics will then be recovered from localized functions by combining steps (2) and (3) above to cover a considerably broader region than the 50 x 20 area used in the present analysis. Also, because of computer time efficiency, the technique of deriving the potential first at satellite altitude and then downward continuing the result to the surface of the earth is being investigated.

ANALYSIS OF SATELLITE-TO-SATELLITE RANGE-RATE BY FOURIER TECHNIQUES

W. M. Kaula
Dept. of Earth & Space Sciences
Univ. of California
Los Angeles 90024

The regular data intervals of satellite-to-satellite range-rates suggest Fourier techniques as a means of avoiding massive inversion computations in data analysis. However, the ignorance of longitudinal & radial derivatives of the unknown potential make imperfect any solution from a single pole-to-pole revolution. Requiring agreement of potential at track crossings essentially solves the longitudinal problem, but the radial problem entails, inevitably, iteration. This iteration can be accomplished quite economically by adopting the Fourier coefficients of range-rate as the residuals to be reduced upon iteration. The main difficulty then becomes choosing the optimum, unbiased, estimate of the ratio of Fourier coefficient for potential to the coefficient for range-rate upon iteration.

A POTENTIAL MODEL

C. L. Lawson, W. L. Sjogren, B. G. Bills, F. T. Krogh
Jet Propulsion Laboratory, California Institute of Technology
4800 Oak Grove Drive, Pasadena, California, 91109

We are modeling the earth's potential function in the vicinity of near circular orbits by an interpolation method in which each parameter effects the value of the potential function only in a relatively limited region of space. Global surface continuity is preserved along with its first and second partial derivatives. The model facilitates computation of the gradient function. Sparse matrix methods are being investigated for parameter estimation using this model.

ERROR ANALYSIS STUDIES FOR A GEOPOTENTIAL RESEARCH MISSION (GRM)

W.D. Kahn
Goddard Space Flight Center
Code 921, Greenbelt, MD 20771

ABSTRACT

The Geopotential Research Mission (GRM), formerly know as Gravsat/ Magsat, has been proposed for the mapping of the earth's gravity field. It is a candidate for a NASA new start in the near future. GRM is composed of a pair of surface-force compensated satellites in identical polar orbits, spaced approximately 3° apart at an altitude of 160 km with a system precision of 1 μm/s.

The objectives of this paper are to discuss the geopotential parameter recovery capability of the SST Doppler sensor flown on GRM

Spectral analysis results show that for a GRM mission altitude of 160 km and a system precision of 1 micrometer/sec., gravity field information can be sensed up to 230 cycles per orbital revolution--beyond that frequency the gravity signal is characterized by white noise. It follows that at the GRM mission altitude of 160 km and a satellite-to-satellite Doppler system precision of ±1 micrometer per second, 1° x 1° gravity and geoid anomalies can be determined to an accuracy of 3.4 mgals and 8.6 cm respectively.

These results are compatible with the scientific requirements for GRM which are: Accuracy - 2.5 mgals; Horizontal Resolution - 100 km; Accuracy of Oceanic Geoid Undulation Difference - 10 cm (over wavelengths of 100 to 3000 kilometers).

Simulations of Magnetic Anomaly Field at GRM Altitude

P.T. Taylor, C.C. Schnetzler, R.A. Langel
NASA/Goddard Space Flight Center/Code 922
Greenbelt, MD 20771

In order to quantify the improvement in magnetic anomaly resolutions anticipated by the Geopotential Research Mission (GRM), orbiting at 160 km altitude, compared to the approximately 400 km altitude Magsat mission we have carried out three simulation studies: 1) The recently completed Composite Magnetic Anomaly Map of the United States was upward continued to 160 km and 400 km to simulate the field at GRM and Magsat altitudes. Before upward continuation a broad trend surface was removed by applying a general two-dimensional polynomial surface (with 8^{th} order terms in longitude and 4^{th} order terms in latitude with cross terms; this is equivalent to 45 degrees of freedom) to the data. The map data were compiled at 0.2^{o} intervals, upward continued to satellite altitude, and the field plotted at 0.4^{o} intervals. The 400 km altitude map closely resembles the anomaly field as measured by Magsat. The field at 160 km altitude shows considerably more detail, having both higher amplitude and finer spatial resolution. 2) Fields produced by two mathematically idealized crustal blocks of different sizes, orientations, magnetic susceptibilities, and separations were simlulated at altitudes between 150 km and 450 km by the use of a Gaussian quadrature integration program (SPHERE). Random noise levels of 0.5, 1 and 2 nT were added to the data. Both anomaly field and inverted dipole moment contoured maps were produced and evaluated from these mathematical simulations. Summary graphs of over one-hundred examples demonstrate improvements gained by flying at lower altitude. 3) Simulations of the same body with differing crustal depths were made with SPHERE. These data demonstrate that changes in gradient of the anomaly are below the noise level for most large size anomalies at Magsat altitude. At the 160 km GRM altitude, however, it should be possible to estimate the depth to source for a significant fracton of the crustal anomalies.

Superconducting Gravity Gradiometer

H. A. Chan, M. V. Moody and H. J. Paik
Department of Physics and Astronomy, University of Maryland
College Park, MD 20742

ABSTRACT

A single-axis superconducting gravity gradiometer is being tested. Various vibration-isolation and common-mode rejection techniques are employed to achieve successful operation of the device in a laboratory cryostat. The noise spectrum observed in the recent cooldowns corresponds to 0.3 E $Hz^{-1/2}$ in the 6-7 Hz window and 1-2 E $Hz^{-1/2}$ below 1 Hz, and was mainly seismic in origin. Coupling mechanisms of the seismic noise through various mechanical modes of the suspension system are under investigation. With a sufficiently high degree of common-mode rejection, a SQUID-limited sensitivity of 0.07 E $Hz^{-1/2}$ is expected for the present design.

This superconducting gravity gradiometer has been used as a null detector in a new test of the gravitational inverse square law. The tensor characteristic of the gravitational field produced by a 1.6 ton swinging pendulum was examined to obtain an experimental limit for the inverse square law at a range of 1 m. A three-axis unit of slightly increased dimension is under construction. In the meantime, the prototype single-axis instrument will be further evaluated and improved.

A SUPERSENSITIVE ACCELEROMETER FOR SPACECRAFT GRADIOMETRY

V. S. Reinhardt
Bendix Field Engineering Corporation
Columbia, Maryland
F. O. von Bun
NASA Goddard Space Flight Center,
Greenbelt, Maryland
J. P. Turneaure
Stanford University
Palo Alto, California

ABSTRACT

Advanced studies in the area of solid earth and ocean physics require, among other parameters, an exact knowledge of the Earth's gravity field. NASA is presently considering a GRAVSAT-A mission to determine the gravity field with an accuracy of 2-3 mgal change and a resultion of 100 km using satellite-to-satellite range rate tracing techniques. The purpose of this paper is to prepare the foundation of an advanced GRAVSAT-B mission in the 1990s with an accuracy of about 1 mgal or less and a resolution of about 50 km. This would lead to another quantum jump in solid earth and ocean physics. Satellite to satellite tracking techniques may not be able to meet the GRAVSAT-B requirements. A new technology, high sensitivity gravity gradiometry, shows promise in achieving the numbers mentioned during the next 5 to 10 years. Flown in low earth (160-180 km) orbits, gradiometers with a sensitivity of 10^{-3} to 10^{-4}EU (1 EU = 1 Eotvos Unit = 10^{-9}cm s^{-1} cm^{-1}) held over averaging times of 1-1000s will be required.

All the gradiometers under consideration for spacecraft use consist of combinations of mass-spring accelerometers which translate accelerations or gradients of accelerations into displacements. This paper shows how the 1-1000s integration time requirements limits the size of the conversion constant for accelerations to displacements. This is used to translate the 10^{-3} -10^{-4} requirement into a 10^{-12}-10^{-13} cm displacement resolution requirements for a mass-spring accelerometer. This paper also shows how consideration of the spacecraft environment leads to requirements on the dynamic range and the calibration accuracy of the mass-spring accelerometers and on the stability of the displacement measurement system.

The second part of this paper proposes a new type of accelerometer for gravity gradiometry utilizing a superconducting microwave cavity controlled oscillator (SCO) as the displacmeent sensor. Unlike other accelerometers being proposed or developed, which convert displacements into voltage changes, an SCO sensor would convert displacements into frequency changes. SCOs have achieved fractional frequency stabilities of better than 10^{-15} which translates into a dimensional stability of $3x10^{-15}$cm since the frequency of an SCO is determined by the dimensions of the superconducting microwave cavity. This paper proposes a practical SCO accelerometer design utilizing a mass-spring accelerometer as one wall of the superconducting microwave cavity. A detailed error anlaysis is given which shows that this device, when used in a gravity gradiometer, would have a sensitivity of 10^{-4}-10^{-5}EU for averaging times of 1-1000s and would have fewer dynamic range limiting problems than voltage based devices.

Satellite Geophysics: Global Distribution and Characteristics of Magnetic and Gravity Anomalies at 400 km Altitude

Herbert Frey, Ann Marie Semeniuk and Sherren Clark
NASA/Goddard Space Flight Center/Code 922
Greenbelt, MD 20771

The distribution of MAGSAT crustal magnetic anomalies and "crustal" free-air gravity anomalies from degree and order 30-180 from a new gravity model are compared at a common altitude of 400 km. At this height only broadscale crustal properties can be resolved, yet both data sets show good general agreement with generalized geologic features and major tectonic structures. Between $\pm 80^{\circ}$ latitude we identified 312 Magsat anomalies with amplitude $\geq \pm$ 2nT, and 405 free-air "crustal" gravity anomalies with amplitude $\geq \pm$ 1.0 mgal. At 400 km altitude the observed amplitude range is -14 to +16nT and -5.5 to +5.0 mgal for the magnetic and gravity anomalies respectively. We have examined the distribution of these anomalies over the continents, oceans and continental shelves for various ages of the underlying crust, and for different tectonic provinces and structures (e.g., shields, platforms, submarine plateaus). Comparisons with other data types (topography, crustal thickness) has also been completed. We summarize our results as follows:

Magsat anomalies: When plotted against geomagnetic latitude, the distribution of Magsat anomalies is non-uniform, showing a pronounced concentration (especially for higher amplitude features) at high geomagnetic latitudes. This is consistent with an induced origin for most anomalies, where anomaly amplitude (A) would depend on field magnitude (F). In order to identify the intrinsically strongest anomalies, we normalize the anomaly amplitude by the local field magnitude, and define the resulting parameter as anomaly "strength". When strength is plotted against geomagnetic latitude, a much flatter distribution results, as would be expected if most Magsat anomalies are induced. The intrincically strongest anomalies (those with large amplitude even though the inducing field is weak) become particularly interesting because they either have a strong remanent component or their causative bodies have susceptibilities significantly higher than the "average" susceptability for Magsat anomalies.

In units of A/F (A = anomaly amplitude in nT, F = field magnitude in 10^5nT), most Magsat anomalies have $|A/F| < 10$. Only 3% have $|A/F| > 20$, of which the strongest is Bangui at -42. Other intrinsically "strong" anomalies include Kursk (+28), Kentucky (+21), Tibet (-27) and a feature in the central Pacific at 19°N, 180°W (-20).

Of the 312 identified anomalies, 45% lie over continents, 44% over oceans and 11% over continental shelves. There is a slight concentration, especially for stronger anomalies, toward continental crust. Of the continental anomalies, less than 20% lie over Precambrian terrains, not counting the 14% over Greenland and Antarctica. About 1/3 of the continental anomalies lie over platforms, and a similar number overlie orogenic zones. The remainder are situated over shields or mixed

terrains. Most oceanic anomalies are found over intermediate age (25-100 my old) crust (55%). However, 25% of all the oceanic anomalies are located over submarine platforms and rises and may therefore not represent normal oceanic crust.

"Crustal" Gravity Anomalies: Free-air gravity anomalies at 400 km with amplitude $\geq \pm 1$ mgal are also concentrated over continental crust (48% of the 405 anomalies), with 36% over oceanic crust and 16% over continental shelves. Of the 191 continental anomalies, 61% are positive features. For those overlying Precambrian terrains, 78% are positive anomalies. Most anomalies over shields, orogenic zones and mixed terrains are positive (70-80%) but free-air anomalies over continental platforms are mostly negative (62%). Most oceanic anomalies are found in intermediate age or old crust, and these are dominantly negative features. Where gravity anomalies are found over young oceanic crust (<25 my) they are 3 to 1 positive in sign. 20% of the oceanic anomalies overlie submarine platforms, and 2/3 of these are positive.

Multiparameter Studies: Magsat anomalies have a distribution of elevations of the underlying crust that is similar to the hypsometric diagram for the Earth. There are two peaks, one at -4 to -6 km and one at 0-1 km relative to sealevel. For the Magsat anomalies the 0-1 km peak dominates slightly when all 312 anomalies are counted, but dominates clearly for the stronger anomalies ($|A/F| > 15$). Stronger anomalies are preferentially concentrated in those elevations corresponding to mean continental crust (0-1 km above sealevel).

Three parameter plots relating topography to crustal gravity at 400 km for magnetic anomalies of different strength reveal the following: (1) the strongest continental anomalies ($|A/F| > 20$) lie over platforms or the boundaries between tectonic provinces. (b) Orogenic zones have generally very weak anomalies, with 78% at $|A/F| < 10$. (c) Magsat anomalies over platforms and orogenic zones have a generally greater spread in gravity and topogrpahy values than those magnetic anomalies over shields. (d) Gravity values associated with Magsat anomalies over shields are small and dominantly negative. This contrasts strongly with the distribution of free-air anomalies at 400 km having amplitudes $\geq \pm 1.0$ mgal, which over shields are generally positive. Shields having satellite magnetic anomalies in general seem to have a different gravity character than general shields. (e) Magsat anomalies over platforms and orogenic zones shows the same positive/negative distribution in gravity values as for gravity anomalies with amplitude $\geq \pm 1.0$ mgal.

Similar three-parameter plots over the oceans show: (a) The mean elevation and range of gravity values at 400 km varies with the age of the crust. Younger oceanic crust has anomalies located at shallower depths (no surprise) but also has a more restricted range of gravity values associated with the magnetic anomalies. (b) Most magnetic anomalies over submarine platforms have positive gravity values associated with them. This is similar to the distribution of stronger gravity anomalies over these features. (c) Magsat anomalies over old oceans have a larger percentage of stronger magnetic anomalies ($|A/F| > 10$) as well as the greatest range of gravity values (-2.0 to -1.5 mgal).

The Effect of Magnetospheric Fields on Models of the Earth's Main Geomagnetic Field

R.A. Langel
NASA/Goddard Space Flight Center/Code 922
Greenbelt, MD 20771
R.H. Estes
Business and Technological System
Seabrook, MD 20706

ABSTRACT

The major currents in the magnetosphere are now well delineated. Such currents flow on the boundary of the magnetosphere (the magnetopause), across the center of the magneto-tail and in an equatorial "ring" or "sheet" current inside the magnetosphere. The Dst index is a measure of the temporal-variation of fields from these currents relative to their values on magnetically quiet days. The dependence of the lowest degree/order terms in a spherical harmonic analysis on the Dst index has been determined. This was done separately for dawn and dusk using Magsat data with the following results:

Dusk Internal: g_1^0 = -29982.6 - 0.161 Dst
Dusk External: q_1^0 = 20.14 - 0.66 Dst
Dawn Internal: g_1^0 = -29985.5 - 0.174 Dst
Dawn External: q_1^0 = 18.22 - 0.64 Dst

Taking these results into account permits:
(1) More accurate determination of the core contribution.
(2) The development of an algorithm to account for some external efforts when using sperical harmonic models.

Torben Risbo
Institute of Geophysics
Haraldsgade 6
DK-2200 Copenhagen

The Geomagnetic Field at the Core-Mantle Boundary

Spherical harmonic models of the geomagnetic field have been estimated on Magsat vector data of unprecedented accuracy and global coverage. Terms of degree less than 14 is believed to represent mainly the core field. Magsat models predict, when evaluated at the core-mantle interface, that the magnetic flux leave and enter the core through a small number of high intensity regions and spots sharply confined against a more neutral background. The main field is generated by four poles. Two equatorial belts of opposite polarity can from the GSFC (9/80) model be identified as the main source of the westward drift, which is as high as 0.5 degrees/year during the last 20 years. Older models and historical data confirm this picture. An interpretation in terms of a dynamo models given; the field is generated by two cylindrical dynamos parallel to the rotation axis, corotating with the mantle. One of them is oscillating with a period of 65 years and expels flux which drift westward as boble pairs forming the equatorial belts. This model explains the correlation between secular variation impulses and minima in the astronomical curve for variations of the earth's rotation. The equatorial belt can be interpreted as a magnetic recording of these phenomena 400 years back.

Improvement in the Gravity Model from Lageos (GEM-L2)

Francis J. Lerch
Goddard Space Flight Center, Greenbelt, MD 20771
S.M. Klosko
EG&G Washington Analytical Services Center, Inc., 6801 Kenilworth Ave., Riverdale, MD 20737-0398
G.B. Patel
Computer Sciences Corporation, 8728 Colesville Road, Silver Spring, MD 20910

ABSTRACT

A refined gravity field model, Goddard Earth Model GEM-L2, has been derived using the Lageos orbital data yielding better baseline measurements for the analysis of tectonic plate motion. This field also contributes to a better understanding of the broad features of ocean circulation through its improvement of the long wavelength geoid (terms through degree and order 4) with an accuracy estimated at ±8 cm. In GEM-L2 two and a half years of Lageos laser data acquired from over 20 well-distributed stations were combined with the existing data from the best satellite-derived model, GEM-9. Testing shows that the Lageos gravity field error at long wavelengths is less than half that for GEM-9. A comparison of global laser "base" stations from independent data sets of alternating 15-day data segments over the 2 1/2 years of Lageos show total interstation position to ±1.8 cm when using this new model. The same comparison using the 1979 versus the 1980 Lageos data yields ±5.2 cm; this difference in agreement reflects the change in data distribution and other systematic errors along with the tectonic motion which has occurred between these chronologically distinct data sets. Polar motion values were adjusted in GEM-L2 to a precision of 10 cm, which is shown to be necessary to achieve the accurate baseline and geopotential results.

The January 1983 1°x 1° Gravity Anomaly Field

Richard H. Rapp
The Department of Geodetic Science and Surveying
The Ohio State University
Columbus, Ohio 43210

ABSTRACT

The last formally documented 1°x 1° mean anomaly field was defined as the October 79 field. A preliminary update of this data set was carried out in December 1981 and we are now completing this new field with complete documentation forthcoming.

This new field started with a recent 1°x 1° data type provided by the Defense Mapping Agency Aerospace Center that contained 38530 anomalies. This tape was merged with our December 1981 tape to form a tape containing 44499 values. Of these values 16472 were based on OSU generated data. Of special interest is a significant number of improved anomalies in and surrounding Japan based on 10'x 10' mean anomalies, and new decision making procedures for anomalies in parts of Africa. The data selection at sea was carried out using comparisons with anomalies derived from Geos-3 and Seasat altimeter data. Note however that no data on our tape will be based on altimeter derived values.

We now have five additional sources to be added to our preliminary merger. When that is done we expect to have a tape containing approximately 44500 anomalies with their accuracy and updated mean elevation. A document will be prepared giving complete source lists, maps, anomaly statistics etc.

DETAILED GEOID GRADIENT MAPS OF THE SOUTH PACIFIC FROM SEASAT AND GEOS-3 ALTIMETER DATA

David T. Sandwell
National Geodetic Survey
Rockville, MD 20853

We have constructed geoid gradient maps of the South Pacific using both Seasat and Geos-3 radar altimeter data. Radial ephemeris error, which typically has an amplitude of a few meters and a dominant wavelength of the earth's circumference, is suppressed with respect to shorter wavelength sea surface undulations by taking the along-track derivative of each profile. This differentiation technique not only eliminates the need for crossover minimization but it also enhances shorter wavelength geoid undulations. North and east components of the geoid gradient are constructed from linear combinations geoid slopes along the ascending and descending orbits of both satellites using a weighted least squares technique (Seasat to Geos-3 weight of 5). An isotropic auto-correlation function, with a 60km width at half maximum, is used to interpolate among passes. This interpolating filter produces a sharp roll-off in the power spectrum at about 60km. Finally, a gray-tone image is produced by sampling the geoid gradient at .2 degree intervals and assigning a dot density ranging from 0% to 100% to each value. Values less than -50m/rad appear as black while values greater than 200m/rad are white. Less distinct features can be enhanced by adjusting the brightness, contrast and sun azimuth.

Shorter wavelength geoid undulations reflect bathymetric features of the seafloor such as large seamounts (e.g. Easter Island) and large age-offset fracture zones (e.g. the Eltanin Fracture Zone). In this region of the South Pacific bathymetric coverage is sparse compared with the dense uniform coverage by the Seasat and Geos-3 altimeters. We use these data to discover bathymetric features that have not been detected previously. The maps show that the Eltanin FZ and the Louisville Ridge are connected. Current bathymetric charts show a 500km gap between these two features. In addition to fracture zones, the maps reveal a number of seamounts that have not been detected previously. In some cases the expressions of these seamounts are greater than the geoid signal around Easter Island. This indicates that they are either taller than Easter Island or they are somewhat shorter and formed on older, more ridgid lithosphere.

GEOID MODELLING USING COLLOCATION

by

C.C.Tscherning
Geodætisk Institut,
Gamlehave Alle 22,
DK-2920 Charlottenlund,

Abstract:

Collocation has been used for the construction of approximations to the anomalous gravitational potential in Scandinavia and Greenland combining geopotential coefficients to degree and order 180, gravity anomalies, deflections of the vertical, Doppler satellite and satellite altimeter derived geoid heights. The method was also simultaneously used to determine a longitude bias of the deflections corresponding to a rotation around the Earth's Z-axis of -0.50 +/-0.26 arcsec.

Approximations were also determined for testpurposes without using the (approximate) geoid heights determined by satellite altimetry. Using a semi-major axis of 6378136 m, the r.m.s. difference between observed and computed values was +/-0.4 m for the sea areas bordering Scandinavia up to a distance of 150 km from the coast, with an even better agreement in areas with available sea gravity data.

A Reduced to Pole Satellite Anomaly Map of the World

R.A. Langel
NASA/Goddard Space Flight Center/Code 922
Greenbelt, MD 20771
S.D. Oh
Computer Science Corp.
College Park, MD 20742

ABSTRACT

Mayhew (1979, 1980) developed a method to reduce satellite anomaly data to common altitude and inclination. At the same time it was possible to calculate an equivalent magnetization. Unfortunately, the method proved unstable when applied to data near the geomagnetic equator. This problem has now been overcome by use of a "principal component" (eigenvalue) analysis wherein only certain eigenvectors of the solution are retained. Eigenvectors associated with "small" eigenvalues are discarded until the condition number of the matrix assumes a reasonable value (<500) and until the RMS of the solution set becomes stable. Application of this technique to data from the POGO satellite has resulted in a new world map in reduced to pole form. In this form, comparisons with tectonic features are less subject to uncertainty.

Geodyn Program Systems Development
Barbara H. Putney
Goddard Space Flight Center
Greenbelt, MD 20771

ABSTRACT

The purpose of the Geodyn Orbit Determination and Parameter Estimation Program System is to recover geodetic and geophysical parameters from satellite and other data in a state-of-the-art manner. As part of the Crustal Dynamics Project, a significantly improved gravity field, pole positions, earth rotation, GM and baselines have been determined. The new solid earth and ocean tidal model and observation normal point technique are currently being used and evaluated. In support of Gravsat, several simulations have been successfully performed. Numerical experiments with block interpolation, more accurate block integration, Fourier analysis of geopotential parameters, and Householder transformation techniques for least squares estimation, have been studied. There is still more work to be done in this area. In preparing for the MERIT campaign the DE118 JPL sun, moon and planetary ephemerides is nearly available in the Geodyn 8210 program. This provides us with improved planetary positions and the Wahr nutation series. In addition, the ocean loading displacement is available in that same program. Conversion of Geodyn and Solve to the Cyber 205 vector computer is underway. Solve is executing on that computer, although not efficiently. Work is underway to rewrite the inversion routine to make proper use of the vector hardware. The Geodyn 1.5 (quick and dirty version) is being debugged. Geodyn 2, the vector rewrite, has been designed and the integrator and interpolator are executing successfully. Despite the Cyber 205 training courses there is obviously a great deal to learn about efficient operation on that computer. Modifications to make this a flexible tool, by allowing multiple satellites (GPS) to be handled at one time, processing multiple observations simultaneously, having variation in numerical stepsize for high and low degree and order spherical harmonics, making easier additions of new adjusted parameters, restructuring of observation and input files to allow for more information and precision, are designed into the new program. Several new versions of Geodyn and Solve have been released. User's Guides and tables (flux, A1-UTC, polar motion) were updated. Versions of Geodyn were requested and delivered to England, Australia, the Netherlands, JPL and Ohio State University this year.

ESTIMATION OF GEODYNAMIC AND GEODETIC PARAMETERS FROM STARLETTE LASER TRACKING DATA

J.G. Marsh/F.J. Lerch
Goddard Space Flight Center
Greenbelt, MD
R.G. Williamson
EG&G Washington Analytical Services Center, Inc.
Riverdale, MD

ABSTRACT

Laser tracking data covering a 4-year period (1975-1978) have been analyzed for the development of a specialized earth gravity model for Starlette precision orbit computations. Rms fits for the GSFC laser data in 5-day arcs have been improved from the level of several meters to a few decimeters. Using this new gravity model, a detailed analysis of the Starlette laser data recorded during 1980 has been performed for the estimation of tracking station coordinates, polar motion, GM and ocean tidal constituents. This solution is a simultaneous least squares solution based upon normal equations for multiple 5-day arcs of laser tracking data. Comparisons between the station coordinate values derived from Starlette with those from independent Lageos solutions indicate an rms agreement of about 20 cm. The recovered values for the K_1, O_1, K_2, M_2, N_2, S_2 and M_1 ocean tidal constituents are in good agreement with the Schwiderski values, with the Parke/Yoder values, and with values from previous work based upon analysis of the long period evolution of the orbit for the recovery of the tidal parameters. With these geodetic model improvements, the Starlette laser data provides a strong complement to the Lageos data for geodynamic investigations.

SEASAT Geoid Anomalies in the Pacific: Two Dimensional Spectra and Relationship to Plate Structure

B. D. Marsh and J. Hinojosa
Dept. Earth and Planetary Sciences, The Johns Hopkins University
Baltimore, Maryland 21218

ABSTRACT

Comparisons of the anomalies from satellite-to-satellite tracking (SST), GEM, and SEASAT now show close correspondence. The principal anomalies in the Pacific are now well defined. Anomalies that previously had no apparent explanation are now found to correlate closely with plate age. And since changes in relative plate age are marked by major fracture zones, these fractures frame and give a marked east-west fabric to the associated anomalies. An offset in plate age of 10 m.y. produces a geoidal anomaly of about 2 m. At the same time the trace of, for example, the Hawaiian hot spot also produces an anomaly pattern, and it is the interference of these two sources of anomalies that gives the Pacific area its distinctive pattern of anomalies. The immediate source of these anomalies is of course the lithosphere itself. To investigate whether or not the hot spot anomalies can be spectrally separated through strike-sensitive filtering from the fracture zone anomalies we have spectrally analyzed in two dimensions four areas of 63°x63°. These spectra show a very strong contribution from east-west trending anomalies, a less strong north-south signal, and only a minor contribution from other directions. The spectra themselves are dominated by a characteristic ∿2000 km wavelength, and there is little sign of strength at the smaller wavelengths seen in a one dimensional spectral analysis of heat flow in this region by Chapman and Furlong. In addition, to gauge the effect of maintaining the buoyancy of a plume ascending from the lower mantle, we have employed the analytical methods developed earlier by us for Rayleigh-Taylor instabilities. It is found that the most probable diameter for such a plume is about 400 km, and to sustain its motion and not cool to ambient conditions it must rise at a mean velocity of at least 2 cm/yr.

Satellite altimetry, seamounts and the tectonic evolution of the Pacific Ocean Basin

A.B. Watts and N.M. Ribe
Lamont-Doherty Geological Obs. of Columbia Univ.
Palisades, New York 10964

The marine geoid has now been mapped to an accuracy of better than 1 meter using radar altimeters onboard orbiting satellites. In the absence of instrument noise and orbital uncertainties altimetric geoids comprise an oceanographic and a gravimetric or tectonic part. We have carried out preliminary studies of how oceanic volcanoes, which rise above the ocean floor as isolated seamounts and oceanic islands or linear ridges, contribute to the marine geoid. Simple models have been constructed in which it is assumed that oceanic lithosphere responds to volcanic loads as a thin elastic plate overlying a weak fluid substratum. Previous studies based on gravity and bathymetry data and uplift/subsidence patterns show that the effective flexural rigidity of oceanic lithosphere and the equivalent elastic thickness, T_e, increase with the age of the lithosphere at the time of loading. The models predict that isolated seamounts formed on relatively young lithosphere on or near a mid-ocean ridge crest, will be associated with relatively low amplitude geoid anomalies (about 0.4 - 0.5 meters/km of height) while seamounts formed on relatively old lithosphere, on ridge flanks, will be associated with much higher amplitude anomalies (1.4 - 1.5 meter/km). Studies of the SEASAT altimeter data set prepared by NASA's Jet Propulsion Laboratory support these model predictions; geoid amplitudes are relatively low over the Mid-Pacific mountains and Line Islands which formed on or near a mid-ocean ridge crest, and relatively high over the Magellan Seamounts and Wake Guyots, which formed off-ridge. Direct modelling of the altimetric geoid over these features is complicated, however, by the wide spacing of the satellite tracks (which can exceed 100 km) and poor bathymetric control beneath satellite tracks. In regions where SASS and SEABEAM multibeam bathymetric surveys are available models can be constructed that fit the altimetric geoid to better than ±1 meter. Studies of geoid anomalies over guyots in the Emperor seamount chain and the Louisville ridge, for example, suggest that these seamounts formed on 20-30 m.y. old oceanic lithosphere consistent with available geologic data. Thus, geoid anomalies over seamounts depend not only on their overall shape, density and crustal structure prior to loading but on their tectonic setting. We examine the implications of these results to studies of the physical oceanography of seamounts, studies that attempt to predict seamounts directly from satellite-derived gravity and geoid data, and geoid effects of deep processes occurring beneath the lithosphere such as those due to layered mantle convection.

An Improved Crustal Gravity Model for Comparison with MAGSAT Data

Herbert Frey, NASA /Goddard Space Flight Center/Code 922
Greenbelt, MD 20771
Steven Klosko, EG&G Washington Analytic Services, Inc.
Riverdale, MD

Anomalies in MAGSAT data remaining after removal of core and external fields are due to sources in the crust, above either the Moho or Curie isotherm, whichever is closer to the surface. This is a consequence of the geochemical makeup of the mantle and the thermal gradient within the upper mantle and lower crust. No such clean separation of crustal sources of anomalies in the gravity field exists. Previous comparisons of satellite magnetic anomaly data with global gravity anomalies have suffered from contamination by long wavelength sources from below the crust.

A special gravity model for the higher degree terms out to 180, 180 has been developed in an attempt to isolate "crustal" contributions to the field, for comparison with satellite magnetic anomaly data. Data sources for this specialized field include: (a) observed $1^{o}x1^{o}$ mean gravity anomalies (Rapp, 1981a), (b) $1^{o}x1^{o}$ oceanic gravity anomalies from a Seasat altimetric geoid (Rapp, 1981b), and (c) geophysically predicted surface data corrected to agree at long wavelengths with recent satellite gravity models. Low degree and order harmonics from GEM-L1 (Lerch et al., 1982) were mated to the new model for comparison purposes. The power spectrum which results for the high degree terms is similar to that for Rapp's (1982) model.

We are interested in the high frequency features out to 180, 180 in the new model. A number of theoretical crustal models were developed to help in estimating where the long wavelength terms should be truncated. Isostatic compensation models were generated using topographic data from DMAAC on 1^{o} blocks, which was used to produce harmonic coefficients which were related to geopotential coefficients through an expression developed by Wagner (personal communication). Uniform depths of compensation of 30, 40 and 50 km were used in the model calculations.

A point modeling approach was also used, in which isostatic compensation was modeled using a $5^{o}x5^{o}$ crustal thickness data set (Soller et al., 1981) to locate the compensating (negative) crustal mass. Depths greater than the Moho were also tried.

The spectrum of the new observed field was compared with the spectra of the various theoretical crustal fields to determine where "crustal" sources become the dominant contributors to the observed field. The highest degree of correspondence was found for the degree and order 30 to 180 terms in the observed field and the uniform depth of compensation = 40 km theoretical model. Although this residual (ℓ= 30-180) field is not entirely free of contribution from deeper sources, we believe it is our best available representation

of the "crustal" gravity field on a global basis.

For comparison with MAGSAT anomalies, a contour map of free-air gravity anomalies at 400 km altitude was generated from the 30-180 field. At this height the anomalies are of low amplitude, with a range of -5.5 to +5.0 mgals. At 400 km both magnetic and gravity anomaly data can resolve only broadscale crustal properties, yet there is surprising agreement in many parts of the globe between the gravity anomaly pattern and the known surficial geology and generalized tectonic structures. The most prominent features in the new field at 400 km are those which appear in most satellite gravity maps: subduction zones and major active foldbelts. Trenches show negative free-air anomalies (-2 to -4 mgal), often with flanking positive features over the overriding plate. The Alpine-Himalayan convergence zone is characterized strong positive anomalies ($\geq$ 3 mgals), which in Asia show excellent correspondence with the topographic structure. The platforms in India and Tibet to the south and north of the Himalayan Mountains are overlain by strong negative anomalies, as are the platforms flanking the Zagross-Caucasus Mountains.

The agreement between anomaly variations and generalized geology extends to weaker features as well. In eastern South America and much of Africa platforms and basins are overlain by negative anomalies, while the intervening outcrops of Precambrian basement have superimposed positive free-air gravity features. A particularily intriguing situation occurs in South Africa, where a negative anomaly over the Kalahari Basin is bounded on the northwest by the Damarides foldbelt, which is characterized by a positive anomaly. Although the Damarides disappear under the platform cover before reappearing to the northeast as the Zambesi Belt, their trace is marked by the positive anomaly which continues with minor attenuation through the platform. In northern Africa the Ahaggar and Tibesti Precambrian outcrops have positive anomalies over them, while the intervening platforms and basins are overlain by negative anomalies. The agreement with known surface and subsurface geology is encouraging, and suggests our new field will provide a useful compliment to satellite magnetic anomaly data for studies of broadscale crustal properties.

Subducted Slabs and the Geoid: Constraints on Mantle Rheology and Flow Pattern

Bradford H. Hager
Seismological Laboratory, California Institute of Technology
Pasadena, California 91125

Postglacial rebound and plate motions suggest that the mantle is not rigid, but responds to long term stresses by viscous flow. Flow results in near isostatic compensation of internal density contrasts by deformation of the upper surface (e.g. ridges and trenches), the core-mantle boundary and any other internal chemical boundaries which may exist. The total geoid anomaly is the sum of the effects of horizontal density contrasts arising from boundary deformations and the competing effects of the internal density contrasts driving the flow. The boundary deformations, and hence the total geoid anomaly for a given density contrast, are strong functions of the variation of effective viscosity with depth and the presence or absence of chemical stratification within the mantle.

The density contrast between subducted slabs and the surrounding mantle can be estimated with a higher degree of confidence than most parameters associated with mantle dynamics; it is constrained by the subsidence of the seafloor with age. Working in the spectral domain, if $S(\ell,m,r)$ represents the slab density contrast of spherical harmonic degree ℓ, order m, at radius r, then $U(\ell,m)$, the Earth's nonhydrostatic gravitational potential, is given by the convolution:

$$U(\ell,m) = \int G(\ell,m,r)*[S(\ell,m,r) + N(\ell,m,r)]dr$$

Here N is "noise" - density contrasts not associated with slabs - and G is the dynamic "instrument" response of the Earth. G gives the total geoid anomaly including the effects of surface deformation. Correlation of U with S allows an estimate of $\bar{G}$ (the radial average of G), as well as an estimate of N.

$\bar{G}$ can be estimated for degrees 4-9, where the correlation between U and S is significant at the 95-99.9% confidence level (except ℓ=6). If the density contrasts associated with subducted slabs are confined to the upper mantle, $\bar{G} \gtrsim 0.3$. If they extend throughout the mantle $\bar{G} \gtrsim 0.1$.

We have calculated $G(\ell,r)$ for a series of radially symmetric, layered Newtonian viscous earth models. G is negative in the upper mantle unless the viscosity increases with depth. Values of G as large as 0.3 in the upper mantle cannot be obtained if the 670 km discontinuity is a chemical barrier separating the upper and lower mantle into separate flow systems. Hence density contrasts associated with subducted slabs must extend into the lower mantle. Either flow extends through the 670 km discontinuity, with viscosity increasing with depth, or the flow pattern and density contrasts in the lower mantle are strongly correlated spatially with those in the upper mantle.

ON THE COMPENSATION MECHANISM OF THE AGULHAS PLATEAU

C.L. Angevine and D.L. Turcotte
Dept. of Geological Sciences, Cornell University, Ithaca, NY 14853

Correlations of geoid anomalies with topography are an important source of information on the compensation of submarine features. We have used this technique to constrain models of the density structure of the lithosphere beneath the southern Agulhas Plateau, in the western Indian Ocean. We explain the correlation in terms of a two-layer Airy isostatic model. Anomalous topography is compensated in part by crustal thickening, relative to crustal thickness in the adjacent ocean basins, and in part by an underlying anomalous mantle layer. Crustal thickness is greatest beneath the shallow, central portion of the plateau. Crustal thickening alone is insufficient to explain the correlation. The anomalous mantle layer underlies all of the plateau and its reduced density may be due to basalt extraction. The anomalous behavior of the Agulhas Plateau is similar to that of the Walvis Ridge.

THE CORRELATION OF BATHYMETRY WITH GEOID HEIGHTS ADJACENT TRENCHES OF THE NORTH PACIFIC

D.C. McAdoo
R. Kolenkiewicz
Goddard Space Flight Center, Greenbelt, MD
C.F. Martin
EG&G Washington Analytical Services Center, Inc. Riverdale, MD
S. Poulose
RMS, Inc., Greenbelt, MD

ABSTRACT

Cross-spectral analyses have been conducted on parallel sequences of altimetrically-derived marine geoid heights and collocated sequences of ocean depths for various regions of the North Pacific, in particular, areal blocks seaward of the Kuril and Aleutian Trenches. Geoid heights are obtained from SEASAT altimeter measurements and are referenced to a degree and order 12 global geoid. Ocean depths are interpolated from the NORDA bathymetric data base. Discrete-space, spectral analysis has been used to estimate the admittance between geoid anomalies and topography at short and intermediate wavelengths (<1800 km). Band averaging of parallel pass segments is employed. Estimates of admittance versus wavelength for block-shaped regions seaward of the Aleutian and Kuril trenches agree approximately with theoretical admittance functions for uncompensated, one-dimensional topography. Specifically, high values of estimated admittance, e.g., 0.005 to 0.015, in the wavelength range, 450 to 1800 km, corroborate earlier gravimetric studies of these regions which suggest that topography of the outer rise is decidedly uncompensated or dynamic. The observed admittances are therefore consistent with those predicted by models of end-loaded elastic oceanic lithosphere as well as by certain convective models.

Insofar as estimates of admittance indicate that topography of the outer rise is essentially uncompensated, mechanical models of oceanic lithosphere in the outer rise environs can be compared with either bathymetric or altimetric (geoid height) data. Separate comparisons have been made between a simple model of end-loaded elastic oceanic lithosphere and both bathymetric and altimetric data. Model parameters, including effective plate thickness and rise amplitude have been estimated using the method of least squares. For the Aleutian region rise amplitude shows an interesting variation across the Amlia Fracture Zone, suggesting a possible mechanical decoupling at the downslab extension of this fracture zone.

SEASAT and other altimetric observations of the geoid are clearly useful in studies of the outer rise, particularly in regions where bathymetric data is lacking. Studies of the outer rise should continue to contribute to our understanding of the nature of the tectonic force balance at subduction zones.

Depth and Geoid Anomalies over Mid-Ocean Swells

Barry Parsons[1] and Stephen Daly[2]
1 - Department of Earth and Planetary Sciences, Massachusetts Institute of Technology, Cambridge, MA 02139
2 - Jet Propulsion Laboratory, MS 183/501, Pasadena, CA 91103

Normal stresses associated with convection in a fluid layer whose boundaries can deform produce topography on those boundaries. For convection in a constant viscosity fluid at infinite Prandtl number integral relations between topography on the boundaries and the temperature structure can be found as a function of wavelength. Similar integral relations can be obtained for the total gravity or geoid anomaly which are the sum of contributions due to topography on the two boundaries and to temperature variations within the fluid. Exact expressions for the kernels in the integral expressions have been derived for a number of different boundary conditions. These relationships have been used together with convective temperature structures obtained numerically to evaluate the relative contributions of different regions in the convecting layer to the geoid and depth anomalies. For cellular convection these largely reflect temperature variations in the vicinity of the upper thermal boundary layer. The slope of the approximately linear relationship between depth and geoid anomalies gives an effective depth of compensation which lies within the region which provides the largest contribution to the calculated anomalies. These observations are consistent with an explanation of depth and geoid anomalies over mid-ocean swells in terms of convection beneath the lithosphere where the lower part of the thermally defined plate acts as the upper thermal boundary layer of the convection. The effective density distributions then lie at depths less than the thermal plate thickness as required by the observed relationship between the geoid and depth anomalies.

LOWER MANTLE EFFECTIVE VISCOSITY FROM LAGEOS OBSERVATIONS

David P. Rubincam
Goddard Space Flight Center
Greenbelt, MD 20771

ABSTRACT

Postglacial rebound appears to have been observed gravitationally by the Lageos satellite. Sixty-four observations of the orbital node made over a 6-year time interval reveal an acceleration of $(-8.1 \pm 1.8) \times 10^{-7}$ arc-seconds/day^2 in the node of the orbit due to a source not presently modeled in the GEODYN orbit determination computer program. This acceleration cannot be explained by the ocean tide with 18.6 year period, assuming it to be a global equilibrium one; it contributes little to the acceleration and mostly to a linear trend in the node. Hence the acceleration appears to be due to postglacial rebound in Laurentide Canada and other formerly glaciated regions of the earth. The rebound is causing J_2, the second degree, zeroth order term in the spherical harmonic expansion of the earth's gravitational potential to decrease at the rate of $(-8.0 \pm 1.8) \times 10^{-19}$ s^{-1} this in turn causes the observed acceleration in the node. This rate is in good agreement with the realistic L1 earth model of Wu and Peltier. Modeling the Laurentide ice sheet with L1, which has a lower mantle effective viscosity of 10^{22} poises, gives a predicted rate of change in J_2 of -6×10^{-19} s^{-1}; this is close to the observed value. On the other hand, their realistic L2 model with its 10^{23} poise lower mantle effective viscosity gives -19×10^{-19} s^{-1} for the rate of change of J_2, which is more than twice the observed value. Thus the effective viscosity of the lower mantle appears to be about 10^{22} poises.

Deglaciation induced polar motion and variations of lod

W.R. Peltier and Patrick Wu
Dept. of Physics, University of Toronto
Toronto, Ontario, Canada M5S 1A7

The wander of the rotation pole at the rate of $0.95^{o}/10^{6}$ years, which is observed in the ILS polar motion record from the period since 1900 A.D., is a rotational response of the earth to the last deglaciation event of the current ice age. This datum provides a useful constraint upon the earth's internal viscoelastic stratification. With the elastic structure fixed to that of earth model 1066B and the deglaciation history to the ICE 1 model of Peltier and Andrews, the predicted polar wander depends jointly upon the thickness of the surface lithosphere and the viscosity profile of the mantle. If the viscosity profile is fixed to that demanded by the relative sea level and free air gravity data of postglacial rebound, then the polar wander datum requires an effective lithospheric thickness near 300 km. This estimate agrees with that obtained on the basis of a new analysis of lithospheric flexure near the margin of the Laurentide ice sheet.

It has also been possible to show that the nontidal component of the observed acceleration of planetary rotation is due to deglaciation forcing. In order to fit the observed acceleration of about $0.7 \times 10^{-10}\mathrm{yr}^{-1}$, which is obtained through analysis of the historical record of solar and lunar eclipses, requires a lower mantle viscosity ν_{LM} which is such that 1.5×10^{21} Pa s $\leq \nu_{LM} \leq 6 \times 10^{21}$ Pa s when the upper mantle value is held fixed at 10^{21} Pa s. The rotational datum is not sensitive to the thickness of the lithosphere and so provides a lower mantle viscosity estimate which is independent of that deduced through analysis of relative sea level and free air gravity data. Furthermore, this estimate agrees nicely with that inferred from the postglacial rebound measurements.

Modern satellite laser ranging data should provide an additional method of testing the value of the viscosity of the lower mantle inferred on the basis of the nontidal acceleration and postglacial rebound observations. It should soon be possible, using these data, to measure the time derivative of the second degree component in the spherical harmonic expansion of the earth's gravitational potential field. This parameter is conventionally referred to as $\dot{J}_2$. Accompanying the relaxation of the earth's shape forced by Pleistocene deglaciation there should be, according to our calculations, a $\dot{J}_2$ of magnitude $0.35 \times 10^{-10}\mathrm{yr}^{-1}$. Since the current accuracy in the determination of J_2 based upon the GEM 10 satellites is about 1 part in 10^9, application of SLR methods to the determination of satellite orbits over a succession of temporal epochs should make feasible a confirmation of our predicted value of $\dot{J}_2$ in the near future. This will in turn provide a very useful additional constraint on the viscosity of the lower mantle.

$\dot{J}_2$ FROM LAGEOS

C.F. Yoder, J.G. Williams and J.O. Dickey
Jet Propulsion Laboratory
California Institute of Technology
Pasadena, California 91109

B.E. Schutz, R.J. Eanes and B.D. Tapley
Center for Space Research, University of Texas at Austin
Austin, Texas 78712

ABSTRACT

One mechanism which affects earth rotation (UT1) is periodic and secular changes in earth oblateness or the J_2 gravity coefficient (1). The orbits of close earth satellites, such as Lageos, are also affected by variations in J_2. The most significant perturbation occurs in Lageos' node Ω where the forced change in Ω is comparable in size to the $J_2(t)$ induced change in UT1: $\delta\dot{\Omega} = -0.47\ \delta\,\mathrm{UT1}(J_2(t))$ (2). Obviously, this kind of perturbation complicates the determination of UT1 from observing the apparent rotation of the earth with respect to Ω as is now done with Lageos, but provides information not available from UT1 alone. However, given an independent record of UT1 (e.g. from lunar laser ranging (LLR) or BIH) and a complete model describing the other forces perturbing its orbit, the residual signature in Ω can be used to separate the variations in UT1 caused by temporal changes in J_2 from variations caused by other mechanisms.

The most provocative signature observed is a secular acceleration in Ω: $\ddot{\Omega} = (-0''.021 \pm 0''.004)/\mathrm{yr}^2$ (" = arcsecond). This result is based on an analysis of 5 1/2 years of Lageos' data (3) using LLR determined UT1 (4). This acceleration is consistent with a secular decrease in J_2: $\dot{J}_2 = -5 \pm 1 \times 10^{-11}/\mathrm{yr}$. This $\dot{J}_2$ could account for the observed non-tidal deceleration of the earth rotation rate ω, estimated from classical observations by Morrison and Stephenson (5) to be $(\dot{\omega}/\omega)_{NT} = 8 \pm 1 \times 10^{-11}\mathrm{yr}^{-1}$. The Lageos' acceleration corresponds to $(\dot{\omega}/\omega)_{NT} = 10 \pm 2 \times 10^{-11}\mathrm{yr}^{-1}$. The most plausible mechanism for $\dot{J}_2$ is viscous rebound of the Canadian shield as a response to the last great deglaciation which began $\approx$18,000 yrs ago (6).

The data span is not yet long enough to establish that the observed acceleration is truly secular. The most plausible alternative is that the apparent quadratic signature results from frictional dissipation associated with the 18.6 yr tidal variation in J_2 which, in turn, is caused by the precession of the lunar node. However, the required tidal $Q(18.6\ \mathrm{yr}) \approx 15$ is unexpectedly small. Several more years of data will be required to resolve this question.

In addition to the acceleration, an annual variation in Ω of amplitude $\approx 0''.02$ is also observed. This signature corresponds to $\approx$2 1/2 ms in UT1 and may be due to the seasonal exchange of water between land and ocean.

(1) C.F. Yoder, J.G. Williams and M.E. Parke (1981). J. Geophys. Res., 86. (2) P.L. Bender and C.C. Goad (1978) in Proceedings Second International Symposium on the Use of Artificial Satellites for Geodesy and Geodynamics. (3) R.J. Eanes, B.E. Schutz, B. Tapley (1981) Ninth Annual Symposium on Earth Tides. (4) J.O. Dickey, H.F. Fliegel and J.G. Williams (1982) in High Precision Earth Rotation and Earth-Moon Dynamics, ed. O. Calame. (5) L.V. Morrison and F.R. Stephenson (1982) in Sun and Planetary System, eds. W. Fricke and G. Teleki. (6) R.J. O'Connell (1971) Geophys. J.R. astr. Soc., 23.

THE INDIAN OCEAN GRAVITY LOW: EVIDENCE FOR AN ISOSTATICALLY UNCOMPENSATED DEPRESSION IN THE UPPER MANTLE

S. M. Ihnen and J. H. Whitcomb (Cooperative Institute for Research in Environmental Sciences, University of Colorado, Boulder, CO 80309)

The broad gravity low in the equatorial Indian Ocean south of Sri Lanka is the largest and most striking feature in the gravitational field of the earth. The most negative long-wavelength free-air gravity anomalies are found there and the sea surface (geoid) lies more than 100 meters below the best fitting ellipsoid. We propose a model of the lithosphere and upper mantle which accurately predicts the observed free-air gravity and geoid elevation. This model is consistent with bathymetry and sediment thickness data and suggests that the crust south of India currently floats as much as 600 meters lower than would be expected if the region were isostatically compensated. This residual depression of the crust is apparently confirmed by observations of ocean depth. An uncompensated depression is consistent with the downgoing arm of a convection cell, and also with the presence of a mechanical wake left in the upper mantle behind India as it traveled toward Asia.

DSN INTERCONTINENTAL VLBI: RESULTS OF INTEREST TO THE CRUSTAL DYNAMICS PROJECT

O. J. Sovers, J. L. Fanselow, J. B. Thomas, G. H. Purcell, Jr.,
D. H. Rogstad, E. J. Cohen
California Institute of Technology, Jet Propulsion Laboratory,
4800 Oak Grove Drive, Mail Stop: 264-748, Pasadena, California 91109

ABSTRACT

Analysis of intercontinental radio interferometric measurements has yielded, as one of its results, a catalogue of some 100 compact extragalactic radio sources. Formal errors of the source positions are approximately 4 milliarcseconds. Internal consistency tests and comparisons with other radio source catalogues indicate that these formal uncertainties (1σ) are accurate estimates of the random component of position error. Comparisons with a number of radio and optical catalogues will be discussed.

Time history of the two DSN intercontinental baselines shows that tectonic motion might be detectable within a few years. The present 3-year span of high-quality data (1977-80) produced measurements of the rate of change of baseline length equal to -6 ± 4 and 4 ± 9 cm/yr for the California-Australia and California-Spain baselines, respectively.

Analysis of the decade-long span of data also suggests a need for reconsideration of the precession and nutation models. Due to the long-period (18.6-year) term involved in nutation, however, the present data is incapable of giving an unambiguous separation of the two.

WESTFORD-FORT DAVIS BASELINE RESULTS: A CASE STUDY OF VLBI PRECISION

James W. Ryan
Code 974
Goddard Space Flight Center
Greenbelt, Maryland 20771

ABSTRACT

The Westford antenna at Haystack Observatory became operational as a Mark III VLBI station in May, 1981. Since then single-day experiments have been carried out weekly on the Westford-Fort Davis baseline as a part of the National Geodetic Survey's POLARIS Project and NASA's Crustal Dynamics Project. Currently, more than fifty data sets have been acquired and each has been used to determine the baseline between Westford and Fort Davis with a formal error in length of 1 to 3 cm. Forty-two of these data sets have been studied extensively at Goddard to probe the precision of the Mark III system. The length repeatability as measured by the RMS of the individual experiment values about the mean is better than 2 cm and the resulting baseline residuals appear to be normally distributed. This data set has also been independently studied at NGS, and solutions done independently at two facilities have been compared. These results indicate that the effect on baseline of subjective analysis decisions is typically 2 cm or less.

Upper Bounds on Rates of Intra-Continental Deformation From Ground Based Geodetic Measurements

Robert Reilinger, Larry Brown, and Jack Oliver
Cornell University
Department of Geological Sciences, Ithaca, NY 14853

ABSTRACT

Rates of apparent tilt are determined by region from repeated geodetic leveling in the U.S. Apparent tilts reflect both true ground motion (tectonic and non-tectonic) and measurement errors and can be treated as upper bounds for rates of surface tilting. The leveling data are sensitive to deformation over characteristic lengths of 10-70 km and time intervals of 10 to 40 yrs. There is a strong tendency for tilt rates to decrease as the characteristic tilt length (length over which tilt is coherent) increases, a tendency which is consistent 'th the behavior expected from random error. However, it is also reasonable to expect true surface tilting to be largest over short distances. Excluding areas of subsidence due to fluid withdrawal, rates of apparent elevation change exceeding 1 cm/yr are, for the most part, confined to a very small percentage of the data in the western U.S. Examination of those areas for which both horizontal and vertical deformation have been reported indicates that shear strain rates are generally of the same order of magnitude as associated tilt rates. The levels of apparent tilt deduced from leveling should serve as guidelines for determining the precision required to monitor intra-continental deformation from space.

Region	Wavelength km	Average Tilt Rate, μ rad/yr (mm/yr)	Upper Bound for 95% of Obs., μ rad/yr (mm/yr)
U.S. (total)	25-35 55-65	.2 (6) .08 (4.8)	0.7 (21) 0.14 (8.4)
E. U.S. (excluding Coastal Plain)	25-35 55-65	0.1 (3) 0.03 (1.8)	0.3 (9) 0.06 (3.6)
W. U.S. (excluding Great Valley)	25-35 55-65	0.2 (6) 0.03 (1.8)	0.7 (21) 0.08 (4.8)
S. Cal. Uplift Area	25-35 55-65	0.2 (6) Not Sufficient Observations	0.5 (15) ---

GLOBAL GEOTECTONICS FROM LAGEOS

D.C. Christodoulidis and D.E. Smith
Goddard Space Flight Center
Code 921, Greenbelt, MD 20771

ABSTRACT

The accuracy with which tectonic plate velocities can be computed is directly proportional to the repetition rate and accuracy in the measurement of interplate distances. As a result, a fair amount of GSFC activity has been devoted to increasing the temporal resolution and precision of baseline determinations for laser instruments deployed surrounding tectonic plate boundaries.

A summary of the results from the most recent analysis of the Lageos laser data for the period May 1976 to mid 1982 will be discussed. These results are approaching the useful accuracies required by Geophysics. For the better determined stations they include consistencies of: 3cm in annual heights, 6cm in monthly heights, 3cm in annual baselines and 8cm in monthly baselines. Better yet, consistencies and temporal resolutions were obtained in the case of specific baselines of moderate length where additional strength was given to the solution through the large number of simultaneously observed passes. Some of the problem areas in the current laser data reductions will be identified and future trends for improvements will be pointed out.

STATION COORDINATES AND BASELINE RESULTS FROM LAGEOS LASER RANGING

B. D. Tapley, B. E. Schutz and R. J. Eanes
University of Texas at Austin
Center for Space Research
Austin, Texas 78712

ABSTRACT

The quality of the laser ranging data has shown a significant improvement during the period since 1979. Both the measurement precision and the geographical distribution have improved. The Transportable Laser Ranging System (TLRS-1) occupied sites at Pasadena, CA, Austin, TX, Bear Lake, UT, Vernal, UT, Flagstaff, AZ, Owens Valley, CA, and San Digeo, CA, since October 1980. The observations and the quality of the TLRS data, as well as the data collected from the global tracking network during this time period, will be discussed. Station coordinates for TLRS and the other laser sites have been estimated, and baselines between these sites have been determined using several techniques. This presentation considers the factors which influence the station coordinate and baseline accuracies, and the baselines are compared with those obtained from other systems. In addition, a recent global tracking station solution based on five years of Lageos data is described and is compared with previously reported tracking station solutions. Finally, baseline rates obtained from independent annual solutions for 1981 and 1982 are reported.

The Tropospheric Problem in Monitoring Crustal Strain: A Microwave Frequency, Doppler-Based Satellite System

H. D. Black, A. Eisner, E. Westerfield
The Johns Hopkins University Applied Physics Laboratory
Johns Hopkins Road, Laurel, Maryland 20707

Abstract

We have designed a satellite system to monitor crustal strain. So that the system will be all-weather and so that it can simultaneously position a large number of sites, we have elected to use microwave frequencies. This choice aggravates the tropospheric refraction errors, particularly the water-vapor problem.

We can deal with all the other error sources in the system.

Ionospheric refraction can be eliminated by utilizing a pair of frequencies in the neighborhood of 400-1200 MHz.

Oscillator-noise is nearly eliminated by using round-trip doppler links. This technique correlates most of the oscillator noise in the system.

Satellite position errors can be effectively removed by simultaneously observing the satellite at several points. The points are separated by small distances; small compared with the satellite altitude. This correlates the satellite errors in determining the relative position of neighboring points.

These three techniques will push their associated errors down to the centimeter level.

Tropospheric refraction is another story. The troposphere is not dispersive, consequently using multiple frequencies will not help. The refractivity at a point within the troposphere depends on the atmospheric state; temperature, pressure, and water vapor density. All three vary temporally and spatially; moreover, the water vapor distribution cannot be rigorously modeled; it is frequently not in equilibrium with the surroundings.

We believe that there is an approach to this problem which is described in the enclosed paper. The theory, as best as we can do it, indicates that we can remove the tropospheric errors down to a few centimeters. Existing data sources and processing techniques show that we are realistically resolving the wet and dry terms. The data currently has insufficient precision to confirm (or deny) quantitively our theoretical findings.

The technique has broad applicability in correcting the doppler data from many satellites, e.g., Seasat, Geos-C, and Transit.

Portable Interferometer Terminals for Geodynamics: Status and Plans

S. A. Gourevitch, R. I. Abbot, C. C. Counselman, R. W. King, A. R. Paradis, and I. I. Shapiro

Department of Earth and Planetary Sciences
Massachusetts Institute of Technology
Cambridge, MA 02139

Portable radio interferometer terminals* that utilize the 19-cm-wavelength signals broadcast by the GPS satellites have been tested in the field over the past 10 months. The one-standard-deviation precision of these instruments has been established at about 2 parts per million (ppm) for each component of baseline vectors whose lengths are in the range from 1 kilometer to 61 km, the latter being the longest measured. This level of precision is about one order of magnitude worse than required for regional applications in geodynamics. In order to reduce to insignificance the error due to the ionosphere, which limits accuracy at present, we are having these instruments modified to receive the 24-cm-wavelength GPS signals. Tests of modified instruments will begin by spring 1983. To obtain a precision of 0.2 ppm or better will also require improved knowledge of the orbits of the GPS satellites. This knowledge will be obtained by using observations from the interferometer terminals to determine the orbits.

Research at MIT has been supported by the Air Force Geophysics Laboratory, Macrometrics, Inc., the U. S. Geological Survey, the NASA Geodynamics Program, and the National Ocean Survey/National Geodetic Survey. The Naval Surface Weapons Center and the NEROC Haystack Observatory, supported by the National Science Foundation, have also provided essential aid. I. I. Shapiro's present address is Harvard Smithsonian Center for Astrophysics, Cambridge, MA 02138.

---

* Manufactured by Macrometrics, Inc.

Spherical Diapirs in a Temperature Dependent Viscosity Medium

Stephen F. Daly[1] Arthur Raefsky[2]
1 - Department of Earth and Planetary Sciences, Massachusetts Institute of Technology and Jet Propulsion Laboratory, Pasadena,CA
2 - Jet Propulsion Laboratory, Pasadena, CA 91103

Several workers starting with Grout and more recently Marsh have argued for the lubricating effect of temperature dependent viscosity in the wall rock surrounding a rising diapir to enable magma to reach the near surface environment from depth. Simply stated, the problem is to get a diapir to rise at a sufficiently rapid rate to prevent the magma from cooling and solidifying. Recently, Morris (1982), employing an analogue model involving the squeezing of fluid between two plates, has used a boundary layer analysis to estimate the effects of this 'lubrication' mechanism. In a series of laboratory experiments Ribe (1982), has also studied the dynamics of hot spheres in a strongly temperature dependent viscosity fluid.

In an initial series of numerical experiments we have studied the drag and Nusselt number as a function of Peclet number and viscosity variation for a hot non-deformable sphere rising in a temperature dependent viscosity fluid. Solutions were obtained over a parameter range in Peclet number from 10^{-1} to 10^{3} and viscosity variations up to 10^{5} for both fluid and solid spheres. The drag is shown to be a function of a single parameter which depends on the deformation layer thickness and viscosity variation in agreement with the work of Morris. A power law relationship between Nusselt number, Peclet number and viscosity variation has also been obtained. The scale height for the rise of a hot spherical diapir in a temperature dependent viscosity medium over the above parameter range is shown to vary by less than a factor of ten. The reason for this is that, although the drag has been reduced with increased viscosity variation, the heat transport increases causing the diapir to cool more rapidly. This suggests the importance of mechanisms such as preheating and shape on the ability of a diapir to penetrate through a geophysically significant distance. Both of these mechanisms will be studied in the future.

DO OCEANIC AS WELL AS CONTINENTAL PLATES HAVE "STRESS PROVINCES"?

Eric A. Bergman and Sean C. Solomon
Department of Earth and Planetary Sciences
Massachusetts Institute of Technology
Cambridge, MA 02139

The concept of "stress provinces," well-defined regions of essentially uniform orientation of principal intraplate stresses, has been successfully applied to the conterminous United States by Zoback and Zoback [1980]. The dimensions and defining characteristics of these provinces are presumably products of a complex interaction between mechanically heterogeneous crust and the thermal and dynamic structure of the upper mantle. Recognition and boundary definition of such stress provinces may be important in the interpretation of changes in intracontinental and interplate baselines. In this paper we address the question of whether the stress province concept may also be applicable to oceanic intraplate regions. Study of this question and its relevance to intraplate deformation in oceanic lithosphere has the advantage that the lithospheric mechanical properties and thermal structure may be better understood in oceanic than in continental areas.

We focus on the Indian Ocean because it is the most seismically active oceanic intraplate region. We began with a comprehensive catalog of intraplate seismicity, and we combined that information with recent syntheses of the spreading history of the region and other geophysical data in order to search for "provinces" with characteristic styles of internal plate deformation. The catalog of intraplate earthquakes for this region includes more than 100 events spanning about 60 years of instrumental records. We have determined significant features of the source mechanisms of as many events as possible, using first motion polarities and P-waveform synthesis for some of the larger events. On the basis of this synthesis, systematic regional patterns of intraplate deformation can be discerned for portions of several plates. To the west of the Ninetyeast Ridge, a preponderance of pure thrust fault mechanisms indicates a nearly N-S compressive strain field extending from at least 12°N (in the Bay of Bengal) to about 4°S, including the area in which Weissel and others have reported reflection profiles indicating compressive failure of the oceanic crust. On the section of the Ninetyeast Ridge immediately adjacent to the most active portion of this zone, focal mechanisms indicate left-lateral strike-slip faulting with generally large thrust components. This slip may represent accommodation of the compressive internal deformation to the west across a boundary between separate Indian and Australian plates, though these plates show little relative motion further to the north and south. Differential motion across the Ninetyeast Ridge can be traced as far south as 15°S with diminishing intensity. From the equator to 8°N, where the ridge meets the Sunda Trench, very little intraplate deformation is apparently taking place.

There are two other regions in the Indian Ocean where significant deformation occurs, both nearer to spreading centers and both characterized by normal and strike-slip faulting with the least principal stress perpendicular to the local spreading direction. One region is in the vicinity of the Kerguelen Plateau and Amsterdam Island. The epicenters of the earthquakes associated with this deformation are restricted to lie within a positive residual-depth anomaly which spans a region between the postulated locations of the Kerguelen and Amsterdam hotspots. A possibly related features is a marked offset of the Southeast Indian Ridge in this region. The second area characterized by strike-slip and normal-faulting earthquakes is adjacent to the Central Indian Ridge in the vicinity of the Chagos Archipelago. This activity may mark a recent change in the spreading regime initiated by the resistance to spreading in the Himalayan collisional zone.

Data on intraplate stress in oceanic regions are still too sparse to reach any conclusions stronger than that the stress province concept is consistent with presently available information for oceanic lithosphere. Hot-spot traces and other loci of intraplate deformation in oceanic regions need to be noted as measurements of long baselines are made in oceanic plates.

Late Cenozoic Tectonics of the Basin and Range Province and San Andreas Fault System: A Progress Report

P.D. Lowman
NASA/Goddard Space Flight Center/Code 922
Greenbelt, MD 20771
R.B. Smith
University of Utah, Dept. of Geology and Geophysics
Salt Lake City, UT 84112
J.E. Estes, J.C. Crowell, and R.E. Crippen
University of California, Dept. of Geography
Santa Barbara, CA 93106

Tectonic and seismic activity in the western United States is concentrated in the San Andreas fault system and the Basin and Range Province, which collectively form the local boundary between the North American and Pacific Plates. Previous studies of these areas have generally been concentrated in one or the other provinces, with little attempt to understand the interrelationship of the San Andreas system and Basin and Range Province. This investigation is intended to study that interrelationship with stress on the Late Cenozoic tectonics. The work is being carried out at the University of Utah (Basin and Range) and University of California Santa Barbara (San Andreas system, with contributions from and coordination by Goddard Space Flight Center. Major results to date are the following.

Basin and Range: A new compilation of seismic events (over 50,000) for the western U.S. has been compiled, using data from 14 seismic networks and catalogues. Digitized compilations of crustal structure (thickness, P-wave velocities, upper mantle velocities, etc.) topography, and gravity have been completed, and computer algorithms for plotting such data have been tested on the University of Utah UNIVAC 1100. Several hundred focal mechanism solutions for the western U.S. have been compiled. A number of these indicate that some present seismic activity may result from listric faulting, and that exposed normal faults in the Basin and Range Province may grade into listric faults at depth.

San Andreas: Studies of the San Andreas system are concentrated in the Little San Bernadino Mountains and adjacent areas. The investigation is using all available imagery, including Landsat, Seasat, HCCM, U-2, and low-altitude air photos, in conjunction with field work. Digital terrain data is also being used to detect subtle irregularities that may indicate unmapped faults. Several unmapped faults or extensions of known faults in the SW Mojave Desert have been found, suggesting a southward bending of the Central Mojave shear system as it approaches the Pinto Mountain fault.

Additional mapping on the San Felipe fault, in San Diego County, supports previous work indicating that the Elsinore fault and related faults to the east are primarily dip-slip rather than

strike-slip. This relation has been interpreted as implying that Late Cenozoic tectonism in the Salton Trough/Peninsular Ranges area involves transection of normal Basin and range type faults by strike-slip San Andreas faults.

ELASTIC STRAIN RELEASE IN THE BASIN-RANGE AND SOUTHERN CALIFORNIA: INFERENCES FROM SEISMICITY AND GEOLOGICALLY DERIVED MOMENT RATES

Robert B. Smith
Department of Geology and Geophysics
University of Utah
Salt Lake City, Utah 84112

ABSTRACT

Using a new compilation of historic seismicity (mostly from regional networks) approximately 14,000 epicenters, M $\geq$ 3, and 320 slip-rate determinations on Late Cenozoic faults we have calculated contemporary moment rates, from the seismicity, and Quaternary moment rates, from the slip data, for the southwestern U.S. These data provide estimates of the direction and magnitude of the strain field due to elastic moment release only. When modeled with various fault geometries in the eastern Basin-Range, inferred from surface geology and seismic reflection information, they allow a determination of the contemporary and Quaternary deformation patterns. Contemporary E-W extensional strain across the eastern Basin-Range occurs non-uniformly at rates of 10^{-19} to $10^{-15} s^{-1}$ (corresponding to maximum extension of approximately 3.9 mm/yr) with the principal deformation occurring in the central Nevada seismic zone and the southern Intermountain seismic belt. Strain across the transition zone from southern California into the Basin Range is comparable to that in the Great Basin but shows an oblique extension. Contemporary N-S compression at rates of 10^{-15} to $10^{-13} s^{-1}$ characterizes southern California including the San Andreas fault. Quaternary deformation rates were remarkedly similar to those determined from the contemporary seismicity and suggest the continuity of the Late Cenozoic lithospheric deformation mechanism. Vertical deformation data are scanty in most of the Basin-Range but a regional E-W profile across the Great Basin (from geodetic releveling) shows a broad 3-9 mm/yr lithospheric uplift (relative to stable Rocky Mountains) centered over central Nevada. An important new finding from the eastern Basin Range, based on new seismic reflection data, is the presence of at least three upper- and intermediate-crustal reflections (at least 120 km in length) that appear to be low-angle detachments. Normal-slip on the low-angle detachments may have accommodated much of the Cenozoic E-W extension. The top-most of the detachment surfaces correlates with the top of an upper-crustal low velocity layer, (with an approximate 10% P-wave velocity reduction) at approximately 8 km. This is the same depth above which 80% of accurately determined focal depths occur. Quasi-plastic, strain-rate dependent deformation modeled for appropriate geotherms and a quartz rheology begins at the same depth and suggests a thermally controlled mechanism for limiting the depth of brittle deformation in the intraplate lithosphere. These data are consistent with a model for contemporary extension above an extending and platically deforming lower crust in the Basin-Range, with intraplate shear coupling across southern California into the Basin-Range. These data bear directly on the expected strain rates measured from laser-VLBI techniques in the southwest U.S.

ESTIMATING CRUSTAL DEFORMATIONS FROM A COMBINATION OF BASELINE MEASUREMENTS AND GEOPHYSICAL MODELS

Yehuda Bock and Ivan I. Mueller
Dept. of Geodetic Science and Surveying, Ohio State University
1958 Neil Avenue, Columbus, Ohio 43210

ABSTRACT

The estimation of crustal deformations from repeated baseline measurements is a singular problem in the absence of external information. One often applied solution is a free adjustment in which the singular normal matrix is augmented with a constraint matrix C such that $C\hat{X} = 0$. These constraints without physical justification impose no net translation nor rotation for the estimated deformations $\hat{X}$. The introduction of an available geophysical model from which an expected deformation vector $\overline{X}$ and its associated covariance matrix $\Sigma_{\overline{X}}$ are computed can direct $\hat{X}$ to a physically more reasonable solution.

Four possible estimators have been investigated for estimating deformations from the combination of baseline measurements and geophysical models. The starting point is the set of observation equations

$$L = AX + V$$

where L is the geodetic observation vector, X the true deformation vector, A the design matrix and V the noise vector. The Σ_L matrix is the covariance matrix of the baseline observations and $P = \Sigma_L^{-1}$. For each estimator the geophysical model $(\overline{X}, \Sigma_{\overline{X}})$ is introduced into the estimation model in a different manner as can be seen in the accompanying table where the statistical properties of the four estimators are summarized. The corresponding estimation models listed on the last line in the table are seen as extensions of the usual Generalized Gauss-Markoff model (L, AX, Σ_L) [Rao, 1973]. The estimates themselves may be found in [Bock, 1982].

These estimators are applied to crustal deformations of a network of VLBI and/or laser ranging stations. The absolute motion model AM1-2 of Minster and Jordan [1978] provides the external geophysical information. By a series of simulations [Bock, 1982] it is found that the BLE is best suited for estimating the deformations. It can improve the unweighted free adjustment estimator (a special case of BLIMBE) if the geophysical model is essentially correct. It is also least sensitive to errors in the geophysical model. Another conclusion is that it is better to apply even a weak but realistic model than none at all.

Statistical Properties of Deformation Parameter Estimators

Property \ Estimate	BLIMBE [1]	BLE [2]	Bayesian [3]	BLICUE [4]
Uniqueness	Yes	Yes	Yes	Yes
Weighted Least Squares Condition	$\hat{V}^T P \hat{V} = \min$	$\hat{V}^T P \hat{V} + \hat{X}^T Q_X^{-1} \hat{X} = \min$	$\hat{V}^T P \hat{V} + \hat{V}_X{}^T \Sigma_{\bar{X}}^{-1} \hat{V}_X = \min$	$\hat{V}^T P \hat{V} = \min$
Minimum Weighted Norm	In the class of P-least squares	Yes	No	No
Biasedness	Minimum bias	Biased	Unbiased assuming $E(\bar{X}) = X$	Unbiased conditional on $E(C\bar{X}) = CX$
Minimum Variance	In the class of minimum bias estimators	In the class of biased estimators	Yes	Conditional
Minimum Mean Square Error	No	In the class of biased estimators	Yes	No
Estimation Model	$(L, AX, \Sigma_L, Q_{\bar{X}})$ $Q_{\bar{X}} = \Sigma_{\bar{X}} + XX^T$	$(L, A\bar{X}, \Sigma_L, Q_X)$ $Q_X = \Sigma_X + \bar{X}\bar{X}^T$	$(L, AX, \Sigma_L, \bar{X}, \Sigma_{\bar{X}})$	$(L, AX \mid CX = C\bar{X}, \Sigma_{\bar{X}}, \Sigma_L)$

[1] Best Linear Minimum Bias Estimate (weighted free adjustment)

[2] Best Linear Estimate (weak Bayesian estimate)

[3] Strong Bayesian estimate (weighted parameter estimate)

[4] Best Linear Conditionally Unbiased Estimate (weighted constraint estimate)

References

Bock, Y. (1982), "The Use of Baseline Measurements and Geophysical Models for the Estimation of Crustal Deformations and the Terrestrial Reference System," Dept. of Geodetic Science and Surveying Rep. 337, Ohio State Univ., Columbus.

Minster, J.B. and T.H. Jordan (1978), "Present Day Plate Motions," J. of Geophysical Research, 83(B11), 5331-5354.

Rao, C.R. (1973), Linear Statistical Inference and Its Applications, John Wiley, New York.

EVIDENCE FOR BLOCK-TECTONIC STRUCTURAL ELEMENTS IN THE EASTERN UNITED STATES AND THEIR INFLUENCE ON CONTEMPORARY CRUSTAL MOVEMENTS

Alexander, Shelton S. and Peter M. Lavin
The Pennsylvania State University
Geosciences Department, 403 Deike Building, PSU, University Park, PA 16802

Multiple types of geophysical and geological observations in the eastern United States indicate, collectively, that the crust in this region is characterized by a block-tectonic structural fabric. The spatial dimensions of these structurally distinct elements typically are on the order of 100 km laterally with reasonably well-defined boundaries that extend at least into the lower crust. The available evidence indicates that these boundaries are fracture zones that have served to decouple adjacent block movements over a long geologic time interval (Pre-Cambrian to the present in some areas). Early lateral displacements between adjacent blocks were supplanted by primarily vertical relative movements from Ordovician time to the present, with corresponding influence or control on depositional environments and emplacement of hydrocarbon and mineral deposits. There is also evidence that this block-tectonic fabric exists beneath the master decollement postulated to be present in portions of the region east of the Appalachians. Therefore, contemporary seismicity and related tectonic movements everywhere in the eastern United States may be strongly influenced or controlled by these block-tectonic structural elements. Some of these elements are nearly aseismic, while others have numerous earthquakes distributed within them and on their boundaries thus defining seismo-tectonic mini-provinces. There is some indication that the larger eastern earthquakes preferentially occur near major block boundary intersections or intersections of block boundaries with other significant crustal structures. Based on the regional magnetic, gravity, and seismic observations currently available, there appear to exist significant variations in crustal structure among adjacent blocks, particularly in the relative thickness between the granitic and intermediate layers comprising the crust above the Moho. Models representing these characteristic crustal features provide a basis for interpreting existing and planned Earth observations from space, such as geodetic and potential field measurements.

THREE-DIMENSIONAL MODELING OF THE 1979 IMPERIAL VALEY EARTHQUAKE

M. A. Slade, G. A. Lyzenga, and A. Raefsky
Jet Propulsion Laboratory, California Institute of Technology,
4800 Oak Grove Drive, Mail Stop 264-748, Pasadena, CA 91109

ABSTRACT

Analysis of data pertinent to the 1979 Imperial Valley earthquake (M 6.6) has produced several rich sets of results: (a) coseismic displacements on the fault have been derived from strong motion and teleseismic data by Hartzell and Heaton (1982); (b) geodetic observations taken between the period (Nov. 1979-April 1979) and between (Oct. 1979-May 1980) have been analyzed by Mason et al. (1981) to produce station displacements which are thought to be dominantly coseismic. These derived motions are located mostly within 6 km on either side of the fault; (c) more regional but sparser suface deformation data are also available from the work of Snay et al. (1982).

In order to attempt a synthesis of these results, we perform three-dimensional finite element modeling of this event using several approaches. First, the coseismic surface displacements are calcuated by prescribing that the slip on the fault be given exactly by the most favored model of Hartzell and Heaton. The vertical elastic structure in the model is derived from compressional and shear wave velocities as used in the seismic data analysis combined with a sediment density profile. Secondly, we consider stresses on the fault plane, rather than displacements, as model variables. To constrain this part of our numerical modeling, we assume that the fault fails when a depth-dependent yield stress (derived from experimental data and a Coulomb friction theory) is exceeded. Furthermore,the coseismic stress drop from point to point on the failed fault is given by the difference between the tectonic shear stress and the frictional stress. The modeled region is taken to be in an average state of uniform shear stress driven by plate motions at large distances from the fault. The fault is assumed to be locked by friction at depth, and the yield stress there sets the scale for the vertical variation of stress in the model zone. (This neglects the likelihood that the shear stress decreased below the seismic zone due to plastic yielding.) Fault 'asperities' which are features of the seismic displacement models are represented as patches of lower than normal friction. The slip on the fault plane and the surface motions are thus both derived quantities in this approach.

Our conclusions include: (a) the geodetic data must contain substantial post-seismic deformation in order to be consistent with the fault plane displacements; (b) and the 1940 El Centro earthquake (M 7.1) may have relieved most of the stress on the southern third of the fault plane of this event.

Aseismic deformation in the Shumagin Islands seismic gap, Alaska

J. Beavan, E. Hauksson, K. Jacob, R. Bilham, J. Armbruster and T. Johnson
Lamont-Doherty Geological Observatory of Columbia University, Palisades, New York 10964

Both seismic and geodetic evidence suggest that an unusual slip event occurred beneath the Shumagin Islands between 1978 and 1980. An event such as the one proposed would lead to an increase of stress on the shallow locked portion of the plate boundary, bringing it closer to rupture in a great earthquake. The area is a seismic gap which has a history of great earthquakes, the most recent having occurred in 1788, 1847 and possibly in 1903. The elapsed time (80-140 yr) since the last great earthquake is of the same order as estimates of recurrence times at this plate boundary (≈100 yr).

We have measured a number of short (up to 1 km) geodetic level lines in the area since 1972 and have operated a local seismic network since 1973. The levelling data show a tilt down towards the trench of 0.9 ± 0.3 μrad yr^{-1} between 1972 and 1978. This is consistent with the deformation expected for interseismic loading at the long-term plate convergence rate of 7.5 cm yr^{-1} with no slip occurring on the plate boundary.

Between 1978 and 1980 the tilt underwent a rapid reversal to -2.2 ± 1.0 μrad yr^{-1} averaged over the two years. This corresponded with a dramatic increase in the number and energy release of teleseismically recorded earthquakes. The energy release was a factor of 6 higher in 1979 than its average for the previous few years. The 1978-1980 levelling data can be explained by a total slip of about 80 cm on that part of the Benioff zone between 30 km and 80 km depth immediately beneath the islands, with the shallower part of the plate boundary, towards the trench, remaining locked.

Estimates using empirical moment-magnitude relationships show that the seismic slip is at least an order of magnitude too small to explain the slip implied by the levelling data. Also, hypocenter locations by the local network suggest that much of the seismicity is located above the Benioff zone, particularly above the shallower end of the surmised slip event. Hence the proposed slip must have taken place mostly aseismically, and the enhanced seismicity during 1979 and 1980 may be a result of stress concentrations caused by the slip event. Detailed analysis of the local seismicity is presently underway.

Since 1980 the levelling data indicate that tilting down towards the trench has resumed at approximately the pre-1978 level.

The interpretation described here represents the simplest model consistent with the data. Vertical and horizontal displacement and strain measurements such as the proposed NASA/JPL occupation of a Shumagin Island VLBI site will provide important additional constraints on the mode of deformation in this region.

UPPER MIOCENE-QUATERNARY WRENCH FAULTING IN THE WESTERN MEDITERRANEAN GEODYNAMICS: EXAMPLE OF ENSIALIC, POST-COLLISIONAL, DEFORMATION.

M. Boccaletti[1], C. Conedera[2], P. Dainelli[2].
(1) Geological Institute, University of Florence
Via G. La Pira 4, 50121 Florence, Italy.
(2) GEOMAP, Via Della Robbia 28, 50132 Florence, Italy.

The comparative analysis of the geo-structural and geophysical data and of the results coming from the interpretation of the Landsat imagery, allowed the recognition, in the western segment of the Mediterranean area, of a system of conjugated wrench faults, reactivating old fractures, which was active during Pliocene and Quaternary, but which started its activity already in upper Miocene. This shear system is the results of the intra-plate deformations that developed in the area concerned, after the Cretaceous-Eocene main continental collisions.

The system consists of two principal conjugated trends, the NE-SW, or Moulouya trend, and the NW-SE, or Gafsa trend. To these, an E-W trend of prevailing wrench character (Gibraltar) and a N-S trend, with mostly tensional movements and subordinate transcurrent components (Thyrrenian), are associated. The trends that characterize the system are always present in all the segments of the circum-Mediterranean chains and continue in the forelands and in the marine areas, although some may locally prevail. The areas where they are observed in the best way are North Africa and the Betic Cordillera.

The orientation and the relative movements of the fractures of the system are consistent with the slip-line field that develops in a plastic-rigid mobile area, when this is placed between two non-parallel converging rigid blocks.

In the Apennine chain some fractures may show opposite movement direction, with respect to the general scheme. These anomalies are related to the differential displacement of segments of the chair, connected to the progressive shifting of the deformational activity towards southeast (Calabrian Arc, active at present).

The system evolves according to a "monoclinic" scheme, which is in turn complicated by the variations of the crustal tickness in the

deformed zone and by some preexisting discontinuities.

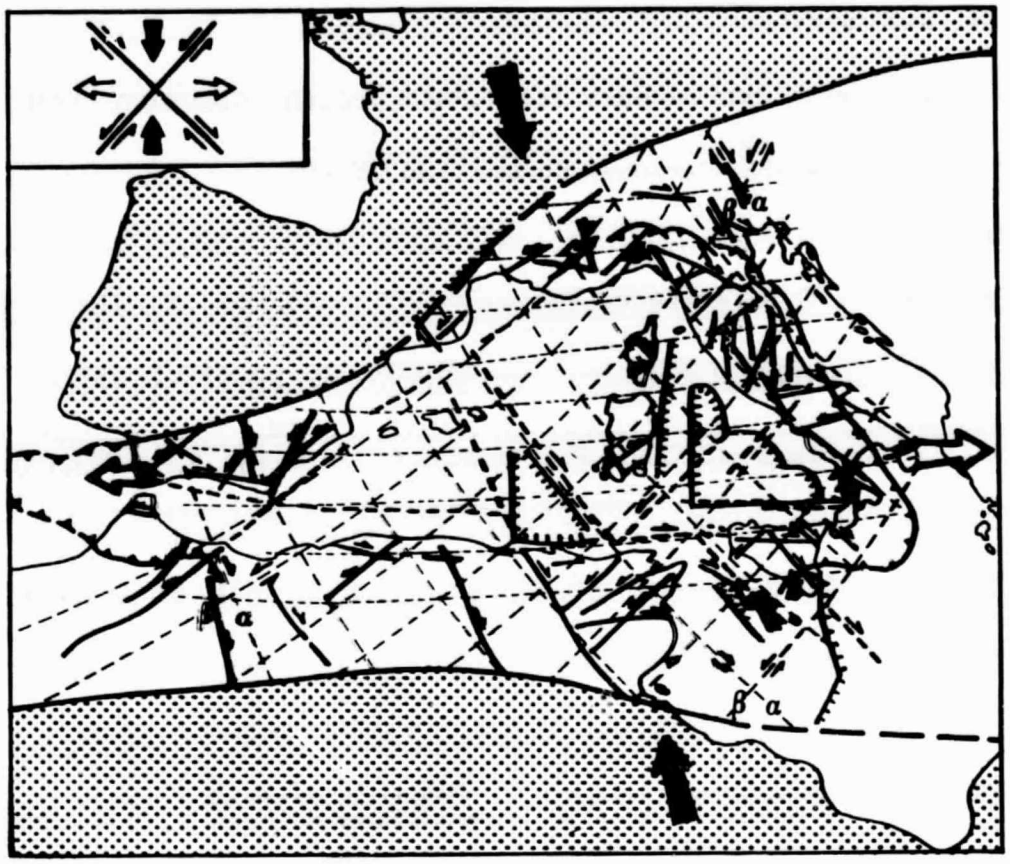

Fig. 1

In this frame, the spreading, since Tortonian, of the Tyrrhenian basin, according to a triangular shape, as well as that of the analogous basin, to the southwest of Sardinia (developed from 11 to 7 m. y.), can be considered as tensional mega-fissures, developed asymmetrically, as lower-order structures, relative to the principal stress between Europe and Africa, orientated between N-S and NNW-SSE from upper Miocene to Quaternary. The asymmetric opening occurs along an E-W rail on the southern edge of each basin. In the Tyrrhenian area, this rail allows also the release and rotation of the southern Apennine, with respect to the Sicilian-Maghrebide segment.

Ensialic "subductions" develop, mainly in the late-Miocene and Plio-

cene phases, induced and guided by the shear system. These subductions involve mechanisms of detachment and formation of listric wedges within the thinned upper crust, relative to the underlying lower crust and mantle.

In this general evolutionary frame, the Neogene Apennine chain assumes the meaning of a lateral chain, relative to the principal stress direction, NNW-SSE, between Europe and Africa.

REFERENCES

- Boccaletti, M.; Conedera, C.; Dainelli, P.; Goçev, P. The recent (Miocene-Quaternary) Regmatic System of the Western Mediterranean Region. Journal of Petroleum Geology, 5, 1, pp 31-42, 1982.
- Boccaletti, M.; Dainelli, P.: Il Sistema Regmatico Neogenico-Quaternario nell'Area Mediterranea: Esempio di Deformazione Plastico-Rigida Post-collisionale. Memorie Soc.Geol.It., XXIV, 1982.
- Boccaletti, M.; Nicolich, R.; Tortorici, L.: The Ionian Area in the Frame of the Dynamic Evolution of the Southern Mediterranean Sea. XXVIIIth Congress and Plenary Assembly of ICSEM, Cannes, December 2-11, 1982.

Modeling Historical Horizontal Crustal Deformation in California

Michael W. Cline, Richard A. Snay, Edward L. Timmerman
National Geodetic Survey
NOAA/NOS, Rockville, MD 20852

The National Ocean Survey/National Geodetic Survey has undertaken the project to model historical horizontal crustal deformation in each of 16 regions spanning California. Model parameters are estimated from triangulation, trilateration, and astronomic azimuth data observed during the past century. Also seismic and geologic data indirectly participate in specifying the models as crustal deformation is related to the episodic movements resulting from large earthquakes ($M \geq 6$), to secular slip rates on geologic faults, and to secular strain rates over large geographic areas. The episodic movement is modeled in accordance with the theory of dislocation in an elastic halfspace. For the secular motion, each region is partitioned into a mosaic of "districts" that are allowed to individually translate, rotate, and homogeneously deform as a linear function of time. Results will be presented for the four regions which in combination span all of California south of the $34^{\circ}.5$ parallel of latitude. Rates of motion between selected laser/VLBI stations will be highlighted.

CRUSTAL DEFORMATION DURING THE EARTHQUAKE CYCLE: TEMPORAL AND SPATIAL DEPENDENCE

Steven C. Cohen
Goddard Space Flight Center
Greenbelt, MD 20771

ABSTRACT

Cycles of stress accumulation and release in seismic zones are accompanied by temporally and spatially varying crustal deformations. The manner, rate, and degree to which the crust is deformed depends on fault geometry and slip and on subsurface rheology. Distance from fault, the earthquake recurrence interval, stress relaxation time, and time since the last earthquake are also key parameters for describing the deformation cycle. In the models presented here the focus is on the influence of asthenosphere viscoelasticity on crustal strain accumulation and postseismic rebound. Finite element computer simulations of the earthquake cycle predict patterns of deformation in which the response of the layered elastic-viscoelastic earth differs from that expected for a purely elastic body. Following strike-slip earthquakes points at intermediate distances from the fault move more rapidly than those in the near or far fields. The transient velocities of the intermediate field points may exceed long term plate velocities and may persist for years or decades following a major earthquake. The near field rate of strain accumulation is much greater than that predicted for an elastic earth after an earthquake and slower later on. In the far field, however, transient episodes of straining with sign opposite to that occurring in the near field can occur postseismically. The propagation of the coseismic and postseismic stress from the fault zone into the far field is retarded when the subsurface layers have a graded viscosity profile compared to when an elastic lithosphere lies over a uniform low viscosity asthenosphere. The postseismic deformation due to viscoelastic flow following a dip-slip earthquake may persist much longer than that for a strike-slip event, and include the effects of several previous slip events. Regions of both crustal subsidence and uplift accompany strain accumulation and postseismic rebound. A common feature of the postseismic rebound, namely a subsidence centered over the fault slip zone, occurs most intensely when the asthenosphere depth is twice the fault depth. Estimates of asthenosphere viscosity derived from postseismic rebound data are $\leq 10^{21}$ poise.

Title of Paper : Finite Element Modeling of the Three-Dimensional Stress Field in Eastern Mediterranean

Author : K. Eren, N. Akkaş, M. Erdik

Institution : Earthquake Engineering Research Center

Address : Middle East Technical University
Ankara-TURKEY

ABSTRACT

On the basis of the focal mechanism of earthquakes and the plane stress analysis, the stress field in Eastern Mediterranean indicates the following complicated features :

(1) Radial compression along Hellenic and Cyprus Arcs

(2) Complete Compression zone in Northern Greece

(3) Pure tension zone around the point of intersection of the Hellenic and Cyprus Arcs

(4) N-S tension in Western Anatolia

The complex features of the Eastern Mediterranean has been investigated by employing a three-dimensional linear, elastic finite element model. The following type of forces are considered :

(1) A northward compressive force due to the movement of the African plate

(2) A northwestward compressive force generated by the movement of the Arabian plate

The synthetic stress distribution has shown sensitivity to the geometry of the Turkish-Aegean plate as well as to the loading.

RECURRENT STRIKE-SLIP FAULTING IN STRESS-DRIVEN FINITE ELEMENT TECTONIC MODELS

G. A. Lyzenga, A. Raefsky
California Institute of Technology, Jet Propulsion Laboratory,
4800 Oak Grove Drive, Mail Stop: 264-748, Pasadena, California 91109.

ABSTRACT

The nature and amount of tectonic stress relief by plastic deformation below the seismogenic lithosphere figures heavily in theoretical studies of the earthquake cycle. Predicted values for transient strain and stress in a given cycle depend upon assumed steady state profiles of stress state and fault slip as functions of depth in the model.

In this work, a finite element model of viscoelasticity is used, which includes provision for stress-regulated brittle failure along a predesignated fault. Using this, no initial assumptions need be made about the steady state distributions of slip and stress, since these are evolved from the model. The only parameters left to be specfied are the rheological parameters of interest (viscoelastic), the far-field boundary conditions (e.g. displacement, stress), and the depth at which plastic deformation replaces brittle yield behavior.

We present the preliminary results of this study, for models with simple layered structure. Resultant profiles of slip, tectonic stress, and stress drop on the fault are presented. In addition, the approach to steady state and the geodetic motions accompanying propagating "stress waves" moving out from the fault zone are discussed.

This work is supported by NASA, Geodynamics Program.

EMPIRICAL STRAIN MODELING USING MOBILE VLBI DATA

K. S. Wallace, G. A. Lyzenga
California Institute of Technology, Jet Propulsion Laboratory,
4800 Oak Grove Drive, Mail Stop: 264-748, Pasadena, California 91109.

ABSTRACT

Using the Mobile VLBI geodetic measurements available through the Crustal Dynamics Data Information System, preliminary values of strain rates for a regional network (100-300 km baslines) have been empirically determined. This data set includes 1979 and 1980 geodetic data from the baselines formed by the VLBI stations at JPL (Pasadena, California), the Owens Valley Radio Observatory (Bishop, California), and the Goldstone Deep Space Network Complex (Barstow, California). Results of various temporal and spatial strain models are evaluated, as well as the significance of these results in light of VLBI measurement uncertainties. Magnitude and direction of these rates are compared to those determined by classical techniques with local scale networks.

FIRST BASELINE RESULTS FROM SERIES

L. E. Young, D. J. Spitzmesser, L. A. Buennagel
California Institute of Technology, Jet Propulsion Laboratory,
4800 Oak Grove Drive, Mail Stop: 264:758, Pasadena, California 91109.

ABSTRACT

The SERIES (Satellite Emission Range Inferred Earth Surveying) RTOP objective is to develop a precise, cost effective geodetic tool. The SERIES technique uses signals from GPS (Geodetic Positioning System) satellites, however, it requires no knowledge of the GPS code. During the previous year two SERIES receivers have been undergoing engineering tests. Some were designed to isolate certain error sources, such as signal multipathing, while others were made to validate SERIES precision and accuracy by comparison with surveys on baselines of various lengths. This paper will present the initial results of tests made with the SERIES system on baselines of 0 meters, 150 meters, 21 kilometers and 171 kilometers.

EARTH STRAIN MEASUREMENTS WITH TRANSPORTABLE LASER RANGING SYSTEM AND STABILITY OF LASER RANGING STATIONS

Yosio Nakamura, H. James Dorman[1] and Thomas Cahill[2]
The University of Texas at Austin, Institute for Geophysics
Austin, Texas 78751

We have conducted a feasibility study to examine the potential of the Transportable Laser Ranging System (TLRS) for monitoring the ground deformation around satellite ranging stations and other geodetic control points. Emphasis has been placed on testing the usefulness of the relative lateration technique. The temporal variation of the ratio of the length of each survey line to the mean length of all survey lines in a given area is directly related to the mean shear strain rate for the area. The data reduction also gives the movement of the TLRS site relative to the surrounding area. The data from a series of experimental measurements taken over the Los Angeles basin from a TLRS station at Mt. Wilson show that such ratios can be determined to an accuracy of one part in 10^7 with a measurement program lasting for three days and without using any corrections for variations in atmospheric conditions. A numerical experiment using a set of hypothetical data indicates that reasonable estimates of the present shear strain rate and the direction of the principal axes in southern California can be deduced from such measurements over an interval of one to two years. Thus, the relative lateration from the TLRS appears to be a very economical way to monitor ground deformations and stability of satellite laser ranging stations, although there has been no opportunity yet to measure the actual ground strain by reoccupying the Mt. Wilson site.

[1]Now with Exxon Production Research Co., Houston, Texas.

[2]Now with Dept. of Geological Sciences, Cornell Univ., Ithaca, New York.

MOBILE VLBI BASELINE RESULTS FROM 1981

J. M. Davidson, D. W. Trask, K. S. Wallace, J. L. Fanselow
California Institute of Technology, Jet Propulsion Laboratory,
4800 Oak Grove Drive, Mail Stop: 264-748, Pasadena, California 91109.

ABSTRACT

The 1981 Mobile VLBI Campaign spanned four "bursts" or data sessions, these being in February, May, August and December. All sessions involved DSS 13 (near Barstow, California), the OVRO 40m telescope (Big Pine, California), and the Ft. Davis 26m telescope (near El Paso, Texas) as fixed base stations, and the 3.7 m transportable telescope (MV-2) as a mobile station. The mobile stations occupied a total of 14 different sites a total of 18 times during these four sessions. We will report on the baseline results from the first three sessions of the 1981 Mobile VLBI Campaign. Sites visited by MV-2 in these sessions include JPL, Palos Verdes, Pearblossom (February), JPL, La Jolla, Monument Peak, Yuma, and Piñon Flats (May) and JPL, Palos Verdes, Pearblossom, Gorman, Santa Paula and Vandenberg AFB (August). Emphasis will be placed on improvements in system precision resulting from the transition to Mark III data recording, introduction of dual frequency (S-X) data recording, introduction of water vapor radiometers, and the introduction of broad bandpass FET receivers.

Predicting Polar Motion & Earth Rotation

A. K. Babcock and D. D. McCarthy
U. S. Naval Observatory
Washington, D. C. 20390

The U. S. Naval Observatory has been involved for some time in the prediction of Earth orientation parameters, and has been publishing its predictions of these values forty days in advance in its weekly "U. S. Naval Observatory Time Service Announcement Series 7". The techniques used to make these predictions are subject to continuous scrutiny and revision in a constant effort to improve both their quality and range. Predicting the variations in the Earth's speed of rotation has presented some special challenges, due to the largely random nature of the short term disturbing forces, apparently meteorological in origin. The techniques used to account for these short term effects are discussed, along with an analysis of the accuracy of the predictions currently available.

The introduction of the IAU 1980 Nutation Theory in the computation of the Earth Rotation Parameters by the Bureau International de l'Heure, a proposal.

Nicole Capitaine and Martine Feissel
Bureau International de l'Heure
61, avenue de l'Observatoire
75014 Paris France

The effect of the nutation theory in the computation of the Earth Rotation Parameters from the different observational techniques is examined. The impact on the combined solution of the Bureau International de l'Heure is evaluated. In view of the improvement brought by the IAU 1980 Nutation Theory, it is proposed that this theory be introduced in the BIH publications without waiting for the adoption by the astronomical ephemerides (1984 Jan. 1).

EFFECTS OF ADOPTING NEW PRECESSION, NUTATION AND EQUINOX CORRECTIONS ON THE TERRESTRIAL REFERENCE FRAME

Sheng-Yuan Zhu* and Ivan I. Mueller
Dept. of Geodetic Science and Surveying, Ohio State University
1958 Neil Avenue, Columbus, Ohio 43210
*(on leave from Shanghai Observatory, China)

ABSTRACT

First, the effects of adopting new definitive precession and equinox corrections on the terrestrial reference frame are presented. The effect on polar motion is a diurnal periodic term with an amplitude increasing linearly in time; on UT1 it is a linear term. Second, general principles are given, the use of which can determine the effects of small rotations (such as precession, nutation or equinox corrections) of the frame of a Conventional Inertial Reference System (CIS) on the frame of the Conventional Terrestrial Reference System (CTS). Next, seven CTS options are presented, one of which is necessary to accommodate such rotations (corrections). The last of these options requiring no changes in the origin of terrestrial longitudes and in UT1 is advocated; this option would be maintained by eventually referencing the Greenwich Mean Sidereal Time to a fixed point on the equator, instead of to the mean equinox of date, the current practice. Accommodating possible future changes in the astronomical nutation is then discussed. Next presented are the effects of differences which may exist between the various CTS's and CIS's (inherent in the various observational techniques) on earth rotation parameters (ERP) and how these differences can be determined. It is shown that the CTS differences can be determined from observations made at the same site, while the CIS differences by comparing the ERP's determined by the different techniques during the same time period.

Reference

Zhu, S.Y. and I.I. Mueller (1982), "Effects of Adopting New Precession, Nutation and Equinox Corrections on the Terrestrial Reference Frame," Bulletin Geodesique, in press.

POLARIS Activities and Achievements

W. E. Carter and D. S. Robertson
National Geodetic Survey, NOS, NOAA
Rockville, Maryland 20852

ABSTRACT

Since November 1980, the partially completed POLARIS network has produced more than 90 measurements of the X-component of polar motion and UT1. The POLARIS UT1 time series is the most accurate series regularly available. It has already contributed significantly to our knowledge of the short period variations in the Earth's rotation. The third POLARIS observatory, at Richmond, Florida, is scheduled for completion during 1983. At that time the network will also begin producing measurements of the Y component of polar motion.

The POLARIS observations also yield baseline length measurements. A tabulation of lengths between the POLARIS observatories and several other fixed observatories, as well as initial results of Mobile VLBI observations at National Crustal Motion Network stations, will be presented and interpreted.

A Fine-Structure Analysis of the Earth's Polar Motion Using ILS Data

B. Feng Chao
National Research Council Research Associate
Goddard Space Flight Center
Greenbelt, MD 20771

ABSTRACT

The 80-year long, homogeneous ILS (International Latitude Service) polar-motion time series reduced by Yumi and Yokoyama (1980) is analyzed by means of the "Autoregressive (AR) method" devised by Chao and Gilbert (1980, Geophys. J. Roy. Astron. Soc., 63, 641-657). Three wobble motions are examined: the annual wobble, the 14-month Chandler wobble, and the 30-year "Markowitz" wobble, with emphasis upon the fine structures in the Chandler wobble.

The AR method, basically, is a frequency-domain formulated Prony's method. It yeilds estimates of the complex frequency (or frequency and Q) and the complex amplitude (or amplitude and phase) for each component in the time series, independent of any other component present in the series. The results are listed in Tables 1-3.

Principal conclusions of this analysis are: (i) the ILS data are consistent with a Chandler wobble model consisting of four components, each of which represents a quasi-steady, nearly-circular, prograde motion--and this is not consistent with the model that the Chandler wobble has been excited randomly; (ii) the four-component Chandler wobble model "explains" the apparent phase reversal during 1920-1940 and the pre-1950 empirical period-amplitude relation; (iii) the annual wobble is shown to be rather stationary over the years both in amplitude and in phase; (iv) the Markowitz wobble appears to have a complicated behavior, but the dataset is too short to resolve any detail--however, a temporal correlation between the amplitude variation of the Markowitz wobble and that of the Chandler wobble is clearly indicated.

Table 1
AR estimates for the Markowitz wobble.

	Period (yrs)	Q	Amplitude (″)	Phase (°)
ILS-X	29.6	-88	0.0246	197
ILS-Y	31.7	-43	0.0230	242

Table 2
AR estimates for the annual wobble.

	Period (days)	Q	Amplitude (″)	Phase (°)
ILS-X	365.20	-1480	0.0884	108
ILS-Y	365.10	1370	0.0840	10

Table 3
AR estimates for the chandler wobble from (a) *ILS-X-CW* (b) *ILS-Y-CW*.

Comp. No	(Period (days)	Q	Amplitude (″)	Phase (°)
I	406.45	1840	0.0267	216
II	426.00	711	0.1199	273
III	437.46	-189	0.0573	342
IV	452.73	180	0.686	150

(a)

Comp. No	Period (days)	Q	Amplitude (″)	Phase (°)
I	406.85	-386	0.0170	132
II	426.15	703	0.1195	185
III	437.43	-184	0.0572	253
IV	452.39	320	0.0569	54

(b)

EARTH ROTATION STUDIES USING LUNAR LASER RANGING DATA

J.O. Dickey and J.G. Williams
Jet Propulsion Laboratory
California Institute of Technology
Pasadena, California 91109

ABSTRACT

The rotational orientation of the earth has been determined from lunar laser ranging (LLR) measurements. The values of UT1 are available through May 1982 in three forms: the raw results, the Gaussian filtered values and the Fourier smoothed values. Improved procedures permit an error estimation of the latter two values. The variation of latitude results will be presented. Comparisons will be made with measurements from other techniques.

LUNAR LASER RANGING: GEOPHYSICAL PARAMETERS, EPHEMERIDES AND MODELING

J.O. Dickey and J.G. Williams
Jet Propulsion Laboratory
California Institute of Technology
Pasadena, California 91109

ABSTRACT

Lunar laser ranging data collected at McDonald Observatory, Texas from August 1969 to May 1982 has been analyzed with respect to the most recent JPL lunar and planetary ephemeris, DE 119/LE 63. The modeling of several systematic effects has reduced the rms residual. Improved results will be given for GM_{earth}, the tidal acceleration and other geophysical parameters.

The lunar and planetary orbit integrator and the ephemeris DE 102/LE 51 are described in a paper to be published in Astronomy and Astrophysics. While this ephemeris has been surpassed in accuracy by more recent ephemerides, its uncommonly long span permits the extraction of the equinox offset and obliquity. The obliquity, $23^{\circ}26'44''.816 \pm 0''.015$ at B1950.0, is $0''.039$ smaller than the recently adopted IAU value. The obliquity and equinox offset implicit in the shorter ephemerides can now be recovered by differencing. Thus DE 119/LE 63 was oriented with the dynamical equinox as its fundamental zero point, a property which achieves consistency with the new IAU conventions and is important to the unification of coordinate systems.

Further Investigation into Effects of the Oceans on Polar Motion

S.R. Dickman
Department of Geological Sciences, State University of New York,
Binghamton, New York 13901

ABSTRACT

The effects of the oceans on polar motion have been studied by treating the fluid oceans and underlying solid earth as a coupled two-body system. From a rotational point of view, oceanic wobble is possible because non-globality allows any misalignment of oceanic rotation and principal axes to be maintained. Wobble characteristics of the uncoupled bodies have been determined and were presented at last year's conference. At that time, the equations governing wobble of the coupled system were also presented, for the case of rigid bodies.

These equations have now been correctly extended to the case of deformable bodies. The underlying earth responds elastically to wobble, and possesses a fluid core. The oceans are assumed to respond in an equilibrium fashion to their own wobble--a reasonable supposition because the wobble periods are long when the coupling strengths are realistically large. Rotation of the deformable system has been investigated with the ocean - solid earth torque assuming for simplicity a variety of general forms.

The retrograde character of free oceanic wobble leads to coupled motions which, depending on the torque, are at best undamped and at worst unstably damped. Those types of coupling which avoid unstable rotational behavior, and also generate one wobble mode similar to the Chandler wobble, predict a second wobble mode with the long period and retrograde (or marginally prograde) sense of the Markowitz wobble. Such coupling, being non-dissipative, implies that both wobbles are attenuated by a combination of shallow-sea interactions and internal friction within mantle and oceans.

From these studies it appears that the Markowitz wobble can be viewed as a natural wobble of an earth possessing oceans.

COMPARISON OF OCEAN TIDE MODELS FOR LAGEOS AND STARLETTE ORBIT ANALYSIS

R. J. Eanes, B. E. Schutz and B. D. Tapley
The University of Texas at Austin
Center for Space Research
Austin, Texas 78712

ABSTRACT

Various questions concerning the application of ocean tide models to the computation of satellite orbits are discussed. These questions include the choice of models, the allowable truncation in their application, the use of equilibrium estimates for zonal tides for which non-equilibrium solutions are not available, and the extension of existing models to nearby frequencies in the tidal spectrum. Recent state-of-the-art global ocean tide models are compared by computing the differences in their effect on the Lageos and Starlette orbits. For example, the difference in the six-constituent model of Parke from that of Schwiderski produces maximum differences in the Lageos node equivalent to about 1 msec of UT1. The RMS difference in Lageos inclination is 10 msec of arc (mas), while the RMS of the residuals from the Lageos long arc LLA 81.12 is 14 mas. Truncation of the ocean tide models above degree 6 produces negligible errors for Lageos, while the errors in the Starlette node are equivalent ot 0.5 msec of UT1. Modeling only even-degree ocean harmonics is sufficient for the inclination and node but not for eccentricity and periapse. Inclusion of the odd-degree terms substantially improves the long-arc eccentricity residuals for both satellites.

EARTH AND OCEAN TIDAL EFFECTS ON THE LAGEOS ORBIT

Peter Dunn and Mark Torrence
EG&G WASC Inc.
Riverdale, Maryland 20737

ABSTRACT

A procedure has been developed for monitoring Earth orientation and station position from laser observations to the LAGEOS spacecraft. This technique also yields precise estimates of the satellite orbit position averaged over the arc-length of thirty days. By comparing these 'short arc' elements with those predicted over the full six year time span of the LAGEOS orbit, any errors in our orbit perturbation model which are longer in period than thirty days can be identified.

The evolution of the satellite's inclination is predictable except for possible errors in the adopted model for the Earth and ocean tidal potential. The tidal perturbations also affect the motion of the satellite's node, which is further influenced by any errors in the adopted series of values for Universal Time. The frequencies of significant tidal effects are predictable and a spectral decomposition of signatures in the inclination and node has been made to yield an improved model including both second and fourth degree terms.

Although the effects of the ocean tides cannot be separated from those raised in the solid Earth, if we assume an Earth tidal model due to Wahr, implicit corrections to the Schwiderski ocean tidal model can be obtained. The significance of these corrections will be described and the use of the improved model in the resolution of Universal Time will be discussed.

EFFECT OF DIFFERENT EARTH MODEL ON LOADING TIDAL CORRECTIONS

H. T. Hsu and W. G. Mao
Institute of Geodesy and Geophysics
Academia Sinica

ABSTRACT

There is close relation between loading tidal correction and structure of crust and upper mantle. By using recent 1066A earth model, we have recalculated the loading love numbers and obtained loading Green's functions for gravity, tilt and strain. It is shown that there are considerable difference of Green's function obtained by these two models, especially for small Ψ. Afterwards, we have estimated the effect of different model on loading correction, in which the evaluation of distant region is carried out by analytical method, and for near region, by using digital method.

LENGTH OF DAY AND THE ATMOSPHERIC ANGULAR MOMENTUM: THE CROSS VALIDATION OF EARTH ROTATION AND METEOROLOGICAL DATA

T. M. Eubanks, J. A. Steppe, J. O. Dickey, P. S. Callahan
Jet Propulsion Laboratory, California Institute of Technology
Pasadena, CA 91109

ABSTRACT

Changes in the circulation of the earth's atmosphere cause fluctuations in the Length of Day (LOD) by exchanging angular momentum with the solid earth. Estimates of the atmospheric polar angular momentum and the earth rotation from May 1976 to June 1981 were compared in both the time and frequency domain. The possibility of exchanges of angular momentum with the core and the oceans was also examined. The Atmospheric Angular Momentum (M/atm) was provided by R. D. Rosen and D. A. Salstein of Atmospheric and Environmental Research in Cambridge, Massachusetts [Rosen and Salstein, 1981] from the zonal wind estimates of the National Meteorological Center operational weather analysis. These data were sampled every five days at the epoch of the earth rotation estimates. Earth rotation measurements included UT1 from the BIH and from lunar laser ranging. The earth rotation measurements were found to be consistent. The measured LOD* [LOD* is defined as LOD minus significant tidal effects with a period of a year or less] was found to have a long period drift not matched by the M/atm data. This drift is probably the result of an exchange of angular momentum between the core and the mantle. M/atm changes were found to dominate the earth rotation fluctuations for periods at and below a year. The spectral power of the M/atm data is proportional to the inverse frequency squared for periods between 1 year and about 3 days, and flattens out at higher frequencies. The LOD* spectra are also proportional to the inverse frequency squared except for periods of < ~40 days where the earth rotation measurement noise seems to dominate. The coherence between the LOD* and m/atm data is highly significant between periods of 700 and 40 days. The phase between the M/atm and LOD* data is near the expected value of zero for periods > 40 days. There is a major discrepancy in the semi-annual component that is probably some combination of errors in the atmospheric data, errors in the model of tidal variations in the earth rotation, and unmodeled exchanges of angular momentum with the oceans. There is a drop in the coherence between the atmospheric and earth rotation data at a period of 100 days which is probably due to errors in the atmospheric model or an unknown source of terrestial angular momentum. A broad spectral peak between 40 and 60 days is clearly evident in all the time series.

Rosen, R. D. and Salstein, D. A., "Variations in Atmospheric Angular Momentum" ERT Technical Report A345-T1, Concord, MA, Environmental Research and Technology (1981).

BASELINE DETERMINATION FROM SIMULTANEOUS RANGE-DIFFERENCES TO LAGEOS

Erricos C. Pavlis and Ivan I. Mueller
Dept. of Geodetic Science and Surveying, Ohio State University
1958 Neil Avenue, Columbus, Ohio 43210

ABSTRACT

Inaccurate or incomplete satellite orbital models are the limiting factors in the estimation of geodetic parameters with accuracies comparable to those of our measurements (SLR in particular). Recent studies have demonstrated that the quality of the results can be improved by simply requiring that the satellite passes are coobserved by several stations.

This investigation studied the possibility of further improving the results by use of the simultaneously observed ranges to Lageos from pairs of stations in a range-differencing mode (Fig. 1.) Simulation tests have shown that model errors are effectively minimized in this mode for a rather broad class of network-satellite pass configurations. Parameters of primary interest here are the baseline lengths.

Lack of strictly simultaneous laser ranging events forced us to examine possible techniques for the generation of quasi-simultaneous range-differences (SRD's). Between least squares approximation with monomials and with Chebyshev polynomials, the latter seems to be a much more stable method. If, however, the data record is dense, cubic splines interpolation is faster, simpler, and circumvents the problem of correlation between the SRD's which cannot be avoided in the approximation methods. With most of the new generation lasers having repetition rates below the 1 pps, this method seems to be the most suitable and economical way for SRD generation.

Analysis of three types of orbital biases (radial, along- and across-track) has shown that radial biases are the ones most efficiently minimized in the SRD mode. The degree to which the other two can be minimized depends on the type of parameters under estimation and the geometry of the problem. In any event, they can be minimized too, without resorting to very restrictive data requirements. Sensitivity analyses of the SRD observation yielded a number of interesting results as far as geodetic parameters go.

For baseline length estimations the most useful data are those collected in a direction parallel to the baseline and at a low elevation. Refraction model biases in this case will be grossly eliminated in the differencing process. When estimating baseline lengths with respect to an assumed but fixed orbit, independent solutions for each baseline further reduces the effects of model biases on the results as opposed to a network solution. Since the baselines are indirectly estimated from the endstation coordinates, enforcing the simultaneity constraint ensures that the results

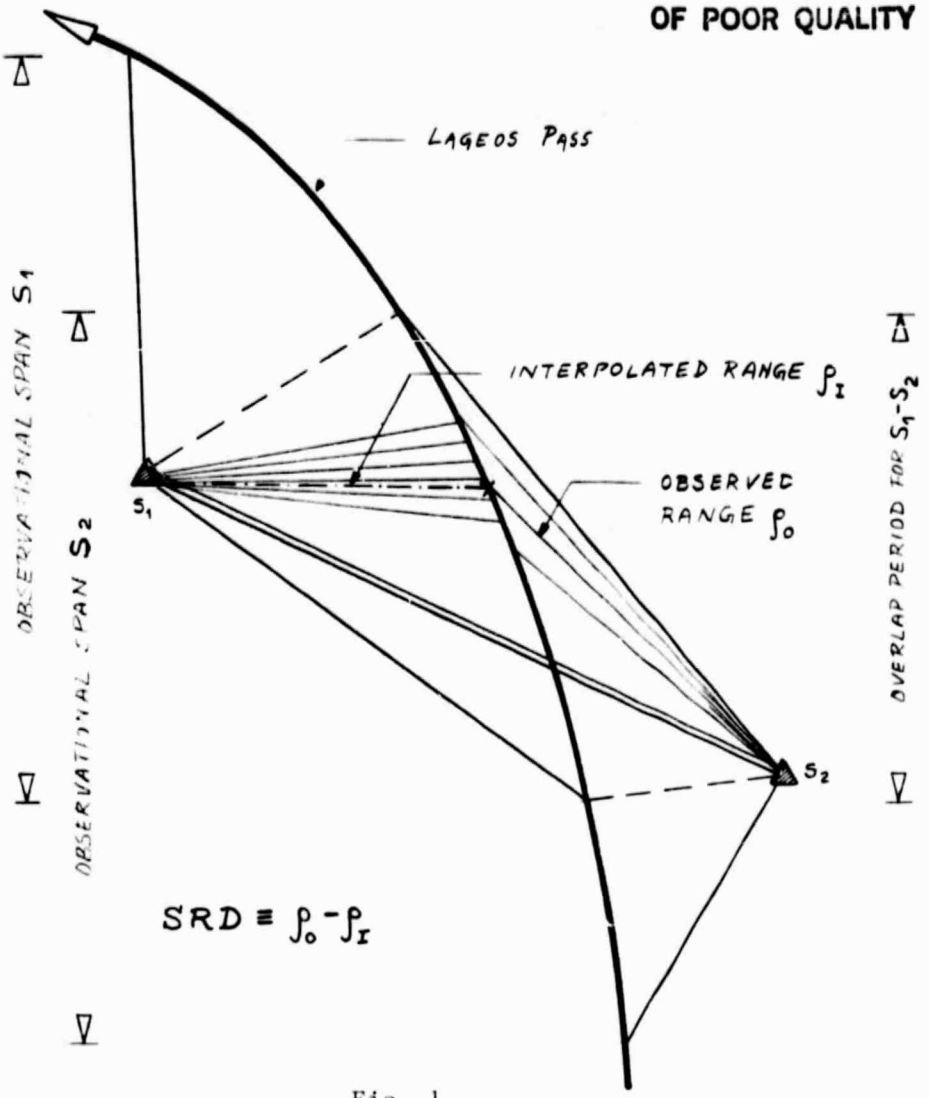

Fig. 1

Table 1

NO.	BASELINE END STATIONS	APRIORI LENGTH	RANGE SOLUTION OBS.	RANGE SOLUTION COORD. NORM	RANGE SOLUTION RECOVERY ERROR	RANGE SOLUTION FORMAL SIGMA	SRD SOLUTION OBS.	SRD SOLUTION COORD. NORM	SRD SOLUTION RECOVERY ERROR	SRD SOLUTION FORMAL SIGMA
1	7901 => 7914	1123487.006	7202	3.572	-0.117	0.017	3601	1.959	-0.003	0.018
2	7095 => 7940	2308853.694	5976	3.489	-0.362	0.019	2988	1.712	-0.047	0.028
3	7942 => 7999	700368.121	7460	3.730	-0.096	0.019	3730	1.198	0.010	0.016
4	7095 => 7942	1484591.097	6954	3.582	-0.228	0.020	3477	1.371	0.004	0.020
5	7091 => 7069	2044497.683	4496	3.544	-0.305	0.022	2248	1.336	0.010	0.029
6	7069 => 7086	2363121.040	4112	3.532	-0.375	0.025	2056	1.250	0.041	0.036
7	7063 => 7051	3701986.397	3944	3.264	-0.666	0.025	1972	1.150	0.038	0.069
8	7051 => 7086	1840222.236	5296	3.641	-0.308	0.023	2648	1.145	0.020	0.027
9	7120 => 7051	3909408.182	2950	3.220	-0.724	0.030	1475	1.386	-0.035	0.083
10	7086 => 7063	2618612.747	4666	3.500	-0.452	0.025	2333	0.925	0.090	0.039

will also be free of possible biases introduced by inconsistent coordinate systems in which independent station determinations refer. Table 1 gives the results of one simulation test for ten baselines (Fig. 2), where ranges to Lageos (σ = 10 cm) were analyzed in the classical as well as the SRD mode. Using identical data and the same orbit (including meter-level biases), the rms of recovery errors between the two solutions shows a ratio of 10:1 in favor of the SRD solution.

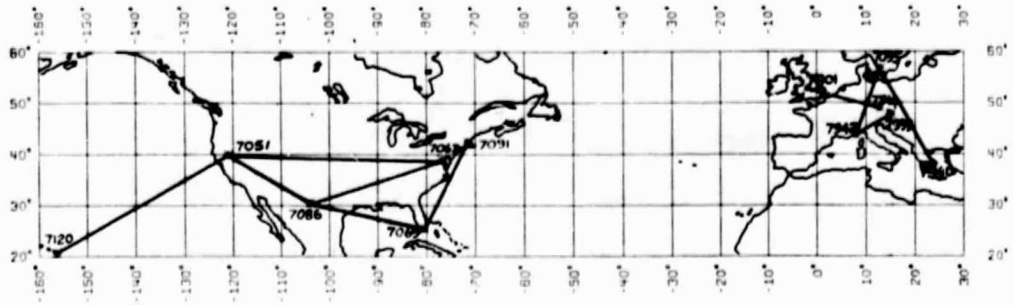

Fig. 2

Simulation studies have also been done for the estimation of polar motion parameters using the SRD mode with similar conclusions as for the baseline case.

Analysis of real Lageos data did not yield any significant conclusions mainly due to the lack of simultaneously coobserved passes. Some preliminary results though have confirmed the conclusions drawn from the simulation studies. A more detailed presentation of the investigation results and the simulation studies performed can be found in [Pavlis, 1983].

Reference

Pavlis, E.C. (1983), "On the Geodetic Applications of Simultaneous Range-Differencing to Lageos," Dept. of Geodetic Science and Surveying Rep. 338, Ohio State Univ., Columbus.

COMPARISON OF JPL EARTH ORIENTATION RESULTS FROM THE TEMPO PROJECT WITH OTHER TECHNIQUES

T. M. Eubanks, P. S. Callahan, J. A. Steppe
Jet Propulsion Laboratory, California Institute of Technology
Pasadena, CA 91109

ABSTRACT

The JPL Time and Earth Motion Precision Observations (TEMPO) program observes station clock behavior and earth orientation to support interplanetary navigation by the Deep Space Network (DSN). TEMPO data will also be used as part of the IAU/IUGG MERIT campaign. The TEMPO program consists of weekly dual-band VLBI observing sessions over both the DSN California-Spain and California-Australia baselines. The data from observations on each baseline are reduced to UT0 and Variation of Latitude for that baseline and combined to estimate all three components of the earth orientation. The TEMPO program goals include weekly determinations of the earth orientation to within 10 milliarcsec.

Almost two and a half years of TEMPO earth orientation data (starting in July 1980) has been reduced using a J2000 coordinate system. The difference between otherwise identical solutions using 1950 and J2000 epochs is a bias of about -3 milliarcseconds in Polar Motion and about 0.7 milliseconds in UT1 (J2000 minus 1950). The observing strategy, data processing and experimental history of the TEMPO program will be described. The internal consistency of the TEMPO results will be discussed, including a comparison of S, X and SX solutions using the same data set and the agreement of the component of earth orientation measured by both baselines in the weekly observations. The results of a comparison of TEMPO data with earth orientation results from the BIH, Satellite and Lunar Laser Ranging, and the POLARIS project will also be discussed. Plans to improve the accuracy and reliability of the TEMPO data for the main MERIT campaign will also be described.

Improved Representation of Earth Rotation For Geophysical Studies

P. J. Morgan, R. W. King, and I. I. Shapiro*

Department of Earth and Planetary Sciences
Massachusetts Institute of Technology
Cambridge, MA 02139

Measurements of the earth's rotation (pole position and universal time or length of day) have improved markedly over the past ten years as new observation techniques have been introduced. We have analyzed time series of earth rotation values obtained using classical astrometric (CA), satellite Doppler (SD), lunar laser ranging (LLR), and satellite laser ranging (SLR) observations in order to obtain more accurate series for geophysical studies. By intercomparing the various results we have been able to bound the systematic and random errors in each series and to determine appropriate weights for their combination. We describe here the characteristics of a combined series, proposed as an improved representation of earth rotation.

Our series for pole position, compiled using a Gaussian filter whose full width at half maximum (FWHM) amplitude was 33 days, is dominated by the SD results from 1971 through 1976; each (independent) element has a one standard deviation error of about 5 milliseconds of arc (mas) (∿15 cm). After 1976, both LLR and SLR observations make a substantial contribution, reducing the standard errors to 3 mas (∿10 cm) for 1976-1978 and 1.5 mas (∿5 cm) after 1979.

For universal time (UT1), where the FWHM of the Gaussian filter used is 8 days, LLR provides the only data set which is free from significant systematic error and spans the entire ten-year period. Gaps in the LLR values have been filled using the CA results before 1976 and the SLR results thereafter. We estimate the standard error in the (independent) elements of the combined series to be about 1 millisecond of time (ms) (∿50 cm) before 1976 and about 0.5 ms (∿25 cm) thereafter.

The accuracy of these series for pole position and UT1 will be further improved in the future by incorporating VLBI values, obtained regularly with comparable accuracy since early 1981 by the National Geodetic Survey's Project POLARIS.

* Now at the Harvard-Smithsonian Center for Astrophysics, Cambridge, MA 02138

Recent Progress in Studies of Atmospheric Excitation of Earth Rotation/Polar Motion

Richard D. Rosen and David A. Salstein
Atmospheric and Environmental Research, Inc.
840 Memorial Drive, Cambridge, MA 02139

Alvin J. Miller
National Oceanic and Atmospheric Administration, NMC/CAC
Washington, DC 20233

Calculations of the atmosphere's angular momentum each day are being made on a continuing basis with wind analyses produced by the U.S. National Meteorological Center (NMC). Study of these wind analyses has helped identify the origin of a near 50-day periodicity that is apparent in both the angular momentum time series and those for changes in the length-of-day.

Beginning with 1 January 1981, daily values of atmospheric angular momentum are also being produced by R. Hide and colleagues at the British Meteorological Office (BMO) using independent atmospheric analyses from the European Centre for Medium Range Weather Forecasts (ECMWF). Comparisons between the NMC and ECMWF results provide a means for assessing the errors present in these estimates of the atmospheric forcing function for earth rotation.

The meteorological data sets from NMC and ECMWF are also being used to examine the role of the atmosphere in exciting polar motion. Recent work by BMO scientists indicates that short-term fluctuations within the atmosphere may indeed play an important role in explaining the irregular motions of the pole.

ATMOSPHERICALLY INDUCED VARIATIONS IN THE LENGTH-OF-DAY DERIVED FROM LAGEOS

D.E. Smith, D.C. Christodoulidis, and G.H. Wyatt
Goddard Space Flight Center
Code 921, Greenbelt, MD 20771

ABSTRACT

Estimates of the length-of-day (LOD) derived from laser tracking of the Lageos spacecraft have been analyzed and compared with inferred changes in length-of-day deduced from atmospheric angular momentum. Six years of data from Lageos and angular momentum beginning in May 1976 have been studied. Earth tidal corrections have been applied to the Lageos LOD at annual, semi-annual, monthly and fortnightly periods and both data sets reduced to 5-day averages. Spectral analyses of the six years of atmospheric data show very little power below 100 days although short lived phenomena are clearly evident at times within the data set. Most of the power is in the annual term with a much smaller amount at 6 months. The lageos data set shows much power at the semi-annual frephency (even after applying a tidal correction) and is, perhaps, the frequency where the largest difference with the atmosphere appears to occur. In addition, the variation in the Lageos LOD clearly shows that the rotation rate of the earth is steadily increasing over the six year period while the atmospheric momentum shows no discernible secular trend, confirming that very long-term changes in LOD of the solid earth are probably caused by motions in the earth's core rather than the atmosphere.

Comparison of the two raw data sets over the six year period shows very good agreement, particularly since 1979 when the Lageos tracking data increased significantly in quality. Over-all correlation of the two data sets is about 0.82 for the entire data span. When all periods greater than 80 days are removed from both data sets the residual variations remain correlated at about 0.6 and the comparison suggests that even on time scales as short as 5 to 10 days that the solid earth is responding to atmospheric changes. Studies of the hemispheric components of the atmospheric angular momentum suggest that the northern hemisphere dominates in the atmosphere-solid earth interaction but that the southern hemisphere winds can, on occasion, cause observable changes in the rotation of the earth.

UT1 FROM LAGEOS LASER RANGING

B. E. Schutz, B. D. Tapley and R. J. Eanes
The University of Texas at Austin
Center for Space Research
Austin, Texas 78712

ABSTRACT

Because of unmodeled or incompletely modeled phenomena in the forces acting on Lageos and in the orientation of the earth, orbit element residuals exist in long-arc analyses using laser range data. Residuals in the location of the ascending node, Ω, of the Lageos orbit plane contain information on UT1, as well as geophysical information, such as tides. Because of the inseparability between Ω and UT1, the accuracy of a UT1 determination is dependent on the accuracy of the Ω modeling. From long arcs of several months duration to those spanning several years, experiments have been conducted for UT1 determinations. These experiments and the models used are discussed. The UT1 determinations resulting from these experiments are compared with those obtained by independent techniques.

CRUSTAL DYNAMICS PROJECT MEASUREMENT ACCOMPLISHMENTS IN 1982

H. Frey
Goddard Space Flight Center
Greenbelt, MD 20771

ABSTRACT

The Crustal Dynamics Project in 1982 conducted Satellite Laser Ranging and Very Long Baseline Interferometry measurements to determine regional crustal deformation in Western United States, global plate motion, plate stability, polar motion, and changes in earth rotation. An overview of the measurements conducted will be presented which details the specific stations used and baselines measured.

PRECISION LASER SATELLITE TRACING FOR CRUSTAL DYNAMICS

Dr. Andrew G. Adelman
Goddard Space Flight Center

ABSTRACT

The Goddard Laser Tracking Network has utilized the extreme precision attainable through laser ranging to make precise geodetic measurements. The fixed, mobile, and transportable laser systems composing the network are located on the boundaries of the earth's tectonic plates and on fault locations. By tracking three satellites whose orbits are precisely known -- Lageos (Laser Geodynamics Satellite), Starlette, and Beacon Explorer -- the system currently measures plate translation, rotation, and elevation changes to a precision of better than 2 cm.

The network of laser stations is made up of seven mobile systems (MOBLAS) and one air transportable system (TLRS-2) operated by the Bendix Field Engineering Corporation, one fixed and one mobile tracker operated by the University of Texas, and a fixed station on Mt. Haleakala, Maui, operated by the University of Hawaii. In addition to these stations, two laser trackers in Australia, one at Yaragadee (MOBLAS 5) and one at Orraral Valley (NATMAP), and one in Arequipa, Peru, are part of the network. Ten foreign cooperative observatories provide continuous tracking data to the network for input to the Crustal Dynamics Science Program.

This paper will address the network expansion and upgrade program, providing statistics on present capability, the addition of stations to the network, and the equipment modifications made to reach a precision approaching 1 cm.

Techniques for Improving the Performance of Satellite Laser Ranging Systems

John J. Degnan
Thomas W. Zagwodzki

ABSTRACT

Satellite laser ranging instruments are subject to two types of error - bias and random noise errors. Through proper choice of commercially available system components, instrumental single shot RMS random errors can be reduced to the subcentimeter level (one sigma). Measurement of the system delay, or system bias, in current field systems is usually performed by ranging to a calibration target before and after the satellite pass and subtracting out a "known" range as measured by a surveyor's geodimeter. If the pre and post calibrations differ, a linear time dependence of the bias is assumed in the data reduction. Bias errors can have a distinctly nonlinear temporal dependence, however, due to ambient temperature fluctuations, changes in voltage conditions, or a varying radiation noise background. This temporal dependence can be cancelled to first order through the use of common detectors and electronics for both the start and stop pulses. In addition, the system delay can be effectively reduced to zero by reflecting a portion of the outgoing laser pulse from the system reference plane (or origin) into the common receiver to start the time interval unit. Thus, it is possible to cancel the system bias on a shot by shot basis and eliminate the need for independent geodimeter measurements which appear to have errors at the one to two centimeter level. The limiting errors in the absolute accuracy of the resulting system should be due to uncertainties in the atmospheric refraction correction at the 5 to 10 mm level.

UPGRADING AND STATUS OF THE SAO LASER RANGING SYSTEMS

Michael Pearlman
Smithsonian Astrophysical Observatory

Through the most recent upgrading program, the performance of the SAO lasers has been improved considerably in terms of accuracy, range noise, data yield, and reliability. With the narrower laser pulse (2.5-3.0 nsec) and a new analog pulse processing system, the systematic range errors have been reduced to 3-5 cm and single pulse range noise has been reduced to 5-15 cm on low satellites and 10-18 cm on Lageos. Pulse repetition rate has been increased to 30 ppm and considerable improvement has been made in signal-to-noise ratio by using a 3Å interference filter and by reducing the range gate window down to 200-400 nsec. The first upgraded system is now in operation in Arequipa, Peru. An upgraded system will be installed in Matera, Italy in early 1983.

THE MCDONALD LASER RANGING STATION

Peter J. Shelus and David K. Aubuchon
McDonald Observatory and Department of Astronomy
University of Texas at Austin
Austin, Texas 78712 USA

The McDonald Laser Ranging Station (MLRS) has been designed to be a joint artificial satellite/lunar laser ranging station to replace similar types of activities which were performed on the 2.7 meter telescope. Although there have been some delays in station implementation, MLRS was deemed to be operational with respect to the LAGEOS target in early summer 1982 and co-location tests were run during the late summer and early fall of 1982 with good success. This report will review the recent history of MLRS/LAGEOS operations and touch briefly on the major milestones encountered along the path to regular operations. Co-location results will be discussed together with what was learned from that co-location test. Data taken with the station will be summarized and the data quality statistics will be presented. Finally, brief comments will be made with respect to MLRS lunar capabilities at the present time.

TLRS-2 STATUS AND PERFORMANCE

Thomas S. Johnson
Goddard Space Flight Center

ABSTRACT

TLRS-2 is a small satellite laser ranging system capable of transportation on commercial passenger aircraft. The system design, collocation testing and performance will be reviewed. The status of the first field operation at Easter Island and future plans will be covered.

ON SITE DATA ANALYSIS/PROCESSING

Paul J. Seery
DBA

ABSTRACT

On-site data analysis and processing has become an integral part of laser system support--especially with respect to the more mobile units being developed today. Data quality assessment at the central facility is considered to be one of the most important issued by the scientific user. But in order to achieve this, the data processing at the site must be of quality standards. The quality assessments are taken from tracking and calibration data. It thus becomes necessary to be able to process both types of data accurately and use same for system diagnostics and performance valuation since this is a cyclic process.

The on-site laser system software for the NASA/MOBLAS Units has improved many fold from the initial system software installation to the current operational system developed by DBA Systems, Inc. DBA's involvement began in 1976 with the Honeywell computers in Moblas 1, 2, 3 and Stalas and later included the Moblas units 4-8 which utilize the Modcomp computer. The improvements to the NASA laser tracking system to date are such items as logging and delogging of raw/processed data, real time visual display of system selectable variables, real time IRV numerical integration, a real time star calibration using a Kalman filter, improved designate techniques for satellite acquisition such as--Cross Track--IRV ephemeris time bias--variable designate range correction with respect to transmitter delay, an improved pre/post calibration process, a more indepth Quick Look analysis, residual range plotting, and the impelementation of a standard user (Mailing) tape for central processing and subsequent scientific applications.

Currently DBA is also involved in supplying on-going software support to accommodate various engineering changes such as Internal Calibration (IC). The final IC system when developed should eliminate the uncertainty and compensate for variations in system delay time, during a pass and calibration frames. The current method of computing system delay time could be maintained to monitor IC variations as opposed to being eliminated.

OVERVIEW OF GSFC/BENDIX LASER DATA PROCESSING

D. R. Edge
Bendix Field Engineering Corporation
One Bendix Road
Columbia, MD 21045

ABSTRACT

The development of laser data processing techniques and procedures has been a cooperative Bendix/GSFC effort since 1975. In performing data processing operations required to prepare and quality control raw laser measurements for scientific research applications, Bendix has developed the data analysis and software maintenance capabilities required for advanced laser ranging technology processing. Bendix has worked closely with GSFC Code 723 in developing new data processing software for the new TLRS-2 laser tracking system.

Working closely with the GSFC technical community in laser data analysis, Bendix has developed special analysis software which has contributed to the understanding of laser tracking system performance. Polyquick, a collocation analysis program developed by Bendix, has provided an efficient means of evaluating the ranging performance of collocated laser tracking systems.

Bendix has purchased and installed a VAX 11/780 computer system specifically designed to support laser data processing requirements. Bendix is modifying both GSFC and Bendix data processing software to run on the Bendix VAX. The transition of laser data processing operations from GSFC computers to the Bendix VAX 11/780 computer will provide responsive processing support which was not possible in the GSFC computer environment.

THE VERY LONG BASELINE INTERFEROMETRY (VLBI) NETWORK FOR CRUSTAL DYNAMICS

John M. Bosworth - Crustal Dynamics Project
Goddard Space Flight Center
Greenbelt, MD 20771

ABSTRACT

The Crustal Dynamics Project is establishing a network of observatory based and mobile VLBI systems to precisely determine baseline lengths, polar motion and variations in the earth's rotation. These systems are located at sites selected by the Project's scientists to provide significant data on tectonic plate motion, plate stability and regional deformation.

During 1982 several observatory VLBI stations were upgraded or added to the network and the correlator facility at Haystack, MA was upgraded. Similarly, the two mobile VLBI systems were significantly upgraded and a new system, MV-3, was nearing completion.

This presentation will review these activities and those occurring in the international community along with an overview of the plans for the forthcoming years.

Development of K-3 VLBI System in RRL for US-Japan Joint Experiment

Y. Saburi, K. Yoshimura, S. Katoh
Radio Research Laboratories
Koganei, Tokyo 184 Japan

F. Yamashita, N. Kawajiri, N. Kawano, F. Takahashi
N. Kawaguchi, T. Yoshino and Y. Sugimoto

Kashima Branch, Radio Research Laboratories
Kashima, Ibaraki 314 Japan

ABSTRACT

In the Radio Research Laboratories, a five-year plan for the development of a high precision VLBI system (K-3) for geodesy started in 1979. After the agreement between NASA and RRL in 1980 as to US-Japan joint VLBI experiment, the plan was revised thoroughly both in hardware and software in order to use K-3 system for intercontinental observation, which must consequently be compatible with the Mark III system.

As to K-3 hardware, the manufacture of the back-end part including hydrogen maser, water vapor radiometer, system delay calibrator and correlation processor will be completed by March 1983. The overall system check and evaluation will be made in 1983 immediately after the installation of S- and X-band front-end. One channel correlation processor was manufactured for trial, and confirmed that it could perform completely well with suitable software. The processor modules of full 32 channels will be expected to perform efficiently in data processing in near future. A hardware compatibility test if the contents of the K-3 recorded tapes are reproduced correctly by using the Mark III recorder was made at Haystack Observatory in Nov. 1982. The delay time error due to the hardware system is estimated to be 70 ps (2 cm in path length) on the joint experiment.

The K-3 software includes programs for automatic operation, correlator control, bandwidth synthesis, baseline analysis, data-base management and antenna tracking. Unified management of VLBI data becomes possible with the aid of one data-base handler. The automatic operation software (KAOS) has already been developed, and confirmation of compatibility between the KAOS and the Field System of Mark III has been started at G.S.F.C. since Nov. 1982, using one computer sent from RRL. The other software will be completed early in 1983.

The joint experiments between NASA and RRL will start at the beginning of 1984 and be continued at least for five years.

A New Generation of VLBI Receivers for the CDP

Thomas A. Clark
NASA Goddard Space Flight Center
- - and - -
Brian E. Corey
Haystack Observatory

ABSTRACT

The fixed VLBI stations used by the NASA Crustal Dynamics Project (CDP) have used a receiver design developed circa 1976 for the support of all the Project's measurement programs. Beginning with the implementation of the CDP's new Mojave Base Station (MBS) in California, several design revisions are being incorporated to improve performance. It is planned that similar receivers will be implemented for the new Transportable VLBI Data Systems (TVDS) currently under construction, for the NGS POLARIS station at Richmond FL, and for the new facility being built at Wettzell, FRG. It is also planned to replace certain of the existing receivers with the new design to improve VLBI system performance. The major changes embodied in the new receivers include:

- The use of cryogenic FET amplifiers which achieve a factor of 2-3 sensitivity improvement over the existing uncooled parametric amplifiers; measured receiver temperatures on the first prototype package yielded receiver temperatures <15K at S-band and <50K at X-band. The development of these new amplifiers was done at the Univ. of California, (Berkeley) under a grant from NASA. In addition to developing the FET amplifiers, this grant funded development of a low-cost closed-cycle cryogenic system. These amplifiers are now available from a commercial source.

- The dual S/X-band prime focus feed originally developed at JPL for interplanetary spacecraft has been further improved. In the previous implementations, this feed over-illuminated a typical f/d=0.43 dish antenna at S-band. An extension to this feed tailors the dish aperture illumination to a more optimum value, resulting in a 10% improvement in efficiency and a decrease of about 20K in the zenith system temperature.

- A simpler local oscillator system has been developed to improve performance and reliability at reduced cost.

- Additional monitor and control functions interfaced to the Mark-3 control computer are included for status verification.

- An improved mechanical package, which allows for greater interchangeability and ease of maintenance, has been developed.

HYDROGEN MASERS-A REVIEW OF RECENT PERFORMANCE DATA AND CRUSTAL DYNAMICS SUPPORT ACTIVITIES

P. F. Kuhnle
Jet Propulsion Laboratory, Pasedena, California 91109

A. Bates, L. Reuger, and M. Chiu
Applied Physics Laboratory, Laurel, Maryland 20707

P. Dachel, R. Kruger, and R. Kunski
Bendix field Engineering Corporation, Columbia, Maryland 21045

ABSTRACT

Hydrogen masers are an important element in Crustal Dynamics VLBI systems. The Jet Propulsion Laboratory(JPL), the Applied Physics Laboratory(APL), and the Bendix Field Engineering Corporation(BFEC) have extensive hydrogen maser programs both in support of Crustal Dynamics and in support of research and development. In this paper, significant data will be presented from these programs of interest to the geodynamics community.

For the past several years, APL has had a program to develop a new field operable hydrogen maser(NR maser) for NASA programs and to produce these masers for the Crustal Dynamics Project. Recent data on the performance of these NR masers will be presented. Data will also be pesen'ed on an NR maser with a new hybrid quartz-aluminum cavity.

At the request of the NASA Advanced Systems Program, JPL conducted an evaluation of the two most recent H. maser designs available at the time. These were the APL model NR, and the Smithsonian Astrophysical Observatory model VLG-11. Data will be presented from this evaluation including extensive data on environmental performance and long term stability(operation over several months and Allan deviate to 10^6s). A summary of recent activities supporting mobile and western VLBI activities will also be given.

For the past several years,BFEC has been supporting Crustal Dynamics activities and the NASA/GSFC hydrogen maser program. Recently in response to increased requirements for Crustal Dynamics support, BFEC has constructed a 5000 sq ft facility in Columbia, Maryland for hydrogen maser maintenance, refurbishment, construction, and development. Data will be presented on old masers refurbished and upgraded at this facility, on R & D activities, and on improvments in BFEC's hydrogen maser thermal chambers.

ERROR SOURCES IN VLBI

Thomas A. Clark
NASA Goddard Space Flight Center
D. W. Trask and J. M. Davidson
Jet Propulsion Laboratory

ABSTRACT

At the October, 1982 Crustal Dynamics Project (CDP) Investigators meeting, the various VLBI groups presented a consensus of the limiting error sources affecting geodetic measurements using interferometric techniques. The major error source was determined to be the uncertainty in the calibration of the tropospheric path delays at each station; the "wet" component due to atmospheric water vapor represents the major contribution.

These error estimates indicate that VLBI baseline determinations (based on one day's data) should be better than 1-2 cm for horizontal components of the baseline, and better than 5-10 cm for vertical components, given the instrumentation currently available and used in CDP measurement programs.

The error estimates formulated by this group will be summarized and discussed. These will be compared with available data to test the validity of the estimates. These comparisons will examine the VLBI measurement precision as determined by repeatability (on those baselines for which redundant determinations exist), intercomparisons between the analysis results of different groups using identical data sets, and intercomparisons between different techniques (e.g. Satellite Laser Ranging vs. VLBI).

STATUS OF THE ONSALA WATER VAPOR RADIOMETER.

Gunnar Elgered
Onsala Space Observatory
Chalmers University of Technology
S-43900 Onsala, Sweden

ABSTRACT

The Water Vapor Radiometer (WVR) at the Onsala Space Observatory is a dual channel microwave radiometer which measures the atmospheric emission at 21.0 and 31.4 GHz. The two channels are conventional Dicke-switched radiometers with two reference loads at the temperatures 77 and 313 K in each channel. The WVR is an integrated part of the MARK-III data acquisition system and has been used in all geodetic radio interferometry experiments in which the Onsala Space Observatory has participated since the summer of 1980. The excess propagation paths measured with the WVR can show significant differences, over both short and long time scales, from those derived from atmospheric models based on ground surface weather data. This is especially true for observations made during the summer period when there are large amounts of water vapor in the atmosphere. The WVR has also been used frequently during the last year in order to study time and space variations of the integrated amount of water vapor in the atmosphere. These data have been compared with data from radiosondes launched at a distance of 37 km from the WVR site. Among interesting results from this comparison are that the WVR does not show any significant long time drift and the long time average of the integrated amount of atmospheric water vapor is about the same at the two sites, but occasional differences up to 35% have been observed.

Tropospheric Calibration of Geodetic VLBI

Bruce R. Schupler
Computer Sciences Corporation
Code 974
Goddard Space Flight Center
Greenbelt, Maryland 20771

ABSTRACT

The effect of the water vapor portion of the tropospheric propagation medium is one of the major remaining error sources in geodetic VLBI. If there is no knowledge of the state of the atmosphere, the variability of the water vapor produces an uncertainty in long baseline length determinations on the order of 3 cm. To account for this effect we have utilized surface weather data alone and in combination with water vapor radiometers. These methods have the potential to reduce the baseline length uncertainty to the 1 cm level.

The calibrations resulting from these methods during a subset of the June, 1982 Crustal Dynamics Project VLBI experiment involving Westford, Owens Valley, and Fort Davis will be presented and compared. The effect of these calibrations on the recovered baselines will also be presented.

Sensing the wet and dry atmospheric path via observations at low elevation angle: A preliminary investigation

A.E.E. Rogers
Haystack Observatory
Westford, MA 01886

T.A. Herring
Massachusetts Institute of Technology
Cambridge, MA 02139

Observations made at low elevation angles provide a method of estimating the differential atmospheric path delays because the low elevation signature is sufficiently unique to be separately parameterized and estimated. The equivalent zenith path estimated by this method can be compared with estimates made using water vapor radiometry and surface meterological data. The accuracy of the method is limited by azmuthal and temporal variations in the atmosphere.

Source Structure and Source Catalog Effects on VLBI Results.

Chopo Ma
and
David B. Shaffer
Code 974
Goddard Space Flight Center
Greenbelt, Maryland 20771

ABSTRACT

While most compact radio sources are not point-like objects at the resolutions used for VLBI geodesy, radio sources do define a fixed reference frame for geodetic and astrometric studies. Errors in this reference frame can cause systematic errors in recovered parameters. The absolute length of VLBI baselines, for example, is affected by source declinations.

With enough observations, one can make maps of the sources that have structure. These maps are used to correct the delay and rate observables measured during VLBI observations. The corrected observations have been used to determine the position of the brightest peaks in several sources, and to redetermine the baseline length between various antennas.

After the corrections are applied, source positions typically change by less than 1 milliarcsecond, and baseline lengths change by up to a few millimeters. The rms residuals sometimes improve dramatically because a few points that were measured near visibility minima have large corrections. These points are few enough that they do not have a large effect on the baseline length results. The effects of leaving these points out of the solution, based on visibility criteria such as proposed by Thomas, are also examined.

Position catalogs have been compiled in the J2000.0 coordinate system from four radio interferometers: 1) Mark III VLBI using stations in North America and Europe, 2) Mark II VLBI using DSN stations in California, Spain and Australia, 3) the Very Large Array in New Mexico, and 4) the USNO 4-antenna array in West Virginia. The positions of sources are compared between catalogs and the effects of using different catalogs are shown. The definition of right ascension origin, now commonly fixed by the source 3C273B, is discussed. The causes for catalog nonoverlap and the usefulness of each catalog are described.

The Accuracy of VLBI Vector Component Determination

W. E. Strange and J. R. MacKay
National Geodetic Survey, NOS, NOAA
Rockville, MD 20852

ABSTRACT

Most discussions of the accuracy and/or precision of VLBI determinations of differential positions are presented in terms of baseline length. Discussions of directional accuracy of the interstation vectors are generally not addressed, primarily because independent determinations of polar motion and Earth rotation with an accuracy of a few centimeters are lacking. Without the availability of independent polar motion and Earth rotation of sufficient accuracy, it is not possible to separate errors in polar motion and Earth rotation from changes in direction of the interstation vector when comparing repeat determinations of a single baseline vector.

However, if three stations observe simultaneously the internal angle between any two of the vectors is essentially independent of the accuracy of the polar motion and Earth rotation values used. Thus, comparisons of repeat determinations of internal angles provide a measure of the accuracy of determination of the direction of interstation vectors using fixed VLBI station observations. Analyses indicate that the errors in the internal angles are of the order of 0".003. For baselines 3000 to 4000 km in length, this implies errors in determinations of the components of the directional position vector which are perpendicular to the interstation direction of the order of 6 to 8 cm. This suggests that strains can be monitored with an accuracy of 2 parts in 10^8 over intercontinental distances.

JPL VLBI INTERACTIVE DATA ANALYSIS

J. E. Patterson
California Institute of Technology, Jet Propulsion Laboratory,
4800 Oak Grove Drive, Mail Stop: 264-748, Pasadena, California 91109.

ABSTRACT

The JPL VLBI data analysis system is being developed tc provide interactive analysis from the point that data leaves the correlator through to final resolution of baselines. The rationale for creating this VAX-based highly interactive, menu-driven system to house existing programs will be discussed. An estimation of processing time and manpower required to reduce a single baseline will be presented. Flexibility, ease of operation, and analytical capabiities will be described. Plans for further enhancement of analysis capabilities as well as the integration of data flow from the new Block II Correlator into this existing system will be discussed.

SOLV2: A Program to Analyze Large Numbers of VLBI Observations

Jay Cee Pigg Jr. and Michael A. Pelizzari
Computer Sciences Corporation
Code 974
Goddard Space Flight Center
Greenbelt, Maryland 20771

ABSTRACT

Over the past several years the GSFC VLBI group has been engaged in the development and operation of an integrated and documented data analysis and management system. The latest least squares analysis element of this system is the newly operational SOLV2 program. This program was developed using matrix techniques which were originally used in satellite orbit determination work. SOLV2 has the capability of solving for up to 128 "global" parameters such as site and source positions as well as a virtually unlimited number of "arc" parameters such as station clock and earth rotation parameters. Work is currently in progress to expand the limit of 128 global parameters and to improve the flexibility of the program.

The results of the first large SOLV2 solution will be presented. It involved more than 500 parameters, 8 stations, and 24000 observations (each consisting of a delay and a rate measurement) taken from 1979 to 1982.

LAGRANGE PLANETARY EQUATIONS FOR ORBITAL RESONANCES OF EARTH SATELLITES TO TEST THE ACCURACY OF EARTH GRAVITY FIELD MODELS

Jaroslav Klokočník

Astronomical Institute of the Czechoslovak Academy of Sciences, 251 65 Ondřejov Observatory, Czechoslovakia

Abstract. Differences among the Earth gravity field models, originally (in Planet. Space Sci. 29, 1981, 653) expressed as dispersions of the relevant lumped geopotential coefficients, are transformed to the differences in variations of the orbital elements.

Theoretical formulas, the Lagrange Planetary Equations (LPE), describing the orbital perturbations near orbital resonances due to the geopotential, have been derived in simple and unified form. Then they are applied to estimate the orbital uncertainty as a function of an inaccuracy of the Earth models. The set of 11 recent models was used: SAO SE 2, 3, 5 or 6, GSFC GEM 6,7,8, 10B, 'Koch 74' or 'Chovitz and Koch 78', HARMOGRAV, 'Rapp 77', GRIM 2.

The amplitudes of the differences in the LPE may reach 10^{-3} deg/day, 10-15 m/day or 200 m/day in inclination, semimajor axis or in mean longitude $L = \omega + M + \Omega$, respectively, for close and polar orbits (about 15revs/day); they are not larger than 10^{-4} deg/day, 1-2 m/day or 20 m/day in these elements for higher orbits (about 6-7 revs/day).

Our test has been prepared for the inclination from 30 to 140° and order 6 - 15. It may be repeated with various sets of the Earth models, for arbitrary orbital inclination and need not be connected to any real Earth's satellite and so limited by its inclination.

A Dynamical Basis for Crustal Deformation and Seismotectonic Block Movements in Central Europe*

Han-Shou Liu
Goddard Space Flight Center
Greenbelt, MD 20771

ABSTRACT

Geological observations have revealed the style of neotectonic near-surface stresses and crustal deformation. Seismic activity, foci depths and fault-plane solutions of earthquakes indicate kinematic reactions and block movements in Central Europe. In order to understand the dynamics of the generating stresses and their directions of tension, compression and shear, a program for the development of crustal stress field as inferred from satellite gravity data has been initiated.

The crust of the earth is considered to be an elastic spherical shell. The solutions of the equilibrium and stresses in the shell of the crust subject to boundary conditions are obtained in terms of series involving spherical harmonics of the geopotential. By applying Kelvin's general solutions and Love's special solutions to the problem of the spherical shell, the six components of the stress tensor at any point in the crust are formulated. Consequently, the orientations of the principal stresses of tension and compression and the maximum shear stresses in the crust of Central Europe are computed according to the theory of elasticity.

The results of the computed stress directions seem to justify the attempt to relate the crustal deformation and seismotectonic block movements in Central Europe to the high degree harmonics in the geopotential. The satellite determined stresses in the crust of Central Europe are consistent with earthquake focal mechanisms, joint orientation, valley trend and in-situ stress measurements. The crustal stress field in Central Europe as inferred from satellite gravity data closely resembles the experimental pattern of crystal deformation. It is shown that much of the intrplate deformation in Central Europe turns out to be related to dynamical processes that govern single crystals which are a billion times smaller in size than seismotectonic blocks.

*Paper to be presented by "title only."

Transient Sea Surface Height Variation and the SEASAT-ALT Data Application

Moon, Wooil, Department of Earth Sciences,
The University of Manitoba, Winnipeg, Manitoba, R3T 2N2

For the reduction of SEASAT-ALT data and the study of ocean bottom friction phenomenon, the hydrodynamic differential equation is solved over the Hudson Bay area and adjacent seas of northern Canada. The surface wind field inputs are from the periods of AUG 5 - AUG 6, AUG 19 - AUG 21, SEPT 15 - SEPT 16 and SEPT 20 - SEPT 22, 1978. For these periods, the ocean bottom friction term is also varied for the correlation of the transient SSH with the SEASAT-ALT measurements. The preliminary results indicate that the numerical simulation of the transient sea surface topography and their correlation with the SEASAT-ALT observation can predict the global average estimate of the ocean bottom friction term and consequently more precise solid Earth and Ocean tide coupling mechanism.

REFERENCES

ICCG, 1981. Application of Space Technology to Operational Geodynamics and Geodetic Measurement Services. Interagency Coordinating Committee for Geodynamics, Washington, DC, July 1981.

NASA, 1980. Geodynamics Program Annual Report for 1979. NASA TM 81978, National Aeronautics and Space Administration, Washington, DC, May 1980.

NASA, 1981a. Data Management Plan for Crustal Dynamics Project. H. G. Linder, GSFC X-931-81-18, National Aeronautics and Space Administration, Goddard Space Flight Center, Greenbelt, Maryland. July 1981.

NASA, 1981b. Geodynamics Program Annual Report for 1980. NASA TM 84010, National Aeronautics and Space Administration, Washington, DC, October 1981.

NASA, 1982a. Geopotential Research Program. Geodynamics Program, NASA Headquarters, Washington, DC, April 1982.

NASA, 1982b. Geodynamics Program Annual Report for 1981. NASA TM 85126. National Aeronautics and Space Administration, Washington, DC, August 1982.

NASA, 1982c. Crustal Dynamics Data Information System User's Guide. H. G. Linder, GSFC X-931-82-14, National Aeronautics and Space Administration, Goddard Space Flight Center, Greenbelt, Maryland. October 1982.

NASA, 1983a. Abstracts, Fifth Annual Geodynamics Program Conference and Crustal Dynamics Project Review. Geodynamics Program, NASA Headquarters, Washington, DC, January 1983.

NASA, 1983b. Geopotential Research Mission - Scientific Rationale. Report of the Geopotential Research Mission Science Steering Group. Geodynamics Program, NASA Headquarters, Washington, DC, February 1983.

NASA/PSN, 1983. Report of the NASA/PSN Lageos-II Study Group. Geodynamics Program, NASA Headquarters, Washington, DC, January 1983.

FIGURE CAPTIONS

III-1. Crustal Dynamics Project sites for global observations in 1982.

III-2. Crustal Dynamics Project sites for observations in Western North America, 1982.

III-3. Mobile VLBI system (MV-3) during construction phase, 1982.

III-4. Laser tracking network sites for 1982.

III-5. Mobile laser system (TLRS-2) in temporary dome at GSFC, 1982.

III-6. McDonald Laser Ranging System (MLRS) at McDonald Observatory, Fort Davis, Texas.

III-7. Moblas-1 during construction at Huahine, French Polynesia, 1982.

IV-1. Present strain rates in the Basin and Range Province, from historical seismicity (R. B. Smith, presentation at the Fifth Annual NASA Geodynamics Conference, January 1983).

IV-2. Atmospheric angular momentum and predicted length of day for 1981, showing variations due to zonal winds in northern and southern hemispheres (R. Rosen, presentation at the Fifth Annual NASA Geodynamics Conference, January 1983).

IV-3. Comparison between earth rotation from lunar laser ranging and BIH values for 1980 (J. O. Dickey and J. G. Williams, presentation at the Fifth Annual NASA Geodynamics Conference, January 1983).

IV-4. Global gravimetric geoid based on GEM-10b gravity field and surface gravity data.

IV-5. Change in the node of the Lageos orbit showing quadratic term consistent with non-zero dJ_2/dt (D. Rubincam, presentation at the Fifth Annual NASA Geodynamics Conference, January 1983).

IV-6. Free air gravity anomalies referred to hydrostatic figure of reference (D. Rubincam, Goddard Space Flight Center).

IV-7. Observations and models of altimetric oceanic geoid and bathymetry in the Aleutians (D. McAdoo, presentation at the Fifth Annual NASA Geodynamics Conference, January 1983).

V-1. Geopotential Research Mission spacecraft being deployed from Shuttle (artist's conception).

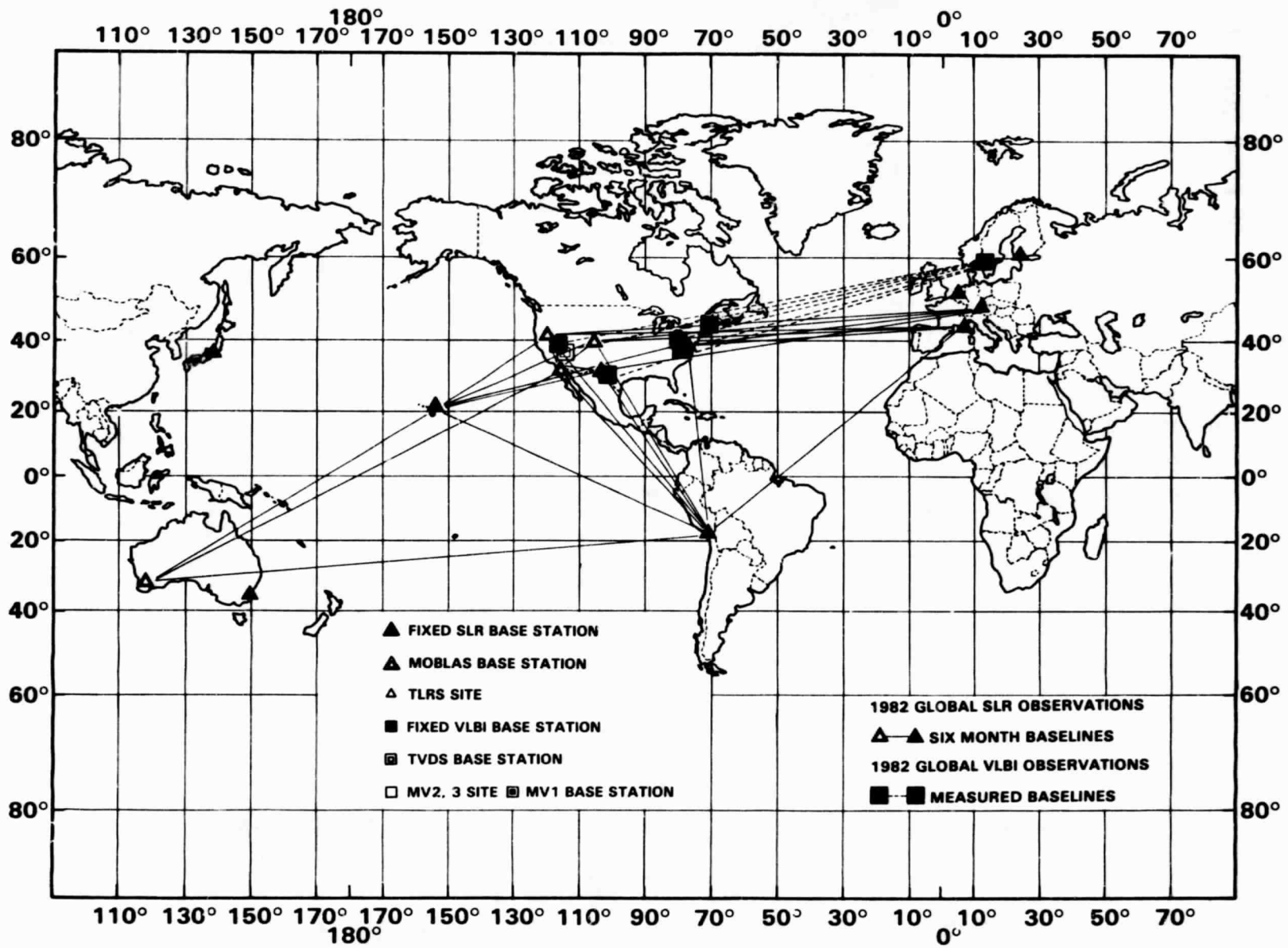

FIGURE III-1

REGIONAL CRUSTAL DYNAMICS PROJECT SITES

WESTERN NORTH AMERICA REGIONAL DEFORMATION 1982

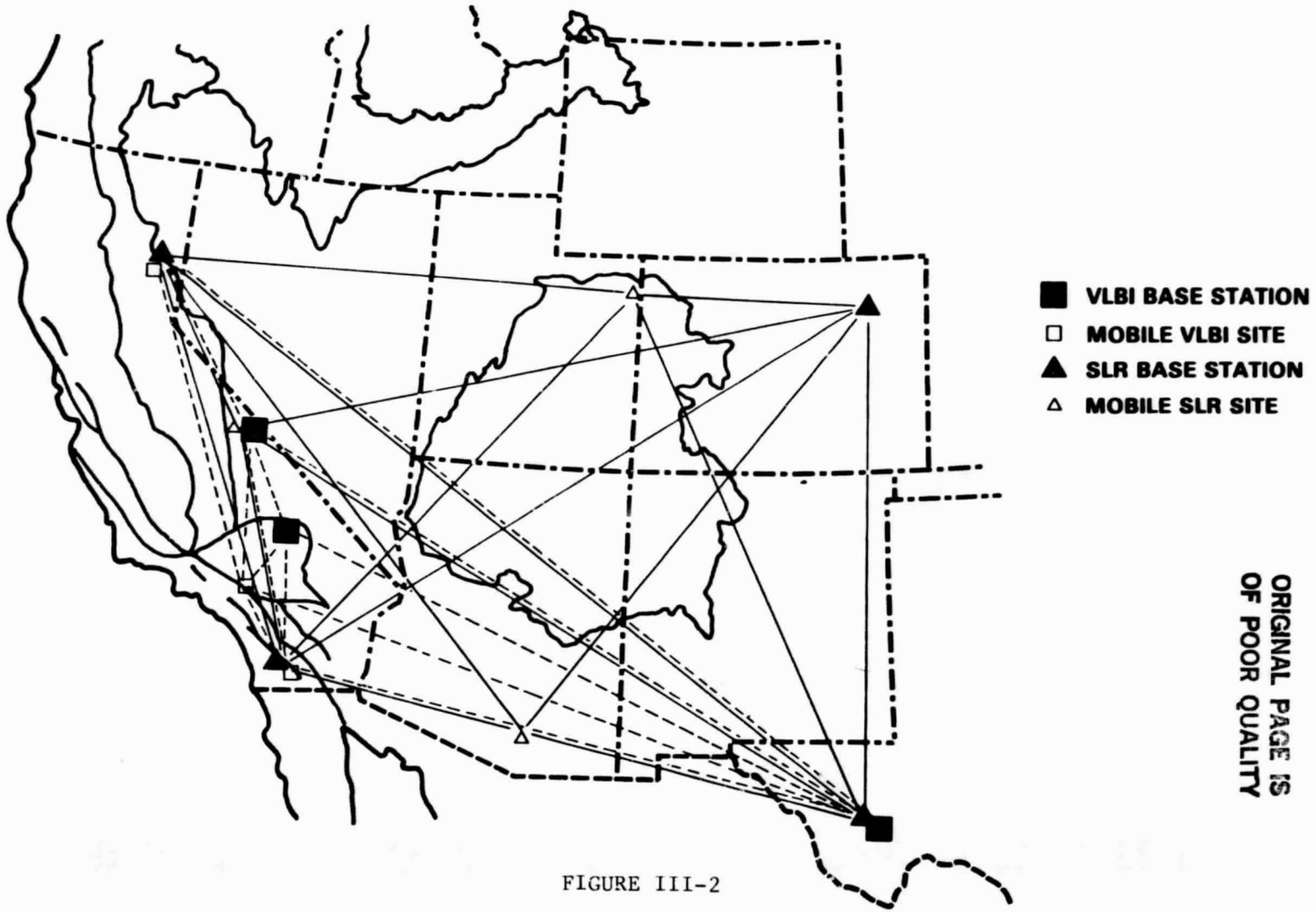

FIGURE III-2

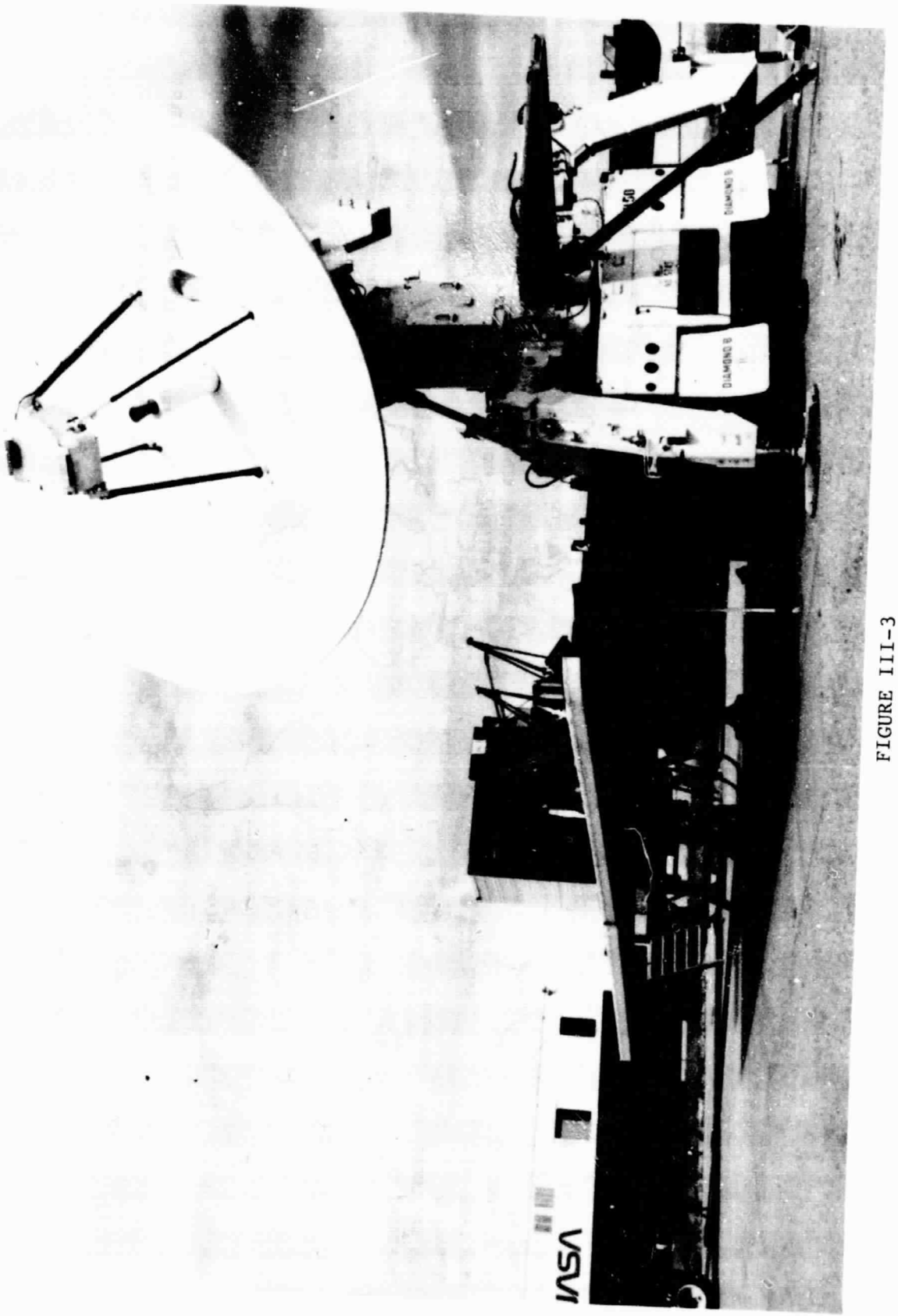

FIGURE III-3

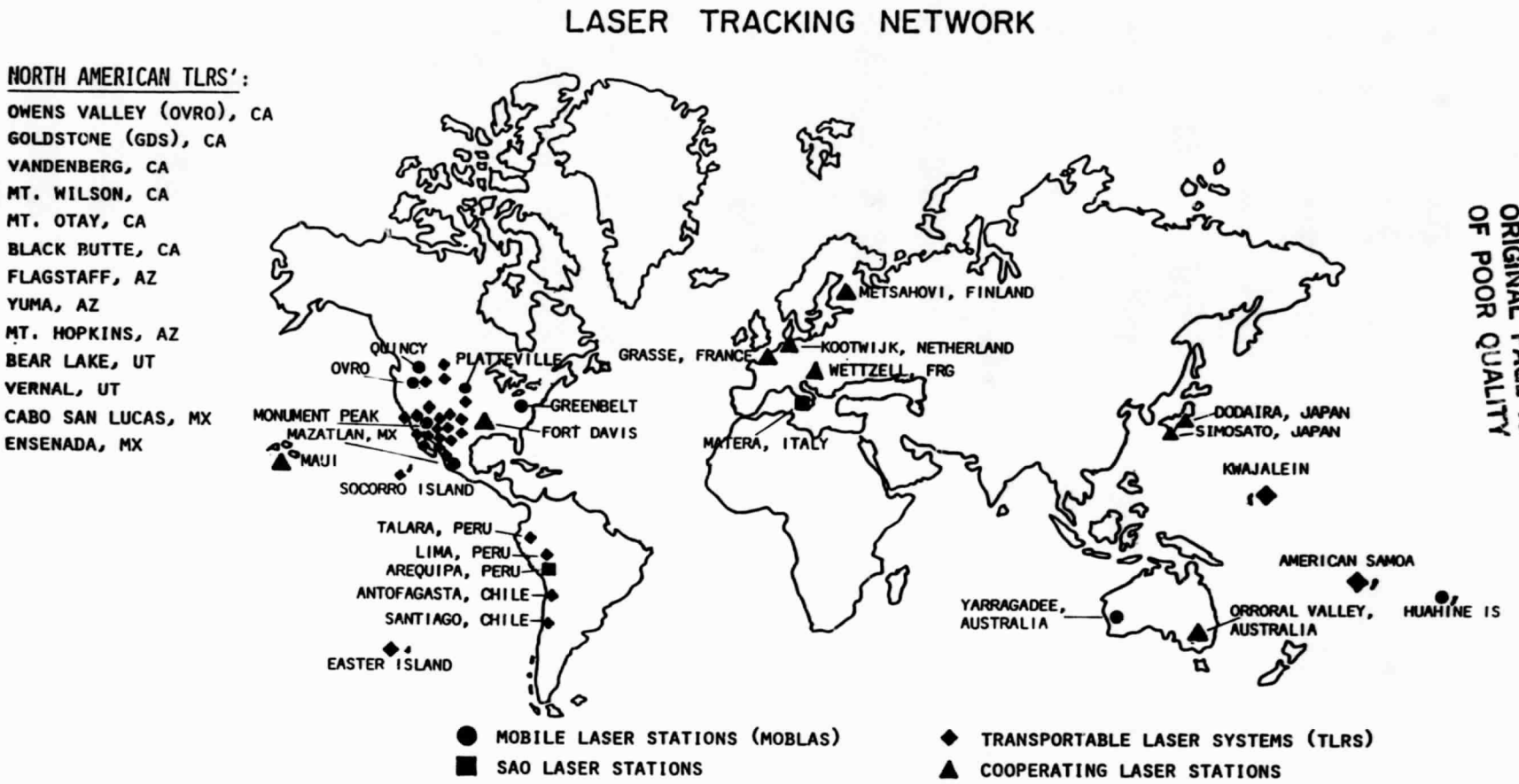

FIGURE III-4

FIGURE III-5

FIGURE III-6

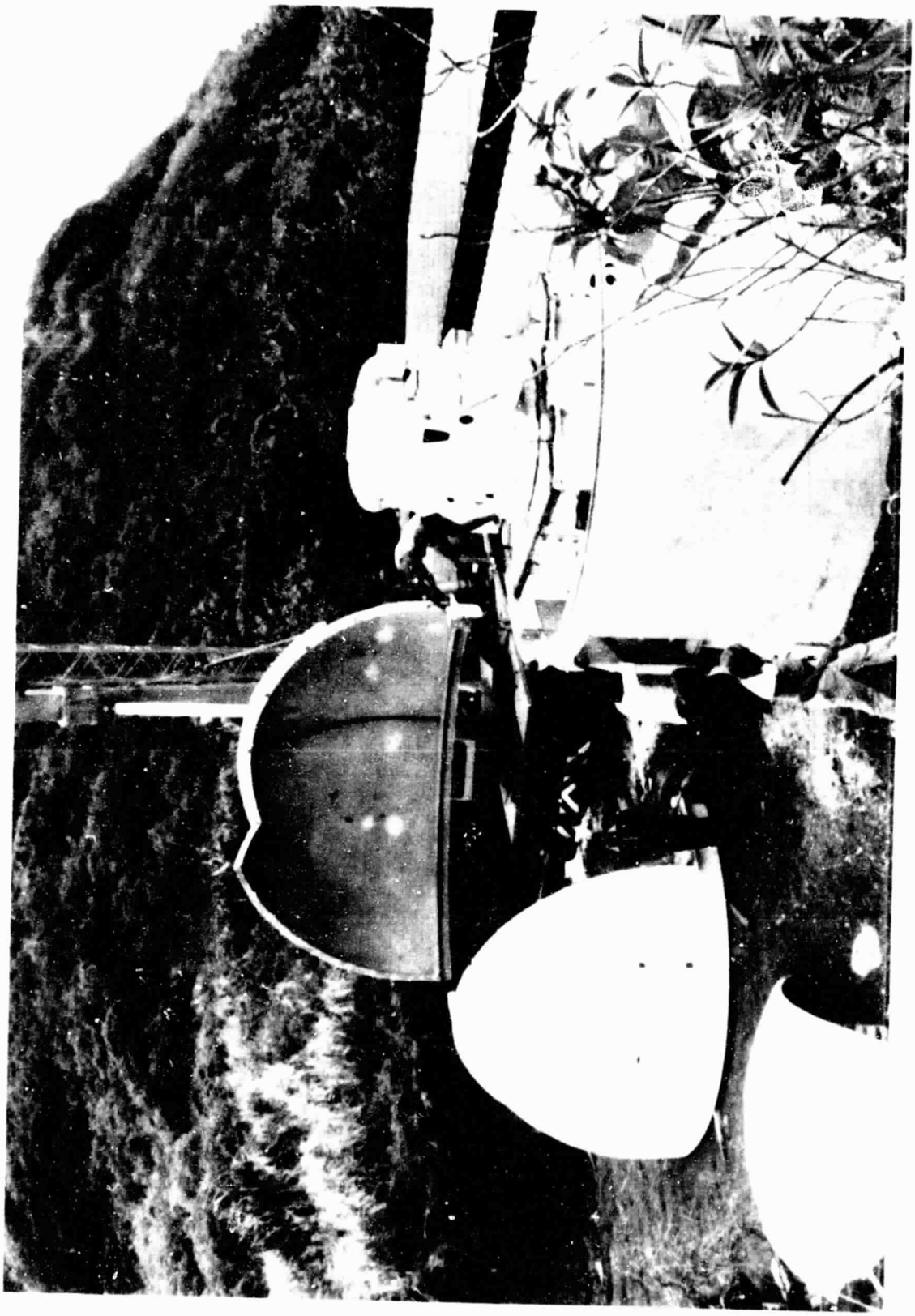

FIGURE III-7

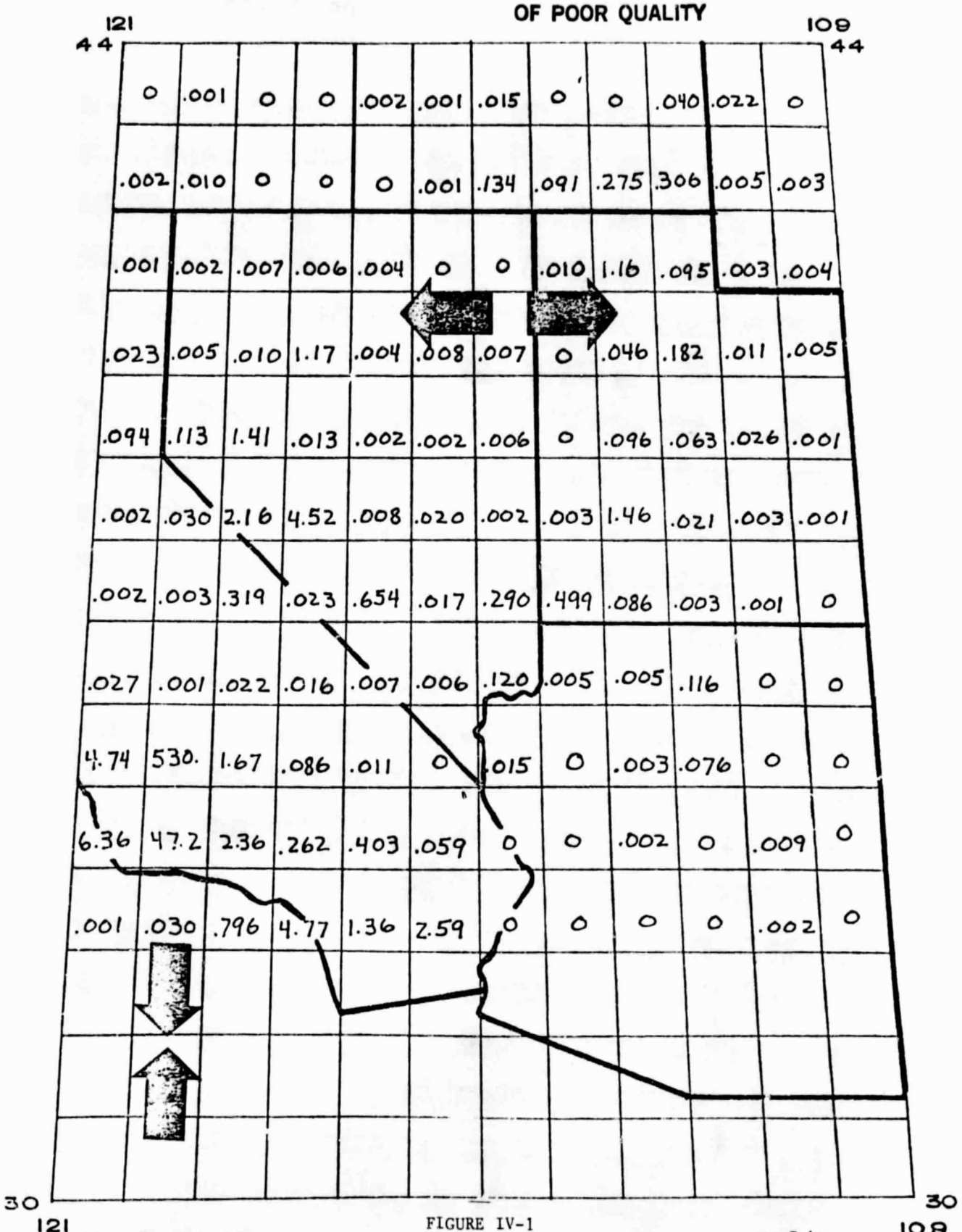

FIGURE IV-1

CONTEMPORARY STRAIN RATES--SEISMICITY ($\times 10^{-8}$/yr)

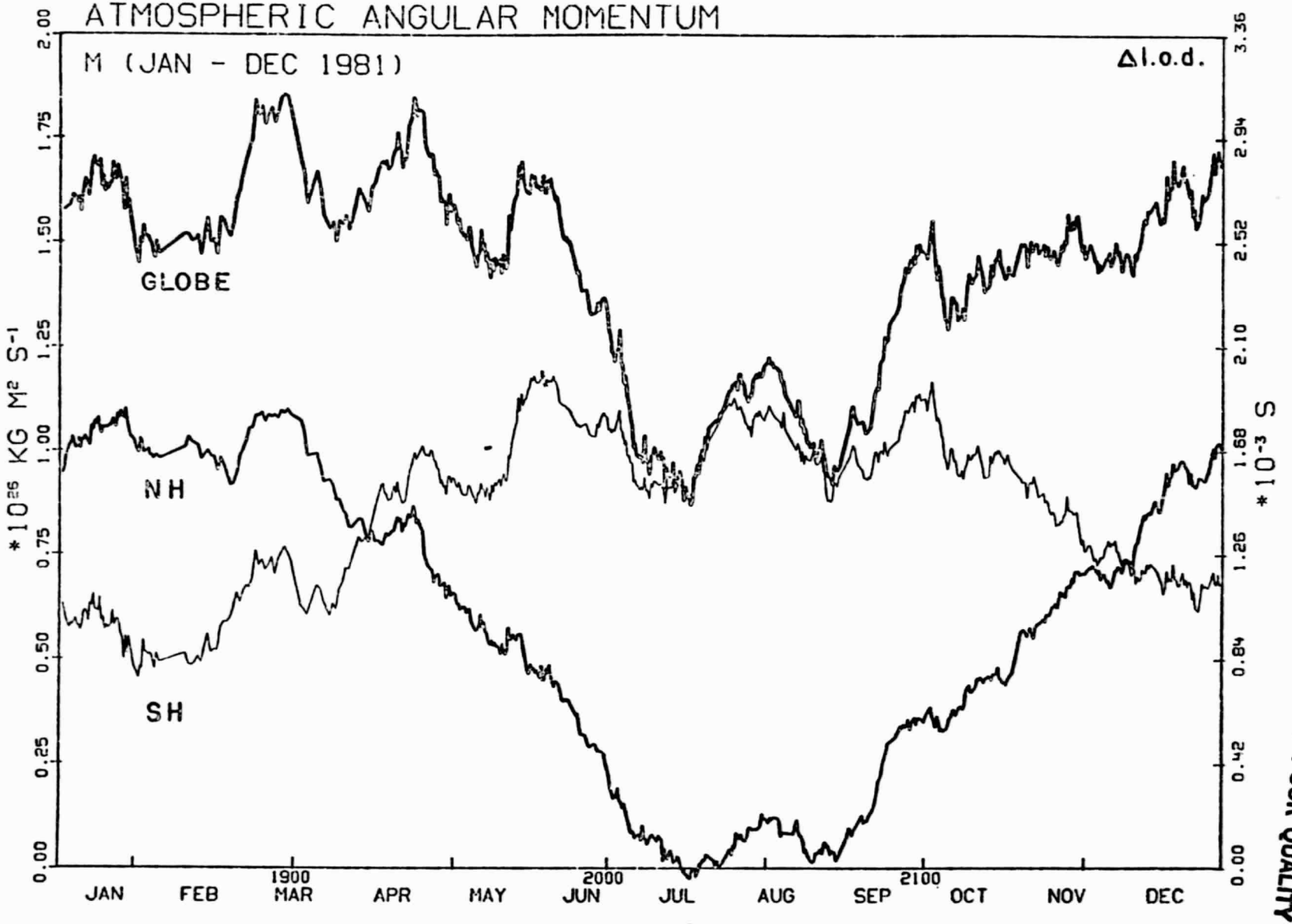

FIGURE IV-2

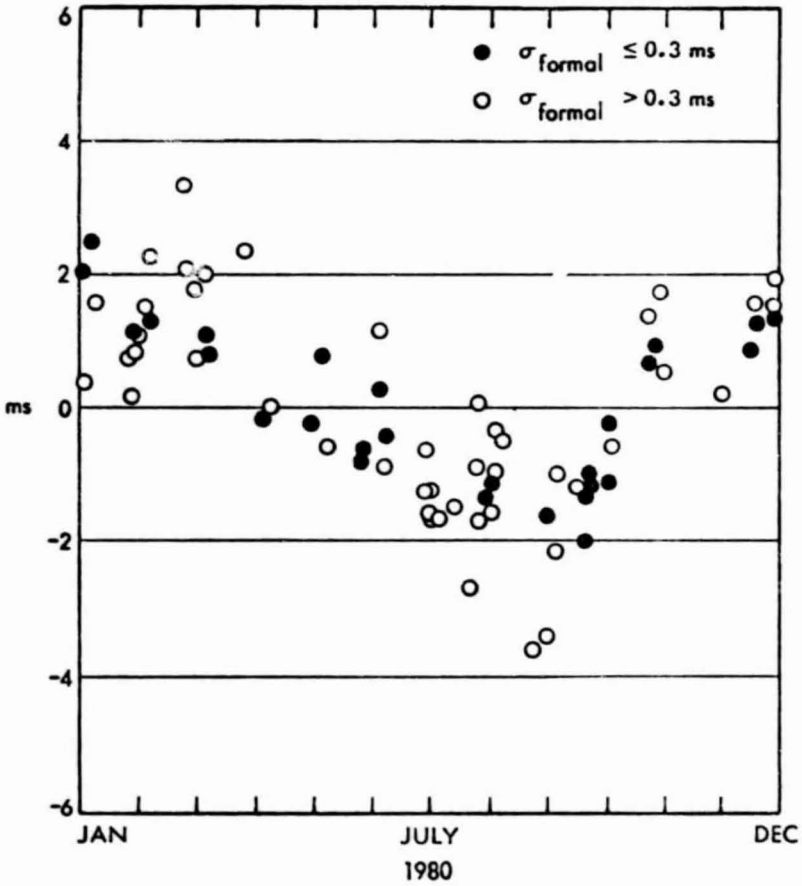

DISTRIBUTION:

$\sigma < 0.3$ ms	40%
$0.3 \text{ ms} \leq \sigma < 0.6$ ms	40%
$\sigma \geq 0.6$ ms	20%

(1 ms OF TIME = 0.015 arcseconds = 46 cm AT EQUATOR)

Differences between lunar laser ranging values of UT1 on individual days and smoothed BIH values during 1980.

FIGURE IV-3

NASA/GODDARD SPACE FLIGHT CENTER GLOBAL DETAILED GRAVIMETRIC GEOID BASED UPON A COMBINATION OF THE GSFC GEM 10B EARTH MODEL AND 1° x 1° SURFACE GRAVITY DATA

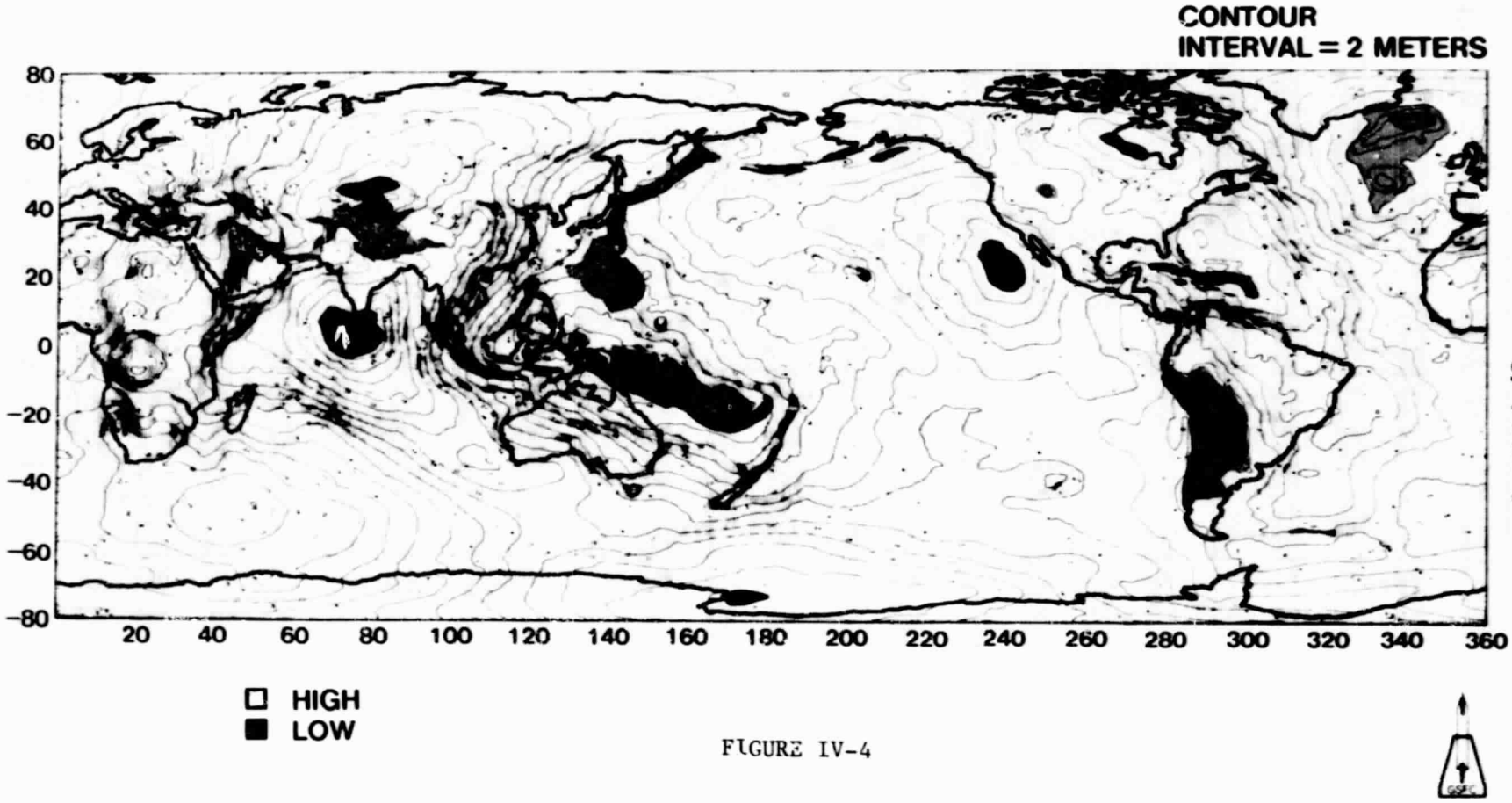

FIGURE IV-4

LAGEOS NODE OBSERVATIONS — SLOPE AND CONSTANT REMOVED

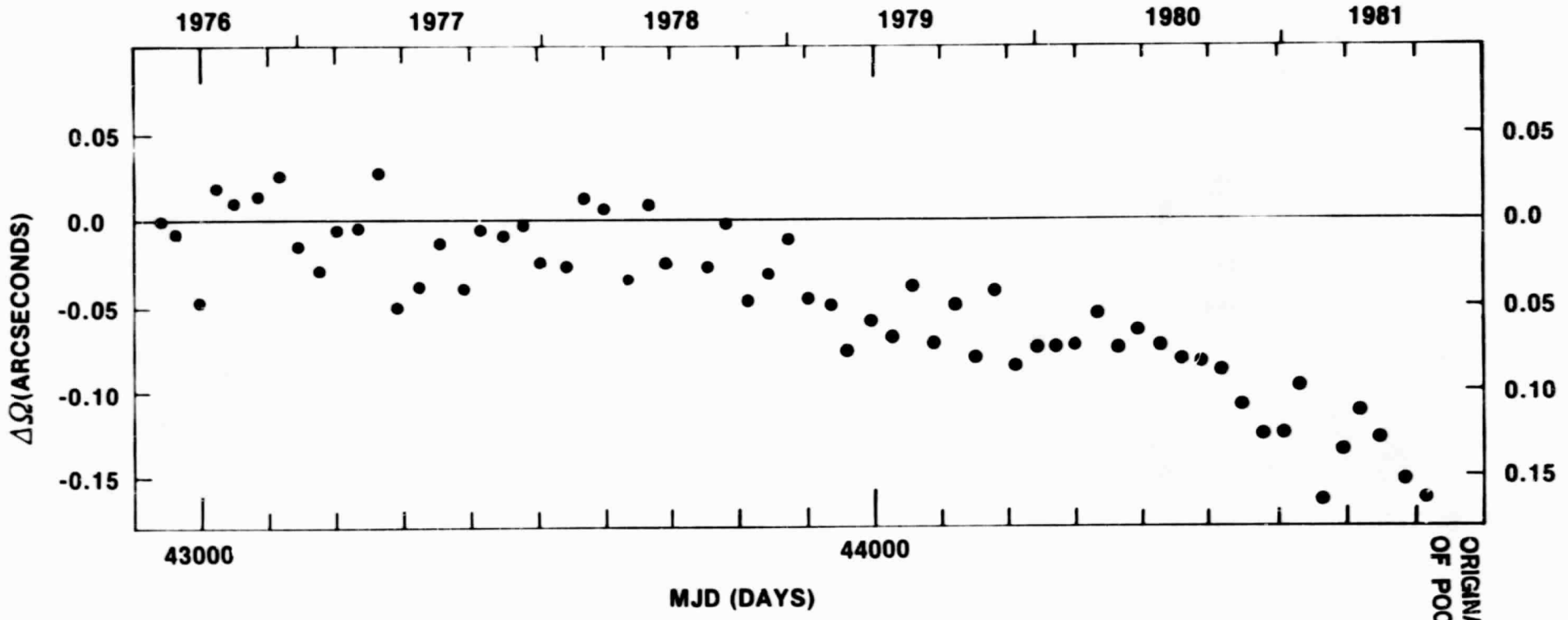

$\Delta\Omega = \frac{1}{2}\ \ddot{\Omega}\ T^2$

$\ddot{\Omega} = -8.1 \pm 1.8 \times 10^{-8}$ ARCSEC/DAY^2

FIGURE IV-5

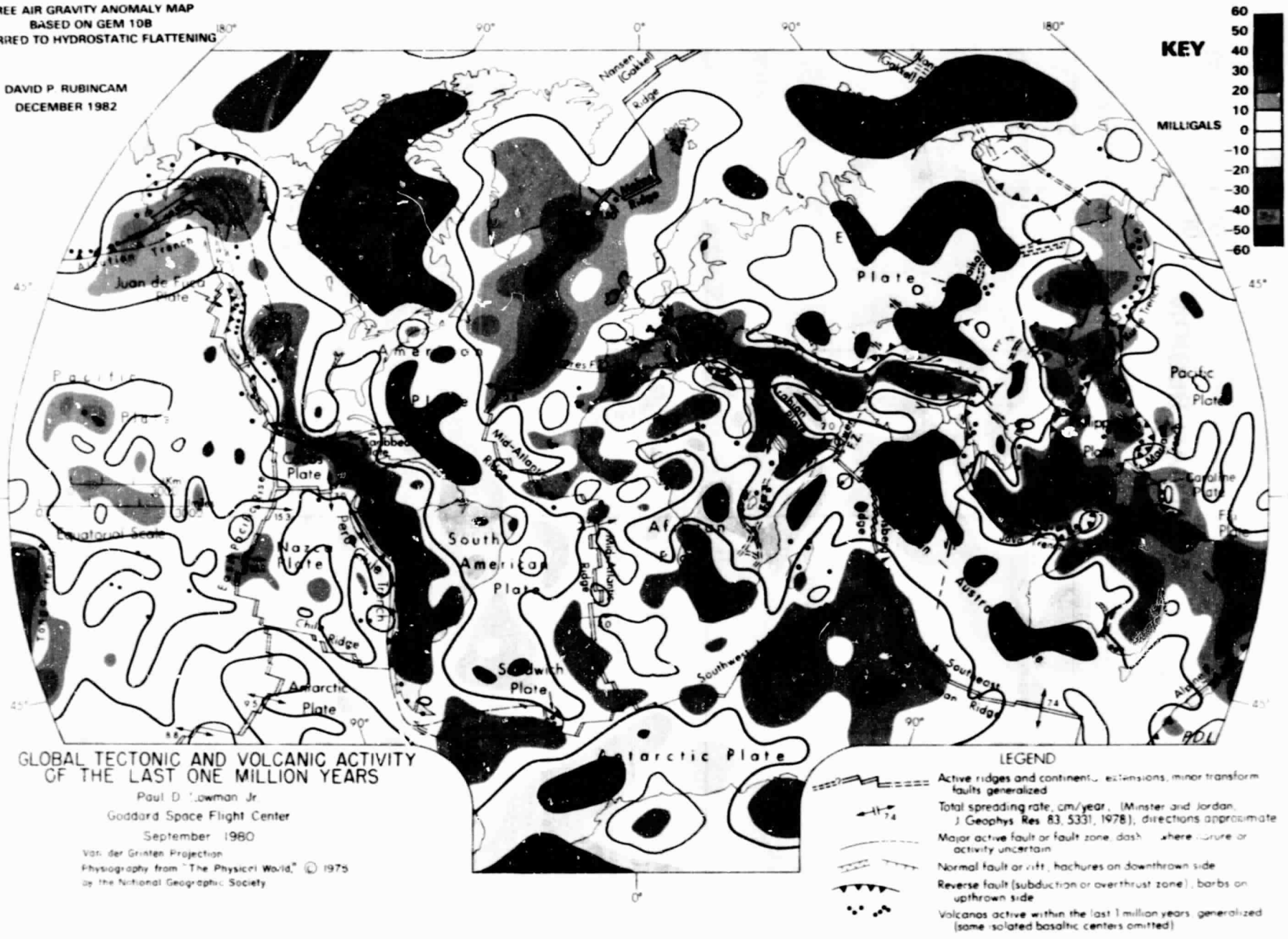

FIGURE IV-6

ALEUTIAN REGION
(E)

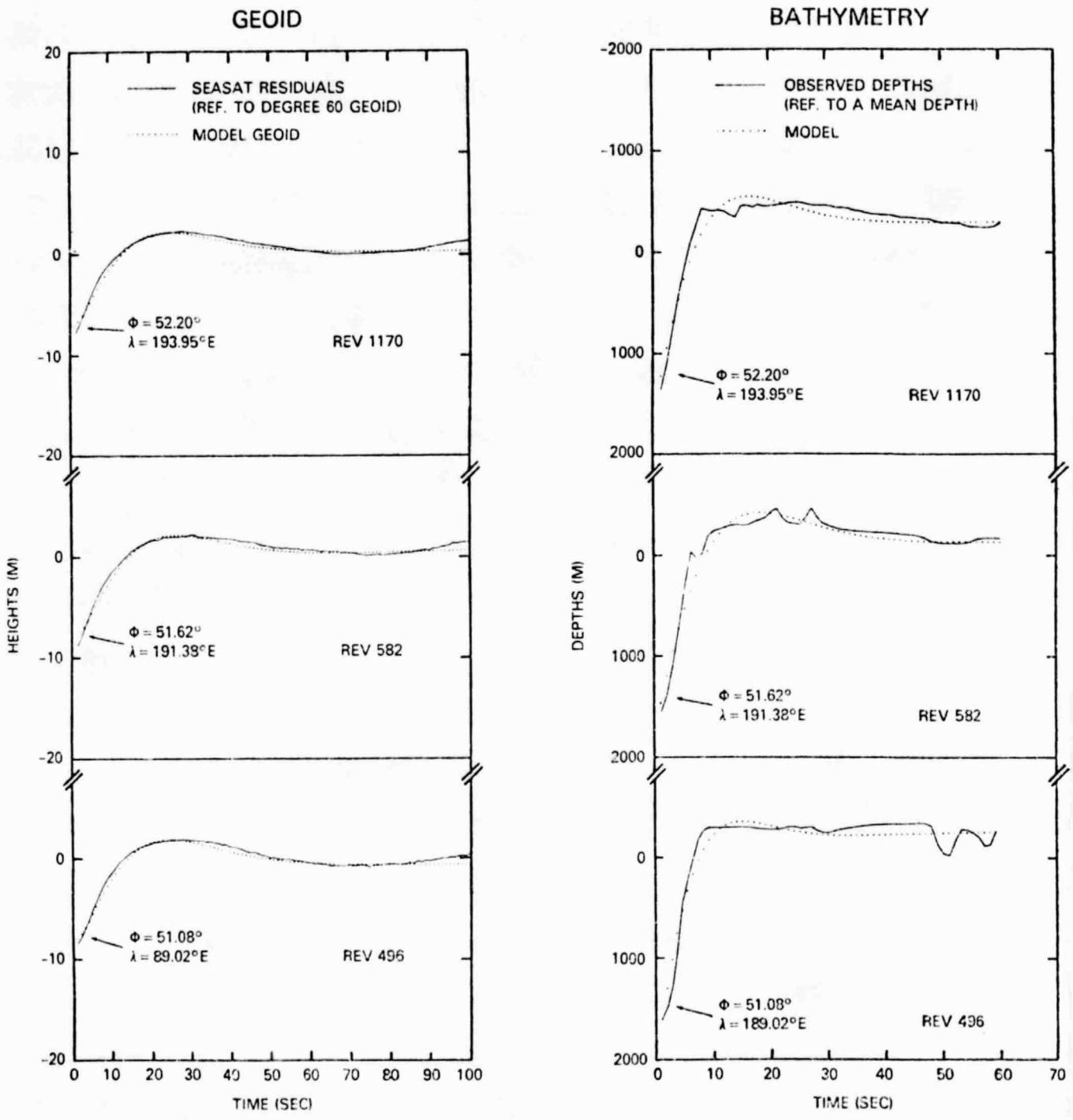

FIGURE IV-7